TURUN
YLIOPISTO
UNIVERSITY
OF TURKU

STATISTICAL PROPERTIES OF SOLAR ENERGETIC PROTON EVENTS

Miikka Paassilta

TURUN YLIOPISTON JULKAISUJA – ANNALES UNIVERSITATIS TURKUENSIS
SARJA – SER. AI OSA – TOM. 690 | ASTRONOMICA – CHEMICA – PHYSICA – MATHEMATICA | TURKU 2023

TURUN
YLIOPISTO
UNIVERSITY
OF TURKU

STATISTICAL PROPERTIES OF SOLAR ENERGETIC PROTON EVENTS

Miikka Paassilta

TURUN YLIOPISTON JULKAISUJA – ANNALES UNIVERSITATIS TURKUENSIS
SARJA – SER. AI OSA – TOM. 690 | ASTRONOMICA – CHEMICA – PHYSICA – MATHEMATICA | TURKU 2023

University of Turku

Faculty of Science
Department of Physics and Astronomy
Physics
Doctoral Programme in Exact Sciences

Supervised by

Professor Rami Vainio
Department of Physics and Astronomy
University of Turku
Turku, Finland

Doctor Athanasios Papaioannou
Institute for Astronomy, Astrophysics,
Space Applications and Remote Sensing
National Observatory of Athens
Athens, Greece

Docent Eino Valtonen
Department of Physics and Astronomy
University of Turku
Turku, Finland

Reviewed by

Associate professor Timo Asikainen
Space Physics and Astronomy
Research Unit
University of Oulu
Oulu, Finland

Doctor Nick Sergis
Academy of Athens and Hellenic Space
Center
Athens, Greece

Opponent

Doctor Pertti Mäkelä
The Catholic University of America/NASA Goddard Space Flight Center
Greenbelt, Maryland
United States of America

ISBN 978-951-29-9256-0 (PRINT)
ISBN 978-951-29-9257-7 (PDF)
ISSN 0082-7002 (PRINT)
ISSN 2343-3175 (ONLINE)
Painosalama, Turku, Finland, 2023

UNIVERSITY OF TURKU
Faculty of Science
Department of Physics and Astronomy
Physics
PAASSILTA, MIIKKA: Statistical properties of solar energetic proton events
Doctoral dissertation, 172 pp.
Doctoral Programme in Exact Sciences
May 2023

ABSTRACT

The Sun is the source of several different kinds of high-energy particles that are most prominently released in sudden large eruptions, known as solar energetic particle events. These particles, which escape the Sun and are accelerated in the coronal plasma, contribute substantially to the radiation environment in near-Earth and interplanetary space and therefore constitute an important consideration in mitigating the risks of space missions and other space-related human activities. Although the basic mechanisms related to energetic particle release and acceleration are fairly well known in principle, electrically charged particles are subjected to multiple complicated physical processes between their point of origin and an observer in interplanetary space. This fact, together with the changing conditions at the particle source, causes the observed particle event characteristics to vary a great deal, seriously complicating any attempt to understand, model, and predict their fluxes in near-Earth space.

In the work forming the basis for this dissertation, we examined three large selections of solar energetic particle events through various statistical methods. Relying on data mainly collected by spacecraft, we identified particle events that fulfilled certain criteria, determined their likely association with other solar phenomena (such as solar flares and coronal mass ejections), and characterised the events by calculating estimates for their intensity rise times, the differences between the particle injection times derived using different methods, the magnetic connectivity between the particle source and the observer, and various other quantities. These observables were studied for statistically significant dependencies in order to uncover information about particle release and transport. The event listing compiled for the first of the three articles included herein was additionally made available as an electronic online catalogue that has been thereafter regularly updated by the author.

We found that the features of solar energetic particle events do not exhibit any general, straightforward dependence on the longitudinal distance or the magnetic connectivity between the particle source and the observer, especially in their initial phase. The studied event populations appear highly variable in this respect, and they might include several different classes of events that are not readily distinguishable based on the available information. However, the intensity rise times, the delays between the event-related X-ray flare and the modelled event onset, as well as the relative durations of events, would seem to be at least somewhat dependent on the magnetic connectivity and the iron abundance of the event: a strong modelled

magnetic connection and iron-rich composition tend to imply a proton event that rises more quickly and lasts for a shorter period of time than does an event with the opposite characteristics. The longitudinal spread of energetic particles in large events is not strongly dependent on particle energy, but might depend on the general solar cycle-specific conditions in interplanetary space. Overall, our results underscore the desirability of combining good observational statistics with reasonably comprehensive numerical modelling of particle transport effects in efforts to gain a better understanding of the processes involved in solar particle events and to develop applications for predicting these events.

KEYWORDS: Solar energetic particles, solar eruptions, space weather, particle radiation

TURUN YLIOPISTO
Matemaattis-luonnontieteellinen tiedekunta
Fysiikan ja tähtitieteen laitos
Fysiikka
PAASSILTA, MIIKKA: Statistical properties of solar energetic proton events
Väitöskirja, 172 s.
Eksaktien tieteiden tohtoriohjelma
Toukokuu 2023

TIIVISTELMÄ

Aurinko tuottaa useita erilaisia suurienergiaisia hiukkaslajeja, joita vapautuu avaruuteen ensisijaisesti äkillisissä laajamittaisissa purkauksissa, niin sanotuissa Auringon suurienergiaisissa hiukkaspurkauksissa. Kyseiset hiukkaset, jotka kiihtyvät Auringon koronan plasmaprosesseissa ja vapautuvat planeettainväliseen avaruuteen, vaikuttavat tuntuvassa määrin Maan lähellä ja planeettainvälisessä avaruudessa vallitsevaan säteily-ympäristöön, ja tästä syystä ne ovat huomionarvoinen tekijä pyrittäessä hallitsemaan avaruuslentoihin ja muuhun avaruuteen liittyvään ihmisen toimintaan sisältyviä riskejä. Vaikkakin suurienergiaisten hiukkasten vapautumiseen ja kiihdytykseen liittyvät perustavanlaatuiset mekanismit tunnetaan periaatteessa kohtuullisen hyvin, sähköisesti varautuneet hiukkaset altistuvat useille monimutkaisille fysikaalisille prosesseille lähtöpaikkansa ja planeettainvälisessä avaruudessa sijaitsevan tarkkailijan välillä. Tämä tosiseikka yhdessä lähtöpaikan muuttuvien olosuhteiden kanssa saa aikaan purkausten ominaisuuksien suuren vaihtelun, mikä puolestaan hankaloittaa tuntuvasti pyrkimyksiä ymmärtää, mallintaa ja ennustaa ko. purkausten intensiteettejä Maan läheisessä avaruudessa.

Tämän väitöskirjan perustan muodostavassa tutkimustyössä tutkittiin kolmea laajaa Auringon hiukkaspurkauspopulaatiota tilastollisten menetelmien avulla. Määrätyt kriteerit täyttävät purkaukset tunnistettiin ja niiden riippuvuus muista Auringon ilmiöistä (kuten aurinkosoihduista ja koronan massapurkauksista) selvitettiin nojautuen lähinnä avaruusalusten keräämään dataan. Purkauksia kuvattiin kvantitatiivisesti laskemalla arviot intensiteettien nousuajoille, eri tavoin saatujen hiukkasten lähtöaikojen erotuksille, lähtöpaikan ja havaitsijan väliselle magneettiselle konnektiivisuudelle ynnä useille muille ominaisuuksille. Näitä tutkittiin tilastollisesti tavoitteena löytää statistisesti merkittäviä riippuvuuksia, jotka voisivat paljastaa uutta tietoa hiukkasten vapautumisesta ja kulkeutumisesta avaruudessa. Purkaustaulukko, joka koottiin ensimmäistä väitöskirjaan sisällytettyä artikkelia varten, on julkaistu lisäksi sähköisenä, tekijän sittemmin säännöllisesti päivittämänä luettelona Internetissä.

Tutkimuksessa todettiin, ettei Auringon suurienergiaisten hiukkaspurkausten ominaisuuksissa — etenkään purkausten varhaisvaiheessa — ole havaittavissa mitään yleistä ja yksiselitteistä riippuvuutta havaitsijan ja hiukkasten lähtöpaikan pituussuuntaisesta etäisyydestä tai kytkentäkulmasta. Tarkastellut purkauspopulaatiot vaikuttavat tässä suhteessa hyvin vaihtelevilta, ja niihin saattaa sisältyä useita eri purkaustyyppejä, joiden erottaminen toisistaan ei ole yksinkertaista

käytettävissä olevien tietojen perusteella. Intensiteettien nousuajat, viiveet hiukkaspurkaukseen liittyvän röntgensoihdun ja mallinnetun hiukkaspurkauksen alkuajan välillä sekä hiukkaspurkausten suhteelliset kestot näyttävät kuitenkin riippuvan ainakin jossain määrin magneettisesta konnektiivisuudesta ja purkauksen rautapitoisuudesta: purkauksilla, joissa magneettinen yhteys on hyvä ja rautapitoisuus suuri, on taipumus nousta nopeammin ja kestää lyhyemmän aikaa kuin purkauksilla, joilla nämä ominaisuudet ovat päinvastaiset. Suurenergisten hiukkasten vaakasuuntainen leviäminen ei riipu merkittävästi hiukkasten energiasta, mutta saattaa riippua kulloinkin tarkasteltuun aurinkojaksoon liittyvistä, planeettainvälisessä avaruudessa vallitsevista yleisistä olosuhteista. Kaikkiaan saadut tulokset painottavat hyvän havaintostatistiikan ja hiukkaskuljetuksen kohtalaisen kattavan numeerisen mallintamisen suotavuutta tavoiteltaessa Auringon hiukkaspurkauksiin liittyvien prosessien entistä parempaa ymmärrystä ja kehitettäessä sovelluksia näiden purkauksien ennustamista varten.

ASIASANAT: Auringonpurkauset, Auringon suurienergiaiset hiukkaset, avaruussää, hiukkassäteily

Acknowledgements

As the lengthy process that resulted in this dissertation is at long last drawing to a close, it is fitting to express my gratitude and the debt that I owe to everyone who helped and supported me along the way. On account of the number of people involved and the great importance of their contributions, this is anything but straightforward to accomplish adequately, but I will strive to do my best.

Heartfelt thanks are due to my supervisors. The lion's share of this task was shouldered by Professor Rami Vainio, whose ideas, advice, guidance, enthusiasm, patience, and overall support made my work possible in the first place. Eino Valtonen and Athanasios Papaioannou served as invaluable mentors all through the course of my doctoral studies, providing me with much-needed feedback and countless excellent suggestions for improving my methods, results, and manuscripts, as well as encouragement that was no less vital for me. I had an opportunity to benefit from their knowledge and experience, and for that, I am and always remain deeply grateful. Timo Asikainen and Nick Sergis, the pre-reviewers of this dissertation, are very much deserving of my gratitude for their thorough work and valuable comments, as is Pertti Mäkelä, who graciously agreed to act as my opponent.

I acknowledge with indebtedness the funding provided by the European Union's Horizon 2020 research and innovation programme, ESA, the Academy of Finland, and the Finnish Centre of Excellence for Research in Sustainable Space (FORESAIL). This financial backing was absolutely crucial as it enabled me to devote my time and energy to scientific research.

Of my current and former colleagues at the Space Research Laboratory, all of whom together made the unit a welcoming and convivial place to work, I feel it appropriate to highlight Osku Raukunen and Esa Riihonen. I was fortunate enough to be assigned to the same work group and office as Osku Raukunen for much of my years as a doctoral student, and I look back very fondly on our brainstorming sessions and entertaining (if sometimes off-topic) conversations, as well as his assistance on a multitude of issues. Esa Riihonen was always ready and willing to help when it came to questions and problems with the IDL software, ERNE data, or any number of other practical matters, making my work immensely easier at every turn. Thank you!

Lastly, I wish to thank my family and friends for their unconditional support and sympathy. Their faith in my ability to bring this undertaking to conclusion may well

have been stronger than my own at times, and I owe them my special gratitude now that it was borne out. In particular, I would like to mention my parents Ulla and Mauno, my sister Anna, Eetu, my cousin Timo Katila and his family, my grandfather Olavi Katila (who sadly passed away before this dissertation was finished), and my close friend Jani Alander; there are many others besides, too numerous to list but all very much due my thanks. If not for you, my road to this achievement would have been immeasurably harder, perhaps outright impassable.

Eurajoki, April 2023
Miikka Paassilta

Table of Contents

Abbreviations

ACE	Advanced Composition Explorer
ASPECS	Advanced Solar Particle Event Casting System
AU	Astronomical Unit
CME	Coronal Mass Ejection
COMESEP	Coronal Mass Ejections and Solar Energetic Particles (a forecasting tool)
EIT	Extreme ultraviolet Imaging Telescope (an instrument aboard SOHO)
EMMREM	Earth-Moon-Mars Radiation Environment Module
EPAM	Electron, Proton, and Alpha Monitor (an instrument aboard ACE)
EPHIN	Electron Proton Helium Instrument (an instrument aboard SOHO)
ERNE	Relativistic Nuclei and Electrons (an instrument aboard SOHO)
ESA	European Space Agency
ESP	Emission of Solar Protons (a mathematical model)
EUHFORIA	European Heliospheric Forecasting Information Asset
EUV	Extreme Ultraviolet
IMPACT	In situ Measurements of Particles and CME Transients (an experiment aboard STEREO)
JPL	Jet Propulsion Laboratory
GOES	Geosynchronous Operational Environmental Satellite
LASCO	Large Angle and Spectrometric Coronagraph (an instrument aboard SOHO)
MHD	Magnetohydrodynamic(s)
NOAA	National Oceanic and Atmospheric Administration
NASA	National Aeronautics and Space Administration (USA)
PARADISE	Particle Radiation Asset Directed at Interplanetary Space Exploration
PFSS	Potential Field Source Surface
PLASTIC	Plasma and Suprathermal Ion Composition (an instrument aboard STEREO)
PPS	Proton Prediction System
PROSPER	Probabilistic Solar Particle Event foRecasting (a statistical model for predicting particle events)
RELEASE	Relativistic Electron Alert System for Exploration

SAPPHIRE	Solar Accumulated and Peak Proton and Heavy Ion Radiation Environment (a modelling tool)
SAWS	Solar Energetic Particles Advanced Warning System
SECCHI	Sun Earth Connection Coronal and Heliospheric Investigation (an experiment aboard STEREO)
SEP	Solar Energetic Particle
SEPEM	Solar Energetic Particle Environment Modelling
SEPT	Solar Electron and Proton Telescope (an instrument aboard STEREO)
SOHO	Solar and Heliospheric Observatory
SOLPENCO	Solar Particle Engineering Code
SPRINTS	Space Radiation Intelligence System
SSN	International Sunspot Number
STEREO	Solar Terrestrial Relations Observatory
SWE	Solar Wind Experiment (an instrument aboard the Wind spacecraft)
SWEPAM	Solar Wind Electron, Proton and Alpha Monitor (an instrument aboard ACE)
TSA	Time Shifting Analysis
TSI	Total Solar Irradiance
VDA	Velocity Dispersion Analysis
VESPER	Virtual Enhancements – Solar Proton Event Radiation (a modelling tool)

List of Original Publications

This dissertation consists of a review of the research topic and is based on the following original publications, referred to in the text as follows:

I **Catalogue of 55–80 MeV solar proton events extending through solar cycles 23 and 24**
M. Paassilta, O. Raukunen, R. Vainio, E. Valtonen, A. Papaioannou, R. Siipola, E. Riihonen, M. Dierckxsens, N. Crosby, O. Malandraki, B. Heber, and K.-L. Klein
Journal of Space Weather and Space Climate, Volume 7, A14, 2017
DOI:10.1051/swsc/2017013

II **Catalogue of $>$ 55 MeV Wide-longitude Solar Proton Events Observed by SOHO, ACE, and the STEREOs at $\approx$ 1 AU During 2009 - 2016**
M. Paassilta, A. Papaioannou, N. Dresing, R. Vainio, E. Valtonen, and B. Heber
Solar Physics, Volume 293, Issue 4, 70, 2018
DOI:10.1007/s11207-018-1284-7

III **Magnetic connectivity and solar energetic proton event intensity profiles at deka-MeV energy**
M. Paassilta, R. Vainio, A. Papaioannou, O. Raukunen, S. Barcewicz, and A. Anastasiadis
Advances in Space Research, Volume 71, Issue 3, 2023
DOI:10.1016/j.asr.2022.11.051

1 Introduction

1.1 Solar energetic particles

As a result of the dynamic processes that are ultimately powered by the nuclear reactions in the solar core, solar energetic particles (SEPs) are ejected from the Sun. These particles include electrons, neutrons, and the ionized nuclei of the elements present in the Sun, the latter of which may attain energies in excess of 1 GeV/nucleon. They are an object of intensive scientific study because their energy spectra, ionization states, relative abundances of different particle species, and other measurable properties carry information about the conditions and physical processes present at their release site and in interplanetary space.

Even though SEPs are in fact continuously released, they are characteristically observed as SEP events, i.e. episodes where the measured particle intensities may increase by multiple orders of magnitude for a period of time that lasts from several hours to several days (e.g. Reames, 2013). While spaceborne instruments are usually required to detect and monitor SEP events due to the shielding effect of the magnetosphere and atmosphere of the Earth, the most energetic cases may be observed through ground-based equipment as so-called ground level enhancements (GLEs; e.g. Asvestari et al., 2017, and references therein). These occur when the flux of the nuclei capable of penetrating the magnetosphere of the Earth increases to such an extent that they become discernible via the cascade reaction caused upon their colliding with the atoms of the atmosphere (see e.g. Poluianov et al., 2017).

The existence of energetic particles arriving from outside the Earth was established by Hess (1912) using balloon-borne electroscopes. During the early part of the 20th Century, the detected energy signatures were assumed to be of gamma rays, which gave rise to the common term ”cosmic rays”; in this broad sense, SEPs are one of the classes comprising cosmic rays. The Sun as the source of some of these energetic particles was specifically postulated by Forbush (1946), who noted a temporal correlation between three large solar flares and increases in cosmic ray activity. Neutron monitors, developed in the 1950s (for a retrospective discussion, see Simpson, 2000), and the first successful unmanned interplanetary spacecraft in the early 1960s (for example, Mariner 2; results reported in Anderson, 1963, and others) added greatly to the scientific understanding of SEPs, and they have been regularly monitored since the turn of the 1970s by various space missions such as the long-running Geosynchronous Operational Environmental Satellite (GOES) series and the Solar

and Heliospheric Observatory (SOHO; Domingo et al., 1995).

SEP events have been traditionally grouped into impulsive and gradual ones (see Figure 1). The empirical work in the mid-1900s led to solar flares being viewed as a direct source of SEPs, and when in situ observations revealed that SEP events display greatly varying maximum intensities, fluences (intensities integrated over time), particle abundances and intensity profiles, the two-way division (e.g. Cane et al., 1986) was adopted, in parallel to a similar, earlier classification scheme applied to flares themselves (Pallavicini et al., 1977). According to this paradigm, impulsive events are characterised by brief duration (a few hours), fast intensity rise, and comparatively low peak intensities. They are typically associated with flares at locations that are magnetically well connected with the observer, and they are rich in electrons, ^{3}He (in relation to ^{4}He), Fe (in relation to elements such as C, N, and O), and very heavy ions (e.g. Hsieh and Simpson, 1970; Anglin et al., 1977; Mason et al., 1986; Reames, 1988; Mason et al., 2004). In contrast, gradual events reach high peak intensities and often last for days, resulting in large overall particle fluences. They are observed to originate from a wide range of solar longitudes, suggesting that their spatial extent is generally larger than that of impulsive events (e.g. Kallenrode et al., 1992). The relative abundances of SEP species in gradual events are much closer to the corresponding values in the solar corona than in impulsive events, and they are generally proton-rich (Reames, 1999, and references therein).

However, the advances in research after the 1980s led to the simple classification outlined above being challenged. Studying a collection of 77 events, Kallenrode et al. (1992) identified a number of events—often termed ”mixed” or ”hybrid” in contemporary literature—that displayed characteristics of both impulsive and gradual types, which they interpreted as probably following from the SEPs being accelerated in a flare at first and then subsequently in a shock. More support for this notion came from the discovery of large or prolonged events that featured a particle composition more typical for impulsive events (Mason et al., 1999; Kocharov and Torsti, 2002). Currently, most researchers (e.g. Cane et al., 2010; Papaioannou et al., 2016) agree that the impulsive-versus-gradual division is a simplification. There appear to be numerous cases that exhibit properties traditionally associated with both groups and no specific parameter that can clearly delineate them. Therefore, SEP events should rather be viewed as existing on a continuum of features.

Many of the details of the various SEP injection, acceleration, and transport mechanisms remain unclear and debated (see e.g. Desai and Giacalone, 2016). However, it seems likely that new space missions enabling observations close to the Sun (most importantly, Solar Orbiter and Parker Solar Probe; Müller et al., 2013 and Fox et al., 2016, respectively), in combination with improving computational modelling techniques (e.g. van den Berg et al., 2020, and references therein), will provide considerable new insight into areas that have so far eluded thorough understanding.

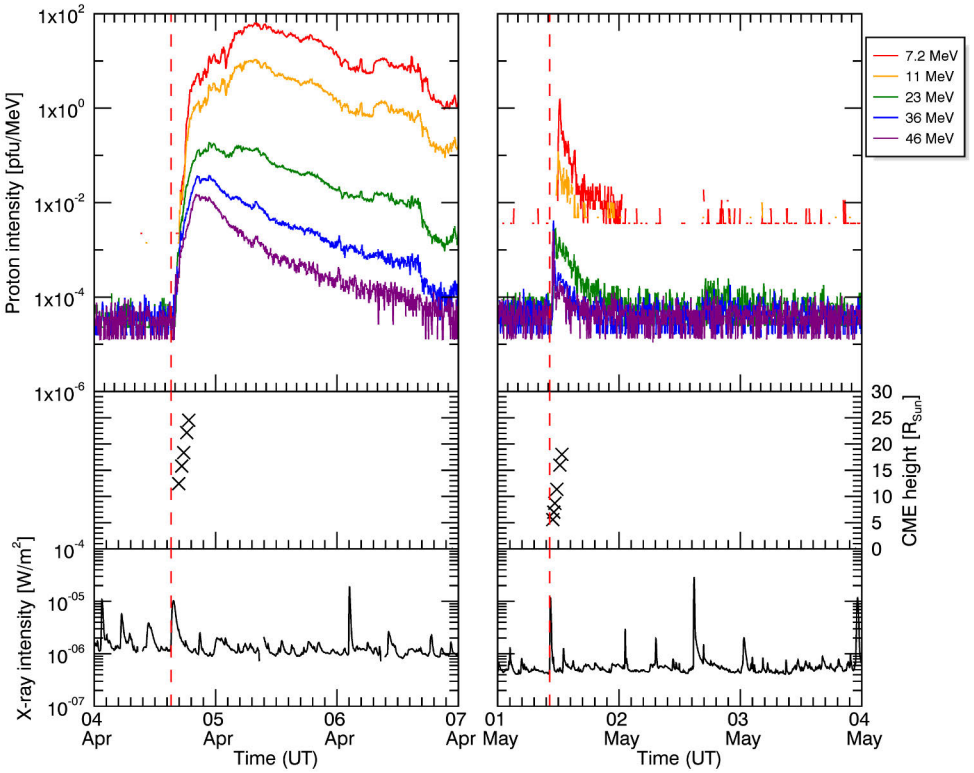

Figure 1. A representative case of a ”gradual” (4 April 2000; on the left) and ”impulsive” (1 May 2000; on the right) SEP event. From the top, the panels present proton intensity detected by SOHO/ERNE on five energy channels in pfu/MeV (where 1 pfu = 1 particle cm^{-2} s^{-1} sr^{-1}), CME height in solar radii (data from the SOHO LASCO CDAW Catalog), and soft X-ray intensity measured by GOES. The onset time of the X-ray flare associated with each event is marked with a dashed vertical red line.

1.1.1 Sources and acceleration mechanisms of SEPs

Since flares were the first kind of dynamic, transient activity discovered on the Sun and a correlation seemed to exist in the timing of SEP intensities and large flares, SEP events were initially attributed solely to flares. Early radio observations lent credence to this idea in that they identified accelerated electrons escaping from the Sun (type III bursts; see also Chapter 1.4), but there were also signs that indicated the existence of propagating shocks (type II) possibly related to particle acceleration (Wild et al., 1963). With the discovery of coronal mass ejections (CMEs) in the early 1970s (see Chapter 1.3) and mounting evidence of two types of events, it became increasingly apparent that more than one mechanism is likely responsible for the acceleration of SEPs (e.g. Kahler et al., 1978; Cliver et al., 1982; Mason et al., 1984). The widespread acceptance of the impulsive-versus-gradual event categorisation scheme was accompanied by the view that these classes of events primarily involve acceleration in flares and CME-driven shocks, respectively (Reames, 1999).

Any model striving to explain the observed properties of classical ”impulsive” events has to account for both ^{3}He and heavy ion enrichments, as well as their observed association with soft X-ray flares. To this end, several models have been put forth that differ in details but generally emphasize some form of stochastic heating process occurring at the flare, either alone (Temerin and Roth, 1992) or as one part of a two-stage acceleration process (Fisk, 1978; Liu et al., 2004; Zhang, 2004). However, attempts to associate SEP acceleration more or less directly with magnetic reconnection have also been made (Drake and Swisdak, 2012). An important factor in many of the stochastic heating models is the ion-cyclotron resonance of the particles with plasma waves, which might explain (via cascading turbulence) the preferential acceleration of certain kinds of heavy ions (e.g. Miller, 1998; Eichler, 2014; Kumar et al., 2017). Impulsive events are at least occasionally associated with narrow CMEs (Kahler et al., 2001) and more often with coronal jets (Pick et al., 2006; Nitta et al., 2008). Based on simulations (e.g. Drake et al., 2009), some have suggested that the combination of a jet and flare might provide an environment where a magnetic reconnection leaves behind a series of collapsing cells, or ”islands”, inside which charged particles experience Fermi acceleration as they are reflected back and forth between the ends (Reames, 2021, and references therein).

Acceleration in propagating CME shock fronts in the solar corona and interplanetary space is considered to play a major role in large gradual events. Fast CMEs—which typically accompany the largest SEP events (Gopalswamy et al., 2012; see also Articles I and II)—are thought to contain ample energy to produce vast numbers of SEPs: Emslie et al. (2012) estimated that although only some 2–3% of the kinetic energy contained in the CME is passed on to SEPs in a representative case, this may still amount to a total on the order of 10^{24} joules. Shocks transfer energy to charged particles via two dominant and simultaneously acting mechanisms,

diffusive shock acceleration and shock drifting. The former is akin to first-order Fermi acceleration and occurs when particles pass through the shock front multiple times and are in the process scattered between waves or magnetic inhomogeneities driven by the particles themselves (e.g. Bell, 1978; Gordon et al., 1999), while the latter describes a drift of the particles parallel to the electric field at the shock front, resulting in the electric potential energy being converted into the kinetic energy of the particles (e.g. Jokipii, 1982; Decker, 1988).

To understand better some of the observed features of SEP events, the geometry of the shock and magnetic field and its variation over time has to be taken into consideration as well. These features have been shown to have a substantial effect on the local details of the acceleration and measured particle intensities (e.g. McComas and Schwadron, 2006; Guo et al., 2010), pitch-angle anisotropies (e.g. Decker, 1990), and abundance variations of various SEP ion species (in conjunction with the event seed population composition; Tylka et al., 2005; Sandroos and Vainio, 2007, 2009).

In actuality, all of the processes mentioned above and others probably occur together, contributing to the large variety of SEP event characteristics observed at a distance from the Sun (e.g. Vlahos et al., 2019). Within the past decade, studies in the field have extended to such pertinent topics as multiple interacting CMEs (e.g. Li et al., 2012; Pohjolainen et al., 2016) and extended SEP injections originating from CME-generated shocks (Lario et al., 2016).

1.1.2 Some features of SEP propagation

All important species of SEPs (except for neutrons, which are not considered in this work) are electrically charged, and owing to the ubiquitous presence of plasma carrying electric and magnetic fields in the near-solar and interplanetary space, they constantly experience electromagnetic forces that govern their movement. The most elementary description of a charged particle under such conditions is the Newton-Lorentz equation, which states that the force acting on the particle is

$$\mathbf{F} = \frac{\mathrm{d}\mathbf{p}}{\mathrm{d}t} = q\left(\mathbf{E} + \mathbf{v} \times \mathbf{B}\right), \tag{1}$$

where $\mathbf{p}$, q, and $\mathbf{v}$ are respectively the momentum, electric charge, and velocity of the particle, $\mathbf{E}$ is the ambient electric field, and $\mathbf{B}$ the ambient magnetic field.

If $\mathbf{B}$ is constant (and $\mathbf{E}$ is negligible), the particle will gyrate in a circular orbit around a magnetic field line, with the direction (handedness) of the gyration determined by the sign of the electric charge of the particle. The radius of the gyration (the Larmor radius) is proportional to the component of $\mathbf{v}$ perpendicular to $\mathbf{B}$, $v_\perp$, and inversely proportional to the magnitude of $\mathbf{B}$, while the parallel $\mathbf{v}$ component, $v_\parallel$, moves the particle along the field line. The result is a spiral motion as seen by an

observer at rest with respect to the particle,[1] and it may be characterised by the pitch angle α, defined as

$$\alpha = \arcsin\left(\frac{v_\perp}{v}\right) = \arctan\left(\frac{v_\perp}{v_\parallel}\right). \tag{2}$$

Equations pertaining to particle transport are typically written so that the so-called pitch angle cosine $\mu = \cos\alpha$ is used instead of α.

Another simplified but instructive treatment, essential to understanding the basics of SEP transport, is provided by the Parker model of solar wind (Parker, 1958). It posits that the lines of the solar magnetic field are embedded in the plasma that makes up the solar wind, and they are extended throughout the heliosphere as the plasma streams outward, with one end of the line remaining anchored near the point of origin of the plasma on the solar surface. A notable consequence is that the rotation of the Sun twists the embedded field lines into an Archimedean spiral (assuming constant solar wind speed), known as the Parker spiral in this context. Since Equation 1 suggests that any SEPs ejected from a certain location on the surface of the Sun have a strong tendency to follow the local magnetic field line, the Parker spiral can be thought of as a preferred path for these particles, i.e. they are more likely to be encountered at the points connected by the spiral than elsewhere. This forms the basis for the notion of magnetic connectivity in SEP events, which is commonly measured in terms of angular distance between the Parker spiral rooted at the site of the particle injection and the one passing through the location of the observer: the shorter the distance, the stronger the connection, which generally implies a larger measured event (e.g. Cane et al., 1988; Lario et al., 2013, and others; see also Articles I, II, and III, as well as Figure 2).

In actuality, however, the electric and the magnetic fields in interplanetary space are spatially and temporally variable in both large and small scales. Even if solar wind flowed smoothly at all times, the density of the magnetic field embedded in it would decrease as the plasma moves further away from the Sun and expands to fill an ever larger volume. Given that the kinetic energy of the particle is conserved, solutions to Equation (1) imply that $v_\perp$ must also decrease, causing $v_\parallel$ to increase; this process, called magnetic focussing, plays an important role in giving rise to anisotropies in SEP events (see e.g. Aran et al., 2018, and references therein).

The situation is made far more complex by the fact that turbulence is known to be prevalent in solar wind (e.g. Bruno and Carbone, 2013, and references therein), leading to fluctuations of magnetic and electric fields. The expansion of the ambient plasma and the magnetic field, when combined with scattering off magnetic field disturbances, causes the SEPs guided by the field lines to decelerate adiabatically

1 A thorough discussion of charged particles in electric and magnetic fields and the derivation of key formulae can be found in several textbooks; see for instance Kivelson and Russell (1995).

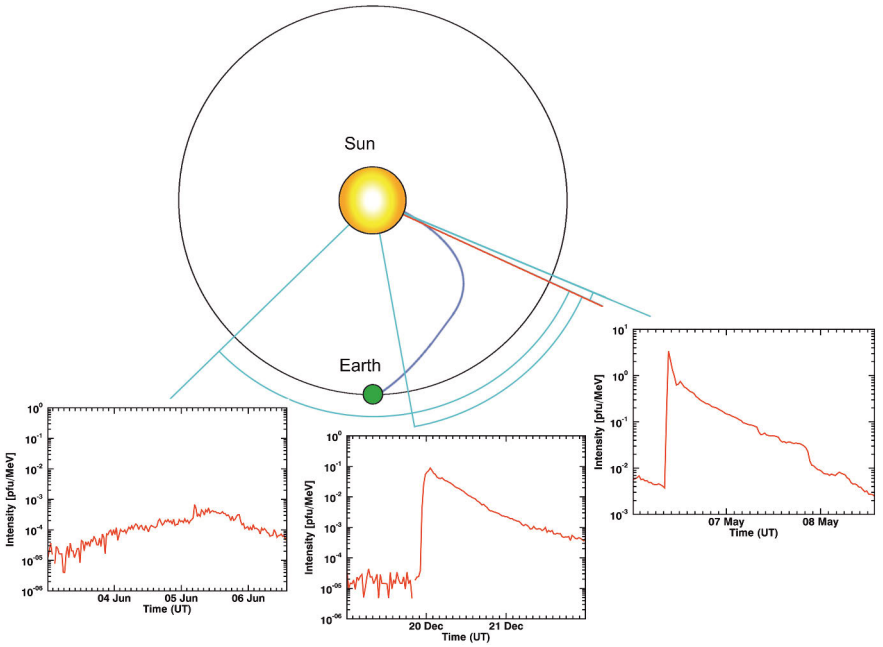

Figure 2. A schematic representation of the effects of magnetic connectivity on SEP event time-intensity profiles. The red line denotes the solar longitude of the footpoint of the Parker spiral (blue curved line) connecting the Earth to the Sun; the cyan lines mark the longitudes of three example events (from the left: 4 June 2000, 19 December 2002, and 6 May 1998), with the cyan arcs denoting their approximate connection angles. The inset graphics show the 21–28 MeV proton intensity detected by SOHO/ERNE before and during the early phase of these events. As can be seen, a small connection angle typically leads to large event maximum intensity and rapid rise (note that the ordinate scale of the rightmost intensity plot extends from 10^{-3} to 10^{1} and that of the others from 10^{-6} to 10^{0} pfu/MeV).

(Parker, 1965; for a more recent treatment, see e.g. Dalla et al., 2015). The magnetic field fluctuations are especially effective in perturbing the pitch angles of any energetic particle population present if its Larmor radii are of the same order as the scale of the fluctuations, and when this process is sufficiently strong, it causes spatial diffusion of the particles along the average magnetic field line (e.g. Dröge, 2000). Under some conditions, changes in the geometry of the interplanetary magnetic field may even cause a substantial proportion of SEPs to reverse direction fully; Bieber et al. (2002) reported that during the massive SEP event of 14 July 2000 (the Bastille Day event), a local magnetic constriction formed by a propagating ICME about 0.3 AU beyond the orbit of the Earth reflected as much as $\approx 85\%$ of the relativistic protons of the event back towards the Earth. For the purposes of modelling, the fluctuating magnetic field is usually treated as the superposition of the unperturbed "mean" field ($\mathbf{B}_0$) and a transient turbulent component. In the simplest case, the latter is considered to manifest as slab turbulence with wave vectors parallel to the mean field lines, that is, the magnitude of the perturbation depends only on the coordinate measured along the length of $\mathbf{B}_0$ (for an in-depth general discussion on the topic, see Shalchi, 2009).

Mechanisms transporting SEPs across magnetic field lines are less thoroughly studied and understood than the parallel transport processes. The former appear to be an important factor in wide-longitude events and must operate fairly efficiently to account for the observed features, although it should be noted that uncertainty about the width of the particle source and injection region itself inevitably complicates any analysis of the net effects of cross-field transport (e.g. Dresing et al., 2012 and Richardson et al., 2014, and references therein). Apart from wide injection region, suggested explanations involve drift and perpendicular diffusion of SEPs. The slab turbulence concept briefly mentioned above is not an adequate approximation in realistic situations since it predicts that there will be no substantial cross-field transport of SEPs and that a particle remains tied to a given field line (Jones et al., 1998; however, see also Shalchi, 2013). Some 80% of solar wind turbulence (measured by energy contained in the fluctuations) is estimated to be transverse to $\mathbf{B}_0$ in the actual solar wind at the Earth, underscoring the need for a more sophisticated model (see Shalchi, 2009 and van den Berg et al., 2020, and references therein).

Several studies (e.g. Zhang et al., 2009; Strauss et al., 2017) show that the explicit inclusion of perpendicular diffusion in the particle transport models allows the simulated SEPs to spread effectively, with the result that any longitudinal fine structure signature from the particle source is largely levelled out. In addition, the observed SEP anisotropy depends on magnetic connectivity so that in wide events, weakly connected observers will measure fewer and weaker anisotropies even when a substantial event occurs at their location. However, these diffusion models tend to have difficulty explaining "dropout" events (Lampa and Kallenrode, 2009), i.e. cases where an impulsive-type event is closely confined to certain magnetic field lines and

there presumably is little perpendicular transport (Mazur et al., 2000).

Adopting a different approach, Laitinen et al. (2016, 2017) considered an ensemble of magnetic field lines that meander randomly as a result of plasma turbulence and simulated an injected group of particles in this environment. They found that under these circumstances, SEPs first follow a given field line and only later gradually diffuse and decouple from it. This model enjoys the advantage that it can account for observed intensity dropouts and it allows for very fast longitudinal spreading of the event during the first few hours after the SEP release occurs at the Sun.

The types of particle drift primarily relevant to cross-field transportation are electric field drift, gradient drift, and curvature drift. Marsh et al. (2013) argued that, somewhat contrary to the then-prevailing notion, gradient and curvature drift in a Parker-style interplanetary magnetic field can produce significant cross-field transportation, especially for high-energy protons and partially ionized heavy ions such as Fe^{15+}. Dalla et al. (2017) have pointed out that these drifts affect and may account for the detected ion charge state-versus-energy spectra for observers with different magnetic connections to the SEP event source. Battarbee et al. (2017, 2018) additionally considered the impact of the drifts caused by the heliospheric current sheet on SEP propagation and found these to be significant and able to affect proton energy spectra for differently located observers. In any case, since magnetic field turbulence is expected to reduce the net effects of drifts (Engelbrecht et al., 2017), as is substantial cross-field diffusion (Wijsen et al., 2019), open questions remain in this area.

1.2 Solar flares

Solar flare is a general term referring to explosive releases of the energy stored in the magnetic fields of the Sun, detected as rapid localised brightenings on the solar disk. They are thought to be triggered when the magnetic geometry of the lower corona changes drastically in a reconnection over a limited area, which leads to effective acceleration of electrically charged particles that become trapped in magnetic loops. The timescale of flares reaches from minutes to tens of minutes, depending on the method of measurement, and they occur at a frequency that varies, along with the overall solar activity, from more than 10 per day to one in several days (e.g. Crosby et al., 1993). The first optical observation of a solar flare is credited to Carrington (1859) and Hodgson (1859), who described an intense transient visual event on the Sun on 1 and 2 September 1859, known today as the Carrington Event.

Flares are closely linked with sunspots and active regions, which typically feature the most intense local perturbations of the Sun's global magnetic field and, consequently, favourable conditions for magnetic reconnection. The reconnection event that causes a flare may lead to expulsion of charged particles at up to relativistic speeds if they reach open field lines (e.g. Reames, 1990), but they usually remain confined in large numbers and are accelerated downward in magnetic loops.

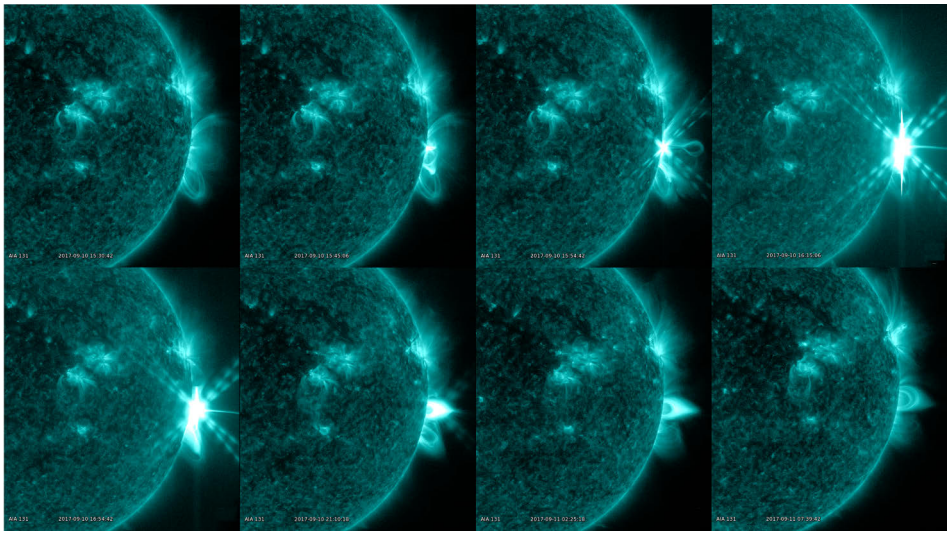

Figure 3. An X8.2-class flare erupting near the western limb of the solar disk on 10 September 2017, as imaged by Solar Dynamics Observatory/Atmospheric Imaging Assembly (SDO/AIA) in ultraviolet light (13.1 nm wavelength). In the last few images (bottom row, right), a gradually dimming large coronal loop can be seen to form and hover above the flare site. (Data courtesy of NASA; image generated with Helioviewer.)

Collisions of accelerated protons and ions in denser layers of the solar atmosphere lead to nuclear reactions and the emission of gamma radiation both as a continuum at energies greater than some 300 keV, and narrow lines from nuclear de-excitation at several MeVs (e.g. Ramaty and Murphy, 1987), as well as the production of energetic neutrons (Hua et al., 2002, and references therein). Electrons are accelerated alongside ions, and they also interact with the surrounding plasma. They are an important contributor to the electromagnetic radiation of the flare, which is emitted over a wide range of spectrum from radio frequencies to hard X-rays ($\gtrsim$ 10 keV, or wavelengths of $\lesssim$ 0.1 nm; e.g. Hudson, 2011, and references therein). Figure 3, featuring a large flare near the western solar limb, demonstrates the great intensity of the ultraviolet radiation output produced during the eruption (compare the relative brightness of the flare and the rest of the solar disk).

The white light and UV signatures of solar flares are commonly used in estimating the coordinates of the source region of an SEP event on the Sun. Since flares can be regarded as another facet of the eruptive processes that also lie at the root of coronal mass ejections and SEP events, an SEP event-associated flare presumably occurs in the vicinity the particle release site. Furthermore, it is possible to infer the time of the particle injection from the X-ray flux of the flare. The so-called Neupert effect (Neupert, 1968; for later developments, see e.g. Dennis and Zarro, 1993; McTiernan et al., 1999; Veronig et al., 2002; Ning and Cao, 2010) refers to the temporal correlation of hard X-ray and microwave intensity on one hand and the time derivative of the

soft X-ray intensity on the other; this is to say, the maxima of the hard X-ray intensity and the soft X-ray intensity time derivative tend to coincide in a fair proportion of all flares. As outlined above, the Neupert effect is regarded as the consequence of flare-accelerated electrons losing their energy through bremsstrahlung upon encountering dense plasma and heating it quickly. If open magnetic field lines exist at the acceleration site, however, some energetic particles are likely to be able to escape into space. Indeed, it has been found that an SEP injection profile derived with the Neupert effect is a reasonably good match for an injection function obtained from observed electron intensities through a full inversion method (Steyn et al., 2020).

1.3 Coronal mass ejections

Coronal mass ejections (CMEs) are expulsions of large clouds of ionized matter from the solar surface. First detected by spaceborne optical instruments in the early 1970s (Tousey, 1973; MacQueen et al., 1974; called at the time ”coronal transients”), they are seen on white-light coronagraphs as bright formations projecting from the solar disk. A number of competing models exist as proposed explanations of the mechanism that gives rise to CMEs (for a review, see e.g. Zhang and Low, 2005), but they are generally understood to be the result of a reconnection in the coronal magnetic field that causes a suspended bubble of plasma to be ejected into the heliosphere. The total mass contained in them is estimated to fall between about 10^8 and 10^{14} kg (Vourlidas et al., 2010), and they may reach speeds ranging from a few tens to over 3000 km/s (Gopalswamy et al., 2010). Due to the CME cloud being composed of electrically charged particles, the field lines of the solar magnetic field remain threaded in it and are carried away as the cloud moves outward. CMEs occur at a rate between once every few days to more than six per day, following the trend of the overall solar activity, and their average speed increases during a solar maximum (Gopalswamy et al., 2009).

CMEs may be categorised by their dynamic behaviour or apparent angular width. Slow CMEs (sometimes called gradual, with speeds of $\lesssim$ 400 km/s) tend to accelerate as they propagate, while fast or impulsive CMEs (speed $\gtrsim$ 400 km/s) occur somewhat lower in the solar corona and conversely have a tendency to decelerate (Sheeley et al., 1999, and others; for a review of later work on this topic, see e.g. Shen et al., 2022). Based on their width (as measured on the viewing plane, with the vertex of the angle at the centre of the solar disk), CMEs are often divided into halo, partial halo, and limb events. ”Halo” refers to CMEs that appear to encompass the entire Sun, and ”limb” to CMEs with a width less than 120°; partial halo CMEs span the gap between these two types (see Figure 4). A greater width implies a more energetic event, and halo CMEs are typically the fastest (usually $>$ 900 km/s) and also involve the largest ejected masses (Gopalswamy, 2010). It should be noted here, however, that since the methods of estimating CME speeds, widths and masses

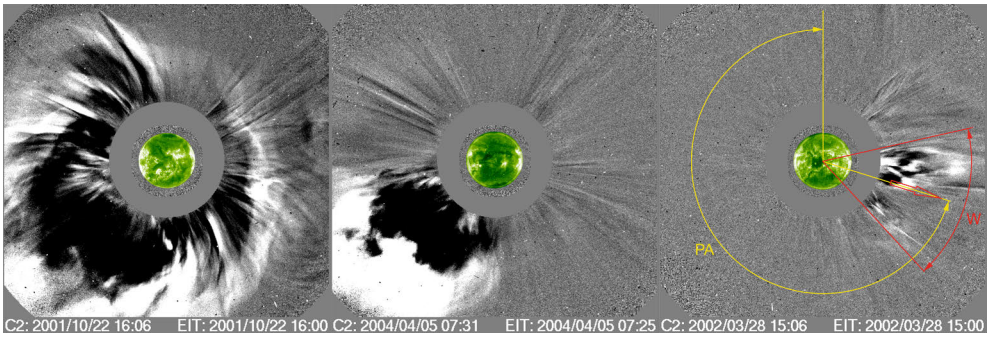

Figure 4. Three different types of CMEs imaged by SOHO/LASCO: from the left, a halo, partial halo, and limb (width $\approx 60°$) mass ejection. Inset in the middle of each panel is the solar disk in ultraviolet light (19.5 nm wavelength), imaged concurrently with the CME observations by SOHO/EIT; the eruption related to the CME can be seen as a brightening slightly to the left and down of the disk centre (the left panel), towards the left-hand edge of the disk (the middle panel), and towards the right-hand edge (the right panel). The rightmost panel additionally demonstrates the definitions used in the CDAW SOHO LASCO Catalog for CME position angle (PA, in yellow) and width (W, in red). (Data courtesy of ESA and NASA; images from the CDAW SOHO LASCO Catalog and Helioviewer.)

are indirect and vary between catalogues and authors (Lamy et al., 2019), the limits given above for these quantities should be regarded as informative but approximate and somewhat flexible.

According to observations, CMEs are typically associated with prominences and flares, as well as EUV waves (Thompson et al., 1998) and radio bursts (see the discussion in Chapter 1.4 and references therein). Since especially the faster CMEs exceed the local speed of sound in the corona and solar wind and thus cause a shock to form as they propagate, they are also considered to play an important part in SEP acceleration (e.g. Reames, 1999; see also Chapter 1.1.1).

However, the exact relationship between flares and CMEs remains disputed. Although large flares and CMEs often co-occur and their evolution seems synchronised—for instance, a phase of fast CME acceleration often coincides with the rising stage of the soft X-ray intensity from the associated flare (Zhang et al., 2001; Vršnak et al., 2004), as do the maxima of CME acceleration and the flare hard X-ray emission (Temmer et al., 2008)—not all flares are accompanied by a CME.

After a CME reaches interplanetary space, it is often referred to as an interplanetary coronal mass ejection (ICME). ICMEs interact with the solar wind and the interplanetary magnetic field, with the result that their speed tends to harmonize with that of the solar wind (i.e. fast ICMEs decelerate and slow ones accelerate towards the solar wind speed). Nevertheless, ICMEs and the shocks driven by them can travel to the outer reaches of the solar system. In the process, they continue to accelerate electrically charged particles, cause magnetic storms when they encounter planetary magnetospheres, and temporarily deflect galactic cosmic rays (the so-called Forbush

decrease; after Forbush, 1937, 1946) so that these arrive at observers within the space traversed by the ICME less efficiently than usual (e.g. Gopalswamy, 2010, and references therein; see also Belov et al., 2014 and Papaioannou et al., 2020).

1.4 Solar radio emissions

In addition to other electromagnetic radiation, the Sun emits vast amounts of energy at radio frequencies ranging from tens of kHz (kilometric waves) to hundreds of GHz (microwaves). This radiation comes from both thermal (thermal bremsstrahlung and gyromagnetic emission) and non-thermal (plasma emission, electron-cyclotron maser emission) mechanisms occurring in the hot plasma in the solar atmosphere, with the thermal processes largely responsible for the quiet-time radio emission. The non-thermal processes, in contrast, play an important role in the so-called radio bursts and storms (for an overview, see e.g. Dulk, 1985). Solar radio emissions were first detected during World War II (Reber, 1944; Hey, 1946); since then, the development of aviation and spaceflight technology has made observation possible at long wavelengths (greater than a few tens of metres, i.e. less than a few tens of MHz) of electromagnetic radiation that are absorbed or reflected by the terrestrial atmosphere.

Solar radio bursts are defined as sudden transient increases in the emitted radio energy at certain frequency ranges, often starting at higher and gradually drifting to lower frequencies. Primarily originating from the oscillation of the excited electrons through the plasma emission mechanism, they are closely associated with active regions and flares and also with CMEs, the frequency decrease generally indicating the propagation of a local disturbance from lower to higher altitudes (with a corresponding decrease in the electron density) in the solar corona. These bursts are generally divided into five distinct main types, numbered I to V, on the basis of their appearance on a dynamic spectrum chart (Wild et al., 1963).

Type I bursts are spike-like features that last from a few tenths of a second to some two seconds and occur over a narrow metric frequency range, in the most common case without displaying any substantial frequency drift (Elgarøy, 1977). When occurring as groups known as noise storms, they are associated with active regions and are thought to arise from processes involving magnetic reconnection (Gergely and Erickson, 1975). Type II comprises radio events that, in a time scale of minutes to a few tens of minutes, decrease slowly in frequency from a few hundred MHz; these result from the excitation of electrons by a propagating magnetohydrodynamic shock front, such as the leading edge of a CME (e.g. Cairns et al., 2003). Somewhat similar to these but falling much more rapidly in frequency and more short-lived (up to about 10 seconds for single bursts and some one minute when occurring in groups) are type III bursts, which also appear associated with active regions and are thought to be generated when near-relativistic electron beams resulting from magnetic reconnection induce plasma emission (e.g. Reid and Ratcliffe, 2014). Type IV

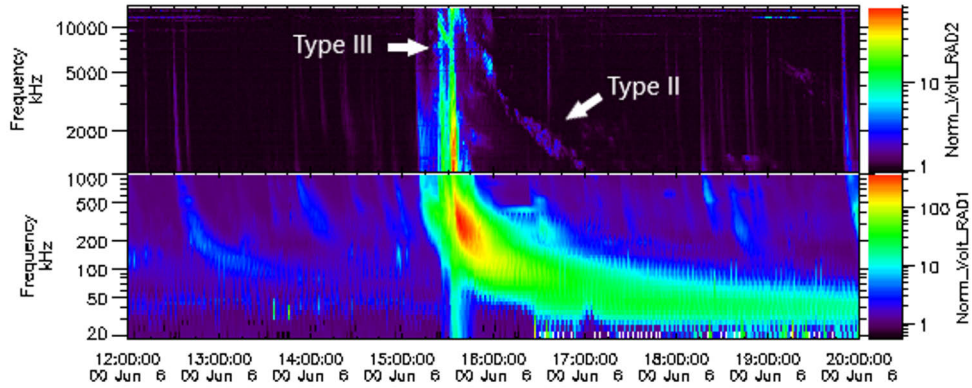

Figure 5. Composite dynamic spectrogram of solar radio flux as recorded by the Wind/WAVES instrument during the high-energy SEP event of 6 June 2000. The type II and type III burst activity commencing shortly before 15:30 UT is related to the particle injection. The vertical, sharply defined features represent type III burst(s); the gently descending, somewhat less conspicuous feature to their right is the type II burst. (Data courtesy of NASA; image generated by CDAW.)

bursts are considered to result from electrons trapped inside magnetic structures, and they manifest as broadband emissions between some 1 GHz and a few tens of MHz, lasting from a few minutes to a few hours. In the metric wavelength range, these include two main subtypes, stationary and moving (Weiss, 1963); the former is associated with type I bursts or flares, while the latter often follow on after type II bursts and are in these cases typically related to outward-moving CMEs (e.g. Hillaris et al., 2016). Lastly, type V refers to diffuse broadband radio events that occasionally succeed type III bursts at frequencies under $\approx$ 200 MHz and last not more than a few minutes. Type V bursts stem from similar phenomena as type III bursts, and they are usually attributed to plasma emission or possibly electron-cyclotron maser emission (e.g. Tang et al., 2013). A dynamic spectrogram featuring type II and III bursts is presented as Figure 5.

From the viewpoint of SEP event identification, the most immediately relevant radio bursts are types II and III because these may indicate a moving shock front (an effective accelerator of particles) and open magnetic field lines in the solar corona, respectively. As found by us and others (Articles I and II; see also e.g. Cane et al., 2002), high-energy SEP events are virtually always associated with CMEs and X-ray flares, and the presence of open field lines suggests that SEPs are possibly being released from the solar corona and injected into interplanetary space. Temporally coincident type III radio burst, large X-ray flare, and the early expansion of a CME are thus a potential precursor to an SEP event at 1 AU, and together these can provide evidence for association with one another, as well as a convenient if approximate measure for the time of departure of the particles from the Sun.

2 Space weather and solar variability

2.1 Space weather

The term space weather refers to the variable physical conditions existing in the heliosphere at a given time, often with a decided focus on the near-Earth space. It encompasses phenomena related to and caused by electromagnetic radiation from the Sun, terrestrial and interplanetary electromagnetic fields and their interaction, space radiation, and solar wind plasma. Some of the most widely known manifestations of these are aurorae and geomagnetic storms; an apparent correlation between the two was discovered as early as 1806 by Alexander von Humboldt (Lakhina et al., 2007), and observations of co-occurring auroral displays and major magnetic disturbances were made on several occasions over the rest of the century, among them the Carrington event of 1859 and a large geomagnetic storm in November 1882 (see e.g. Tsurutani et al., 2003, and references therein). Later, Maunder (1904) explicitly linked magnetic storms with sunspots. ”Space weather” as an expression in its current meaning came to use in the late 1950s, by which time the effects mentioned above were known to be the result of the activity in the Sun, and it was popularised in the 1990s along with the increasing awareness of the possible dangers posed by solar eruptions to human activity (see Cade III and Chan-Park, 2015 for discussion). The study of space weather builds on heliophysics, space physics, and geophysics, with all of these disciplines contributing to the general understanding of the Sun–Earth relationship.

The facets of space weather primarily considered in this work are SEPs, solar flares, and CMEs. As mentioned in Chapters 1.1, 1.2, and 1.3, the common mechanism ultimately responsible for powering them is magnetic reconnection in the lower corona and upper chromosphere, which can rapidly convert very large amounts of magnetic potential energy into kinetic energy.

Even when no CME or substantial SEP release occurs in conjunction with flares (so-called confined flares; e.g. Schmahl et al., 1990; Green et al., 2002), their electromagnetic radiation and X-ray emission in particular may be intense enough to cause changes in the electron density profile of the ionosphere of the Earth (the solar flare effect; e.g. Nagata, 1966) that potentially disturb radio communications, as well as to pose a lethal radiation hazard to an unprotected human being outside the atmosphere (e.g. Smith and Scalo, 2007). For SEP events falling into the traditional ”impulsive”

category, flares have been identified as an important source and site of energetic particle acceleration (Chapter 1.1.1 and references therein). Through the generation of shock waves in the solar corona that accelerate charged particles, CMEs contribute in a substantial fashion to the increased particle intensities during SEP events, especially for those cases that have typical ”gradual” characteristics. The most energetic protons released and accelerated in SEP events traverse the distance between the Sun and the Earth within 10 minutes, but the shock acceleration may continue in interplanetary space (when an event-related CME has become an ICME; see Chapter 1.3) and produce elevated SEP fluxes that last for several days. When an ICME comes in contact with the magnetosphere of the Earth, the interaction between the magnetic field embedded in the ICME and the terrestrial field may give rise to a geomagnetic storm that can be particularly severe if the ICME field has a strong southward component (Gosling et al., 1991; Landi et al., 1998; Webb et al., 2000; Cane et al., 2000).

Ionising particles are present in significant numbers in the upper atmosphere (especially at high magnetic latitudes), in space near the Earth, and beyond. At altitudes less than a few tens of thousands of kilometres, the populations constituting the particle environment are SEPs, galactic cosmic rays, and magnetically trapped particles, mainly protons and electrons, circling the Earth in the Van Allen belts (e.g. Vainio et al., 2009). The most energetic of the former two groups of particles can penetrate into the atmosphere, where they contribute to the radiation dose received by aircrews and airline passengers, mainly through causing a cascade reaction upon interacting with the ambient matter (e.g. Mishev, 2014; Tobiska et al., 2015).

Prolonged or intense exposure to ionising particles leads to a variety of deleterious effects on both biological organisms and technology. In the case of living beings, the harm caused by radiation can in general be divided into two categories, chronic (or stochastic) and acute (or deterministic). The former of these refers to long-term effects, which typically include different types of cancer in humans (Jones et al., 2010), and the latter to results of large and often rapidly sustained doses, known as acute radiation syndrome. Absorbed doses larger than a few tenths of a gray, received over a brief period of time, disturb the functioning of the human bone marrow, the gastrointestinal system, and the neurovascular system (in this order, corresponding to increasing dose). The syndrome manifests early on as nausea, vomiting, and a number of nonspecific symptoms such as fatigue, headaches, and skin erythema; depending on the severity of the case, diarrhoea, dizziness, loss of consciousness, sepsis, and eventually death may follow (Donnelly et al., 2010).

A somewhat comparable situation exists with respect to electronic devices in that they may be damaged and degraded over time, as the received radiation dose accumulates, or suddenly in single hit events. Incident particles may displace atoms within the lattices that make up the material of components of a semiconductor device, causing noise and malfunctions after sufficient damage has occurred (e.g. Marshall et al., 1991), or deposit an electric charge in dielectric materials that can lead to electric

interference and destructive discharges (Frederickson, 1996). On the other hand, a single passing particle might fortuitously strike a critical location (McNulty, 1996), such as a computer central processing unit or a memory bank, and cause either lasting physical damage (a ”hard” error, e.g. the destruction of a transistor; Sexton, 2003) or a transient software disturbance (a ”soft” error, e.g. a change in the value of a variable stored in memory; Dodd and Massengill, 2003). Several spacecraft malfunction incidents and even outright losses of unmanned spacecraft have been attributed to system failures resulting from exposure to ionising radiation. An example of a total loss is the geosynchronous communication satellite Telstar 401, which failed in 1997 during a magnetic storm that changed the geometry of the electron radiation belts around the Earth and exposed the spacecraft to unusually intense > 2 MeV electron flux (Reeves et al., 1998).

Space weather affects activities on ground level as well. During an intense geomagnetic storm, the changes in the magnetic field of the Earth may lead to induced currents occurring in large conductors, such as power and telephone lines, and structures made of conducting materials, such as oil pipelines (see Boteler, 2000, and references therein). In a well-known incident, considerable damage to the electric network and an extensive power outage took place in Quebec, Canada, on 13 March 1989 after a magnetic storm that resulted from two fast ICMEs colliding with the magnetosphere of the Earth in quick succession (e.g. Boteler, 2019; Love et al., 2022). In addition, and aside from the solar flare effect mentioned above, radio transmissions used in communication and radar systems may be directly disturbed by the radio noise and radio bursts of the Sun (Lanzerotti, 2005, and references therein).

Analogously to the usage of the term in terrestrial meteorology, the long-term and large-scale state of and changes in space weather are collectively called space climate. More recent as a scientific concept than space weather, the study of space climate is concerned with periods extending from a few solar rotations (i.e. a multiple of about 27 days) to several millennia. Among its central aims are understanding solar variability over these spans of time, with a special view to explaining observed extreme conditions and identifying any recurring patterns, and the development and refinement of exploitation of proxy data (such as cosmogenic isotopes; e.g. Beer et al., 2006). For an introductory discussion on the topic, see Mursula et al. (2007).

2.1.1 SEP event forecasting

In view of the risks stemming from solar activity, summarized above, there is understandably a decided worldwide interest in and need for developing techniques and tools for predicting space weather. A very brief, non-exhaustive overview of some of the efforts that pertain to SEP event forecasting is presented in the following. (For a more general and somewhat more comprehensive discussion on the topic, see e.g. Temmer, 2021 and Whitman et al., 2022.)

Even though our knowledge regarding the state of the Sun and interplanetary space at any point in time is necessarily quite limited because of the scarcity of measuring instruments and locations available in practice, the developments in flare and CME modelling have nevertheless made SEP event warnings with a lead time of a few hours a reasonable prospect. Following Anastasiadis et al. (2019), the existing forecasting methods and systems with this kind of capability may be characterised as empirical (or semi-empirical), physics-based, or other.

Notable examples of the empirical category are the PROTONS algorithm (Balch, 1999), in use with the NOAA Space Environment Center, and the Proton Prediction System (PPS; Smart and Shea, 1989). Drawing on information about a solar flare that may potentially be followed by an SEP event (as well as associated radio bursts in the case of the former), these systems provide predictions of event occurrence, together with either the estimated maximum proton intensity at $E > 10$ MeV (PROTONS) or a SEP time-intensity profile at multiple, selectable energy ranges (PPS). Since they were originally developed before the importance of CMEs as drivers of SEP events was fully appreciated, neither of them incorporates CME data; in contrast, the Coronal Mass Ejections and Solar Energetic Particles (COMESEP) SEP forecast tool[1] makes automated use of both flare and CME information to arrive at an SEP forecast and to generate warnings as necessary. Yet another ”nowcasting” (very near-term) concept, Relativistic Electron Alert System for Exploration (RELEASE), exploits the fact that the intensity of high-energy SEP electrons, travelling almost at the speed of light, often increases as a precursor to the corresponding SEP proton enhancement (Posner, 2007).

Physics-based SEP prediction assets attack the forecasting problem through (simplified) mathematical modelling of SEP acceleration and transport, including interplanetary shocks due to ICMEs. For instance, the Solar Particle Engineering Code (SOLPENCO; Aran et al., 2006), an operational tool designed for proton intensity prediction, is built around several hundred pre-calculated, simulated proton time-intensity profiles at 1 AU and 0.4 AU and multiple energy channels; each of the profiles corresponds to a certain set of prevailing conditions (e.g. the solar longitude of the event-related flare and the mean free path of 0.5 MeV protons). The Earth-Moon-Mars Radiation Environment Module (EMMREM; Schwadron et al., 2010) is oriented towards estimating the time-dependent radiation exposure in the vicinity of the celestial bodies in question, as well as in interplanetary space. To this end, it includes a component for modelling SEP propagation in the inner heliosphere and another for target penetration by incident energetic protons and the secondary products (such as alpha particles) resulting from the interaction of the primary protons with the target material. Efforts that model SEP particle populations against the

1 https://www.comesep.eu/

backdrop of a simulated interplanetary magnetohydrodynamic (MHD) environment include SEPMOD (a combination of the heliospheric simulation with the ENLIL software, the Wang-Sheeley-Arge solar wind model, and a cone model for CMEs; see, respectively, Odstrcil et al., 2004; Arge et al., 2004; and Luhmann et al., 2017) and the Particle Radiation Asset Directed at Interplanetary Space Exploration (PARADISE; Wijsen et al., 2019). The latter is an SEP propagation code module coupled with the three-dimensional MHD simulation provided by the European Heliospheric Forecasting Information Asset (EUHFORIA; Pomoell and Poedts, 2018).

A number of recent studies and projects falling under the ”other” label seek to utilize techniques such as automatic detection through machine learning or high-order statistical relations. An example of the former is the Space Radiation Intelligence System framework (SPRINTS; Engell et al., 2017), which features a machine-learned decision tree model relying primarily on the X-ray fluence, heliolongitude, and decay phase duration of solar flares to generate an SEP event forecast. Representing the latter avenue, Papaioannou et al. (2018) performed a study where principal component analysis is applied to six flare and CME variables in order to produce a numerical index representing the probability of SEP event occurrence in the near term. A Bayesian statistical approach forms the basis of the Probabilistic Solar Particle Event foRecasting (PROSPER; Papaioannou et al., 2022) model, which was incorporated as the core of the Advanced Solar Particle Event Casting System (ASPECS),[2] a forecasting and nowcasting tool operational online since 2021 as part of the SEP Advanced Warning System (SAWS) of ESA.

Long-term forecasting of individual SEP events is not possible at present, and may in fact be essentially impossible even in theory (Xapsos et al., 2006). To address this problem, several statistical models based on previously observed data have been developed. Their aim is to determine the greatest peak SEP intensity or the total fluence that will not, at a given level of confidence, be exceeded during a given length of time. The first such widely used model was constructed by King (1974), who based his work on an extension of Poisson statistics by Burrell (1972) and considered proton data recorded by the Interplanetary Monitoring Platform (IMP) series of satellites during solar cycle 20. Relying on a generally similar approach but extending the data coverage to include solar cycles 19–21 to improve the statistical basis, Feynman et al. (1990, 1993) developed the more advanced Jet Propulsion Laboratory (JPL) model and its revised 1991 version. Since then, Rosenqvist et al. (2005) have further refined the values of the parameters used in the JPL model.

Using the maximum entropy theory (e.g. Jaynes, 1957) as a starting point, Xapsos et al. (1998, 1999, 2000) constructed the Emission of Solar Protons (ESP) model, which is designed to estimate the highest peak intensity, fluence, and the cumulative

2 http://phobos-srv.space.noa.gr/

fluence. Later work employing related methodologies include the proton peak intensity and fluence model (Jiggens et al., 2012) incorporated in the Solar Energetic Particle Environment Modelling (SEPEM) project of the European Space Agency, and the Solar Accumulated and Peak Proton and Heavy Ion Radiation Environment (SAPPHIRE; Jiggens et al., 2018). A fundamentally different approach based on modelling the physical energy spectrum and overall size of the SEP event has been used to construct the Moscow State University (MSU) models (Nymmik, 1998, 1999, 2007). In these, the event frequency is considered to be dependent on the sunspot number, and heavy ion intensities and fluences are included by utilizing an averaged relation (based on the studies of Mazur et al., 1992 and Mazur et al., 1993) between proton and heavy ion spectra.

Recently, Raukunen et al. (2018) introduced two proton fluence models, both based on proton fluence spectra recorded during ground level enhancement events. One of these employed on a JPL-type approach (calculating time-integrated integral fluences from function fits to fluence spectra and then modelling their distributions with exponentially cut off power law functions) and the other on an MSU-type approach (modelling the spectral parameters as normally distributed variables). The results were found to be generally in good agreement with those given by the JPL, ESP, and SEPEM models. This work was later complemented with a proton peak intensity model for very high particle energies (Raukunen et al., 2020). Other noteworthy developments within the last few years include the Virtual Enhancements – Solar Proton Event Radiation model (VESPER; Aminalragia-Giamini et al., 2018), which creates a virtual time series of differential proton intensity based on observed data. Its primary advantages are independence of the particle energy range of interest and the lack of the need for a priori assumptions about the spectral shape of SEP events.

2.2 Solar variability

The magnetic field of the Sun is thought to be generated through a dynamo process, similarly in principle to the planetary fields in the Solar System. Although some of the details of this process are not clear and remain debated, it is understood that the field probably arises in the interior of the Sun as the star rotates, and becomes self-sustaining due to the turbulent motion of the electrically conducting plasma. In addition to the massive convective flows powered by the nuclear reactions in the core, the Sun exhibits pronounced differential rotation (i.e. it revolves at a higher angular velocity at the equatorial than the polar latitudes) on its surface and in the convective zone that makes up approximately the outer 30% of the diameter of the Sun, but likely not in the deeper layers. This introduces shearing forces within the convective zone and especially at its base (Schou et al., 1998, and references therein).

A characteristic feature of the global solar magnetic field, as represented in the

so-called $\alpha\Omega$ model (see Babcock, 1961 for an early and simplified formulation), is the interplay between its poloidal and toroidal components: At solar minimum, the field is initially almost purely poloidal, but the differential rotation causes its lines to be wound horizontally and continually enhances the toroidal component until it reaches its maximum close to sunspot maximum. During this stage, the overall geometry of the field becomes increasingly complex, giving rise to a wealth of local details and limited areas of high magnetic intensity. There then follows a declining phase of the sunspot cycle where the global field is reorganised and the poloidal component is restored from the toroidal component (to opposite polarity compared to the previous solar minimum) and the process begins again. While they are simplifications, models of this sort provide an explanation for the cyclic nature of solar activity and the appearance of sunspots, which are manifestations of intense vertical magnetic fields—corresponding to the aforementioned toroidal component of the global field—on the surface of the Sun. For an introduction to and review on solar dynamo models, see e.g. Ossendrijver (2003) and Charbonneau (2010).

Sightings of sunspots have been recorded since antiquity (Clark and Stephenson, 1978), and it had also been noted that sunspots vary in number and size. Even though the idea that this variation could be periodic had been proposed earlier, the identification and definition of the basic 11-year solar activity cycle is credited to Samuel Heinrich Schwabe (1844), who found out that the average sunspot number increases and then decreases more or less regularly over time. Now commonly known as the Schwabe cycles, they are numbered sequentially so that cycle 1 began in 1755 and cycle 25 in December 2019; this scheme was originally laid out by Wolf (1852) and remains in use.

In the early 20th Century, Hale (1908) showed sunspots to have intense magnetic fields, which later led to the discovery of a rule known as Hale's law (Hale et al., 1919) governing the polarities of the sunspot fields. Hale's law postulates that the magnetic polarity of the spot leading a group in a given solar hemisphere is constant during each cycle, with the corresponding leading spot in the other hemisphere having the opposite polarity, but that these polarities are reversed when the next cycle begins (Figure 6). Two consecutive Schwabe cycles thus form a 22-year (Hale) cycle, after which the global magnetic configuration of the Sun returns approximately to its initial state. However, the Schwabe subcycles of a given Hale cycle are usually not identical but the average sunspot number of an odd-numbered cycle tends to be greater than that of the preceding even-numbered cycle (the Gnevyshev–Ohl rule, as cited in e.g. Hathaway, 2015). The reason for this asymmetry is currently not well understood.

Lengthy periods with very large or small numbers of sunspots, called grand maxima and minima, have been identified in the historical record and proxy data (Usoskin, 2017, and references therein). Perhaps the best-known example is the Maunder Minimum that occurred between about 1645 and 1715; sunspots are in-

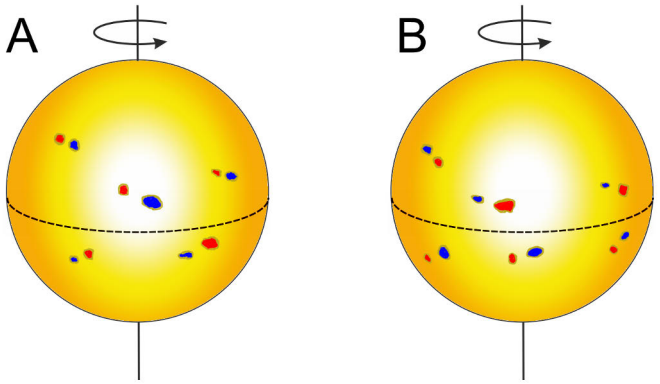

Figure 6. A diagram demonstrating Hale's law; the red and blue colours represent different magnetic polarities (north or south) in the sunspot pairs. During one 11-year solar cycle (A), the leading spot of a sunspot group in one hemisphere typically exhibits a certain polarity, and the opposite polarity in the other hemisphere. In the next cycle (B), the situation is reversed in both hemispheres.

ferred to have been all but completely absent during these years (Spörer, 1889; Spörer and Maunder, 1890), and this situation may have contributed to a prolonged trend of unusually cold temperatures particularly in the North Atlantic region (the "Little Ice Age"; e.g. Owens et al., 2017). Furthermore, several studies (e.g. Rigozo et al., 2001; Usoskin et al., 2003; Solanki et al., 2004) propose a so-called Modern Maximum that may have begun in the early 1900s and ended with solar cycle 23 in 2008 at the latest.

Other, longer cyclical patterns of solar activity have been postulated in addition to the Schwabe and Hale cycles. Examples of these are the Gleissberg cycle of 70–100 years (7 or 8 Schwabe cycles; Gleissberg, 1939), the Suess cycle (also known as de Vries cycle) of some 210 years (Suess, 1980), and the Hallstatt cycle of approximately 2400 years (Sonett, 1984; for later work on the topic, see e.g. Vasiliev and Dergachev, 2002 and Usoskin et al., 2016). On the other hand, several studies (e.g. Feynman and Gabriel, 1990; Rozelot, 1995; Greenkorn, 2009) have suggested that the dynamo process in the Sun is largely chaotic in nature, which might imply that the apparent long-duration cycles are tendencies rather than fully regular and predictable features.

The most widely used measure of solar variability is the International Sunspot Number (SSN), also known as Wolf's Sunspot Number or Zürich Sunspot Number, due in large part to the available record reaching several hundred years into the past (when reconstructed observations are included). It is calculated for each day as the sum of observed sunspot groups, multiplied by 10, and the number of individual sunspots, with an additional correction factor included to account for differences

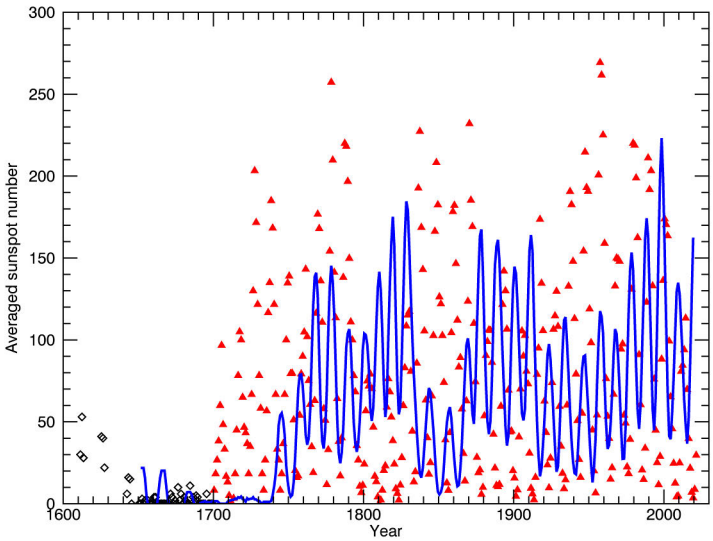

Figure 7. Annual average sunspot numbers (SSN) and their 5-year sliding average (the blue curve) since 1610. Data from 1610 to 1699 (black hollow diamonds) are estimated by Eddy (1976); later data (red filled triangles) courtesy of World Data Centre for the Sunspot Index and Long-term Solar Observations, Royal Observatory of Belgium, Brussels. The Maunder Minimum can be clearly seen in the lower left-hand corner of the plot (although it should be noted that data coverage is sparse in this period), and the Modern Maximum comprises the generally somewhat elevated sunspot numbers appearing throughout the 20th Century.

between observers. For the purposes of determining solar maxima, minima, and the changing of a Schwabe cycle, the daily sunspot numbers are often smoothed with a 13-month running mean centred on the month of interest. Alternative methods of gauging and reporting sunspot prevalence include the Boulder Sunspot Number, the American Sunspot Number, Group Sunspot Number (Hoyt and Schatten, 1998a,b), and total sunspot area calculation. The annually averaged SSN for the years between 1610 and 2021, together with a 5-year sliding average of this number, is shown in Figure 7.

Apart from sunspot observations, solar variability is commonly characterised with two quantities, 10.7 cm Solar Flux and the Total Solar Irradiance (TSI). The former refers to the radio flux density integrated over the area of the solar disc at the wavelength of 10.7 cm (Tapping, 2013), and the latter to the radiative energy per unit area arriving at 1 AU from the Sun, as integrated over the entire electromagnetic spectrum (the so-called solar constant; see Fröhlich, 2012 for an overview). Their principal advantage over sunspot numbers is that they are more objective and, given the availability of spaceborne instruments in the case of TSI, immune to problems

resulting from the terrestrial weather such as heavy cloud cover. While they in general correlate well with SSN, the relationship is not quite linear for the 10.7 cm Solar Flux (Tapping and Morgan, 2017) that also tends to lag behind changes in the SSN; both additionally exhibit disagreement in details. Furthermore, the absolute accuracies of the instruments used to derive quantities approximating the TSI vary, which has led to various methods of calculating a numerical estimate for the solar constant, and some controversy (e.g. Hathaway, 2015, and references therein).

Solar eruptions (flares, CMEs, and SEP events; see above) are thought to originate from foci of magnetic activity known as active regions (e.g. Toriumi and Wang, 2019), which, when sufficiently large and dynamic, are typically marked with concentrations of sunspots. It is therefore unsurprising that the frequency and the intensity of solar eruptions are correlated with the overall level of solar activity (see Chapter 1 and references therein); however, significant eruptions that involve SEP events can and do occur during the ”quiet Sun” periods as well (e.g. Shea and Smart, 1990; see also Article I).

3 Statistical studies of SEP events

Due to the great diversity of solar energetic particle events, the complicated and intertwined nature of the physical processes that cause them, and the difficulties stemming from the fact that the observational coverage of any single event is necessarily limited to a few (mostly near-Earth) locations, researchers frequently resort to statistical approaches to study SEP events as a class. This involves collecting observations from a period of time that typically spans several years, often entire solar cycles, and attempting to discern and interpret correlations and dependencies in the data. Combined with the existing theoretical knowledge and numerical modelling, such discoveries are potentially valuable because they can provide information about the mechanisms behind SEP release, acceleration, and transport, as well as pointing out areas where further research is needed.

In practical terms, statistical studies typically investigate and report such SEP-related quantities as the onset time, maximum intensity, and fluence of the events of interest for a given particle species and energy range. These are compared against other phenomena associated with the event—active regions, X-ray and white light flares, magnetic field data, radio bursts, and CMEs—to determine the probable location, time, and other relevant conditions of SEP release. In many cases, data concerning solar wind and interplanetary magnetic fields are included since they reflect the situation with respect to particle transport (e.g. the approximate shape of the interplanetary magnetic field and the presence and passage of ICME-induced shocks) from the Sun to the observer.

A brief, non-exhaustive summary of relatively recent research into SEP events from the statistical perspective is presented in this chapter. In accordance with Articles I to III, it is mainly limited to studies that feature energetic ($E \gtrsim 10$ MeV) protons or near-relativistic and relativistic ($E \gtrsim 50$ keV) electrons, and includes studies (similar to Article II) based on observations from multiple vantage points.

3.1 SEP event lists and catalogues

In their influential work, Cane et al. (2010) gave a listing of 280 proton events at energies of > 25 MeV from 1997–2006, complete with radio, flare, and CME associations, interplanetary shocks at 1 AU, and electron/proton and some heavier ion abundances. Data from SOHO/Energetic and Relativistic Nuclei and Electron exper-

iment (ERNE; Torsti et al., 1995) and IMP 8, as well as from Wind, were utilised, and the authors performed an in-depth statistical study of the observed quantities. The most important result was confirmation for the observation that no clear differentiation between ”impulsive” and ”gradual” SEP events exists; furthermore, it was found that all of the studied events were associated with a CME, SEP event size was positively correlated with flare intensity and CME speed and width, and that virtually all events were associated with type III radio bursts. This led the authors to propose a model where in large SEP events, particle acceleration processes related to flares are an important contribution to the acceleration in the interplanetary shock.

Vainio et al. (2013) presented a catalogue[1] of SOHO/ERNE 55–80 MeV proton events from 1996 to 2010, together with the related electron events (at 0.18–0.31 MeV and 0.7–3.0 MeV), yielding 115 cases in total. Velocity dispersion analysis (VDA; see Chapter 5.3) and time-shifting analysis (TSA; Chapter 5.2) were performed for protons and TSA for electrons to estimate the SEP release times, and solar phenomenon associations were determined. The VDA results were mostly regarded as reasonable, with the majority of cases indicating an effective path length between 1 and 3 AU, but the path length would occasionally fall outside these realistic boundaries, implying that the basic assumptions of VDA (simultaneous release and the same path length for particles at all energies) are mostly but not strictly correct. If large apparent path length values are ascribed primarily to particle scattering, the mean ratio of spiral field line length divided by VDA path length of 0.54 for the proton events suggests a proton scattering mean free path shorter than 1 AU, given that even the first protons to arrive travel about twice this distance before they reach the near-Earth observer. According to the TSA results, high-energy electrons are released on average a few minutes later than low-energy electrons. The time difference between the onset of the event-related flare and the electron release was noted to be the shortest for the best-connected events, with a linear fit yielding an estimate of 600 km/s for the expansion of the particle source region. Decametric-hectometric type III emission and proton release coincided for events with a realistic VDA result, lending support to the idea that there is a connection between the aforementioned longitudinal expansion and proton and electron release as well.

Making use of the event listing provided in Vainio et al. (2013), Kouloumvakos et al. (2015) additionally considered Wind electron data at energies of 20–646 keV, performed VDA on proton as well as electron data, and then compared the estimated proton release times against type II, III, and IV radio burst activity. Electron release times were estimated using type III bursts as proxies, and proton energy spectra and peak intensities were examined. The majority of events appeared to feature electron release prior or simultaneously to proton release, and the VDA-indicated path

1 This is part of the SEPServer project of ESA and available online at `http://server.sepserver.eu/`.

lengths were typically greater for protons than for electrons. Hardening of spectrum was noted in proton events that include type II but not type III radio burst association. The results generally confirmed that flare- and CME-accelerated events are not two fully distinct categories but overlap, and the contributions of flares and CMEs to SEP acceleration are not straightforward to disentangle. The SOHO/ERNE proton event catalogue and the statistical study performed by Vainio et al. (2013) were updated with an additional 61 events from 2011–2016 in Article I. Another conceptually and methodologically related study was undertaken by Biji and Prince (2022), who only considered SOHO/ERNE proton events from solar cycle 24 (2008–2019) and focussed on correlations between various observed and estimated quantities, such as CME and proton release times and CME speed and proton peak intensity. They came to the conclusion that CME association and acceleration apparently dominate for low-to-mid-energy particles, while flare association dominates for high-energy particles (see also Chapter 3.2).

Drawing on the Solar Energetic Particle Environment Modeling Refererence dataset (SEPEM RDS), Papaioannou et al. (2016) compiled a catalogue of 314 proton events observed by the GOES satellites (at $E > 10$, 30, 60, and 100 MeV) from 1984 to 2013. For the events after 1997 (174 cases), the associated near-relativistic electron components (with data from Advanced Composition Explorer, ACE) were included; flare, CME, and radio burst associations were determined, as were Fe/O abundances. The flare–CME associations were arrived at by estimating the CME liftoff time via extrapolation from observed visual data and requiring that the flare location is within the position angle covered by the CME, with VDA used to yield an estimate for the particle release time. Almost all post-1997 events included a significant electron signature, 83% a recognizable type III radio burst, 73% both a type II and type III burst, and 35% a type IV burst. It was confirmed that neither the Fe/O ratio nor the radio bursts can be used to divide the SEP events into clear-cut categories as per the classical picture. High proton peak intensities typically occurred in events that involve large flares and fast, wide CMEs, and they may originate from a wide range of solar longitudes (although those from near the centre of the visible disk of the Sun usually posed the most significant radiation hazard). In quantitative terms, however, proton peak intensity and fluence were not strongly correlated with CME speed and flare size and X-ray fluence, and increasing particle energy seemed to weaken the correlation with CME speed. A definite conclusion about the relative importances of CME and flare(-related) acceleration proved challenging to attain, but CMEs generally appear to be more important for lower energies. Papaioannou et al. (2018) later relied on this catalogue in their extensive analysis to identify and quantify the correlations between flare size, longitude, rise time, and duration, as well as CME size and speed on one hand and SEP event occurrence on the other, aimed at developing SEP event forecasting and "nowcasting" applications (see Chapter 2.1.1).

The 25 and 50 MeV proton events detected by Wind during the years 1996–2016

were catalogued by Miteva et al. (2017a) and Miteva et al. (2018b), who present the onset times, peak intensities, and fluences for the rise phase of each event at both energy channels, as well as flare and CME associations.[2] Unlike in many other listings and studies, the latter were deduced heuristically by considering flare and CME activity within a time window that was deemed reasonable; no precise particle injection times were calculated as VDA is not viable with only two energy channels and TSA was considered too uncertain by the authors. The energy channels and the first eight years of solar cycles 23 and 24 were compared to each other. Similar numbers of events are present on both channels, but the peak intensities are approximately an order of magnitude lower on the higher channel; for both channels, a western origin on the Sun for the SEP events is about three times more common than an eastern origin. When both energy channels are considered, there were about 40% fewer events during cycle 24 than cycle 23, with a corresponding decrease in the numbers of large flares and fast CMEs. Flares had slightly longer rise times in cycle 24, but halo CMEs were more prominent, and the largest CMEs were somewhat faster than in cycle 23. Proton fluence was found to correlate better than peak intensity with flare class, X-ray fluence, and CME speed, but the statistical significance of most of these correlations and partial correlations remained marginal. An electron event counterpart[3] of the proton event catalogue was later introduced by Samwel and Miteva (2021). Based on near-relativistic electron data from ACE, they identified 800 events at 175–315 keV and 965 events at 103–175 keV as having occurred during the years 1997–2019, noting that some 30% of the low-energy and some 40% of the high-energy electron events were associated with corresponding 19–72 MeV proton events.

Listings and statistical studies of proton events at very high energies (from 80 MeV to some 1 GeV) include works by Kühl et al. (2017) and Bruno et al. (2018). In both cases, the energy spectra of the events were additionally studied. 500 MeV proton intensity in near-Earth space and neutron monitor count rates on the ground were found to be typically correlated (Kühl et al., 2017). Interestingly, however, no qualitative differences seem to exist between the spectra of GLE and large non-GLE events, and even a poorly connected event may cause significant rises in > 1 GeV proton fluence at the Earth (Bruno et al., 2018).

Dresing et al. (2020) investigated Solar Terrestrial Relations Observatory/Solar Electron and Proton Telescope (STEREO/SEPT; Müller-Mellin et al., 2008) 45–425 keV electron data from the time period of 2007–2018 and identified 781 events in total. Rise times for these were calculated and the intensities were fitted with single and broken power laws to estimate the energy spectra of the events. About half of the cases were found to conform to the broken power law spectral shape; rise times vary widely, but hard spectra generally appear to correlate with rise time length (the

2 This catalogue is accessible at `http://newserver.stil.bas.bg/SEPcatalog/`.
3 `http://www.nriag.sci.eg/ace_electron_catalog/`

harder the spectrum, the longer the rise time) as well as the presence of MeV electrons and 60–100 MeV protons, and the latter two are further correlated between themselves. The electron spectral index does not depend clearly on the connection angle or absence-versus-presence of a type II burst in events with a $>$ 25 MeV proton component. The authors concluded that slowly-rising electron events probably do not originate purely from flares but involve acceleration and injection mechanisms operating over an extended period of time, and that there may be a shared acceleration mechanism for relativistic electrons and high-energy protons, although MeV electrons occasionally appear without a related 60–100 MeV proton intensity enhancement.

Rotti et al. (2022) presented a correlation and compilation of three different SEP event catalogues—PSEP (Papaioannou et al., 2016), CDAW-SEP (`https://cdaw.gsfc.nasa.gov/CME_list/sepe/`), and the NOAA SPE list (`http://ftp.swpc.noaa.gov/pub/indices/SPE.txt`)—based on harmonized GOES integral proton intensity data from solar cycles 22–24 (years 1986–2017). Their list contains 341 events in total, with 245 exceeding the "significant" limit as defined by Space Weather Prediction Center of NOAA. Other similar works on synoptic catalogues that draw on multiple sources and cover several solar cycles, primarily with respect to large $>$ 10 MeV proton events, include Bazilevskaya et al. (2021) and Vlasova et al. (2022).

An example of an SEP event catalogue centred on particles other than protons or electrons is the ^{3}He enhancement listing of Hart et al. (2022). The authors give the properties of 854 ^{3}He intensity enhancements (SEP events, shocks and co-rotating interaction region crossings) detected by ACE and the STEREO spacecraft between 1997 and 2021, including the ^{4}He, O, and Fe fluences and ^{3}He/^{4}He and Fe/O abundances at 0.32–0.45 and 0.64–1.28 MeV MeV/nucleon. A strong correlation in ^{3}He/^{4}He and in Fe/O between the two energy ranges was found during the enhancement periods, but ^{3}He/^{4}He and Fe/O exhibit either no correlation (at large ^{3}He/^{4}He values) or only moderate correlation (at small ^{3}He/^{4}He values) with each other. The exact cause for the latter was left as an open question by the authors.

Attention has at times been called to the fact that the available SEP event catalogues are based on dissimilar assumptions, definitions, and data sources. Richardson et al. (2015) compared the event-associated CMEs as reported in several catalogues, cautioning that the properties of a given CME may disagree significantly between any two listings because different techniques are used to estimate CME speed and width. In particular, the authors note that the strong halo CME–proton event association apparent in the CDAW SOHO LASCO Catalog does not generally hold for other catalogues. Nevertheless, if the observations from the quadrature spacecraft (that is, the spacecraft viewing the CME from as close to a right angle to its path of propagation as possible) are used, CME width seems to be clearly correlated with CME speed and SEP peak intensity. In their extensive comparison of

seven prominent SEP proton event catalogues, Miteva et al. (2018a) further highlighted differences in the approaches, definitions, data coverage, and methods. They underscored that such issues can lead to divergence in statistical results, depending on which catalogue the basic event information is drawn from, and that researchers should bear this in mind.

3.2 Comparison and correlation studies

It is common for an investigation of a given facet of SEP events to rely on a previously published event listing but to limit the selection of cases in order to concentrate on a particular type of event (for instance, large or well-connected events, to minimise interpretation difficulties stemming from complicated processes like substantial cross-field transport effects). A reasonable expectation is that such selective inclusion renders any dependencies between various observed and calculated quantities easier to find, even if there might be certain types of events where the discovered correlations do not exist. For example, several authors (e.g. Ji et al., 2014; Kahler and Ling, 2017; Wang et al., 2022) have applied this approach to find functional forms that could be used to describe the time-intensity profiles of SEP events.

Pertinent works of SEP event data correlation analysis published within the last ten years include Miteva et al. (2013), Park and Moon (2014), Ji et al. (2014), Dierckxsens et al. (2015), Trottet et al. (2015), Le et al. (2017); Le and Zhang (2017), Kahler and Ling (2019), and Iwai et al. (2020). In general, these agree that CME speed, width, and event origin longitude are the most important factors determining the likelihood of SEP event occurrence and that particle peak intensity is, depending on data selection, at least moderately correlated with CME speed, flare peak X-ray intensity, flare rise phase X-ray fluence, and microwave radio burst fluence. Park and Moon (2014) found stronger correlations when several observed solar parameters were combined. Another correlation appears to exist between the bandwidth of the hectometric type II burst and SEP peak intensity (meaning that a wider bandwidth implies a greater peak intensity; Iwai et al., 2020), as well as between SEP rise and decay times on one hand and the X-ray flare (peak intensity, fluence, and rise time) on the other (Ji et al., 2014). Furthermore, the correlations between SEP peak intensity and CME speed and SEP peak intensity and flare peak intensity are thought to vary according to the particle energy of interest and solar wind conditions: at high energies (> 100 MeV), SEP peak intensity is better correlated with flare than CME parameters, but the opposite could be true at lower energies (Le et al., 2017; Le and Zhang, 2017). When the observer is immersed in a passing ICME during an event, the peak intensity correlation between protons and the flare and electrons and the flare are much stronger than otherwise, whereas the SEP peak intensity–CME correlation does not seem to be similarly affected (Miteva et al., 2013).

The results mentioned in the foregoing are often interpreted as confirming the

notion that the processes related to both flares and CMEs contribute substantially to SEP acceleration but that the former might be more important at high particle energies, the latter at low energies. Kahler and Ling (2019) reported significant correlations between suprathermal particle intensities and event peak intensity for events originating from longitudes between 0° and 40° west and in most cases from over 83° west, but not from the range of 41° to 83° west, which is expected to be the best connected to the near-Earth observer; they suggested that this finding might reflect the difference of quasi-parallel versus quasi-perpendicular shock geometry and acceleration with respect to the observer, as outlined in Kahler (2016), and that the suprathermal particles could represent the seed population of the shock-accelerated SEPs from the corona. However, Trottet et al. (2015) notably cautioned that if interdependencies between SEP, flare, and CME quantities in their data set are taken into account, many of the apparent correlations vanish and only CME speed and flare rise phase X-ray fluence appear to be independently correlated with SEP peak intensity.

Making use of the listing of SEP events in Cane et al. (2010), Lario and Karelitz (2014) examined 147 western proton and electron events, with a special emphasis on the relationship between SEP peak intensities, rise times, and the presence (or absence) and location of the event-associated ICME. Apart from confirming that large SEP events are typically associated with fast CMEs, their results lend support to those of Miteva et al. (2013) in that the highest peak intensities are typically observed when the ICME is at the observer, and the second-highest when an ICME has passed beyond the observer, presumably due to mirroring of particles. A CME that is launched while a preceding CME from the same active region is still fairly close to the Sun tends to have the effect of increasing the SEP peak intensity. Covering a broadly similar topic, Kahler and Vourlidas (2014) investigated the solar wind conditions at the Earth during 96 20 MeV proton events for which the source location was more westerly than W40, CME information was available (in the SOHO LASCO CDAW Catalog), and a detectable proton signature was found at 2 MeV. The ambient solar wind condition was considered to be one of three types, transient, fast, or slow. Event onset and rise timescales of 20 MeV protons showed no dependence on the solar wind, but the peak intensities of SEP events were significantly elevated during transient solar wind conditions (this last point was later confirmed by Kahler and Ling, 2019). If the 20 MeV proton peak intensity is normalized to the 2 MeV proton background intensity, the former is only weakly correlated with CME speed. In the transient solar wind cases and possibly others, the 2 MeV protons might provide a seed population for the more energetic event protons.

Miteva et al. (2017b) presented a synoptic statistical study of proton events from 1996–2016 (data from several sources and catalogues; energy range about 10 to 70 MeV) and their flare, CME, and radio burst (type II, III, and IV) associations. The median flare class for the proton events was found to be M2.8, CME speed 1055 km/s, and width 360°; type II and IV bursts are accompanied by somewhat larger

flares and faster CMEs than are type III bursts. SEP events with a western origin outnumbered eastern events by almost three to one, but no major statistical differences with respect to the relative numbers of radio bursts exist between different longitude ranges. Miteva et al. (2022) extended this study to the near-relativistic electron events detected by ACE/Electron, Proton, and Alpha Monitor (EPAM) during the entirety of solar cycles 23 and 24. The combined results suggest that interplanetary type II radio bursts may be more often associated with proton events and coronal type II bursts with electron events, but otherwise the trends concerning particle events and radio bursts appear similar for both particle species. Type III bursts are more closely related to electron than proton events. The authors categorized the events according to their presumed type of primary particle acceleration as flare-dominated (prolonged type III burst, with type II absent), CME-dominated (type II present), or "mixed" (simultaneous type II and type III), finding that 29% of electron events and 19% of proton events were flare-dominated, whereas the respective figures are 18% and 42% for CME domination, and 17% and 32% for the mixed type, with the rest of the cases uncertain.

Tan and Reames (2016) investigated directional near-relativistic electron intensities in 93 large SEP proton events from solar cycle 23 to identify cases where a "dropout" (see Mazur et al., 2000 and Chapter 1.1.2) occurs in an impulsive-type event. They discovered that directional electron intensities may exhibit a dropout when the effect is very small in omnidirectional intensities; the dropout periods last about 0.8 hours on average, which is consistent with the scale derived from solar wind turbulence observations. Electron dropout might occur in gradual-type events in addition to impulsive events if turbulence of magnetic flux tubes changes their connection to the SEP source region on the Sun. Ion dropouts, on the other hand, were generally interpreted to signify a compact source but in at least some cases could result from turbulence as well. Tan (2017) followed this work with a further study of 29 gradual SEP events from the same time period, again searched for evidence of electron and ion dropout with a view to disproving an earlier model by Giacalone et al. (2000), who had suggested that the dropouts are due to magnetic field line mixing and so should be rare in events where the SEP site of origin is large. Dropout periods were indeed found in 12 cases in 10 separate events, five of which were characterized as Fe-poor (implying quasi-parallel shock acceleration). Additionally drawing on interplanetary magnetic field observations, the author surmised that the dropout phenomenon in the studied events is more likely to result from solar wind turbulence than field line movement.

Bronarska and Michalek (2017) conducted a study of $84 > 10$ MeV proton events detected during the SOHO mission (1996–2014) with respect to their associated active regions. They found that SEP events commonly originate from complex active regions that feature sizable bipolar structures, large sunspots with asymmetric penumbrae, and many small spots in the group. Large peak intensity of the SEP event

was positively correlated with the magnetic complexity of its parent active region as well. Eastern active regions producing SEP events are typically larger than their western counterparts, possibly implying that eastern event-related CMEs are wider on average than western ones. In addition, they suggested a method for predicting peak SEP intensities (applicable to western SEP events) based on active region category. Cliver and D'Huys (2018) investigated the distributions of soft X-ray flare maximum intensities and 25 MeV proton event maximum intensities for different samples of cases between 1996 and 2011 by utilising a maximum likelihood estimator (e.g. Clauset et al., 2007) and assuming power law distributions. The slopes of the power laws fell generally between about 1.3 and 2.1, with those of the SEP- and CME-associated flare samples closer to that of SEP peak intensities than that of all flares. The difference between the SEP and flare peak intensity distributions was interpreted as mainly following from SEP-associated flares being especially energetic in general. The authors emphasised that for an effective shock and shock acceleration to occur, the event-related CME must exceed the local Alfvén speed and the motion of the plasma must be perpendicular to the ambient magnetic field; this leads to a selection effect that favours some types of flares and CMEs over others as drivers of large SEP events. Tan (2018), who mainly examined low-energy (a few to a few tens of keV) electron data from both impulsive and gradual SEP events during solar cycle 23, found a correlation between CME speed and flare soft X-ray peak intensity, as well as a steepening of electron energy spectrum in impulsive but not gradual events. This may be evidence of a situation where particle acceleration in magnetic reconnection sites causes a beam configuration to form as the parallel speed of electrons is limited by the electron Alfvén speed. In conclusion, the author proposed a scenario where the bremsstrahlung radiation from the coronal loops and type III radio emission from open field line regions are due to the same initial electron population from a "reconnection exhaust" in both main types of events.

The solar release times and heights of SEPs, often derived from CME and radio observations and then compared to results obtained by methods such as TSA and VDA, are another active topic of study. Xie et al. (2016) selected 28 large $>$ 10 MeV proton events from December 2006 to March 2014 and estimated and compared the release times of 10–100 MeV protons (derived using VDA and TSA) and 0.25–10.4 MeV electrons (using TSA). The results indicated that high-energy electrons are systematically released later than lower-energy electrons; for protons, the release times are almost identical for high and medium energies, and slightly later on average for the low energy range, probably due to interplanetary scattering. In the majority of the events, protons were released within some 8 minutes from near-relativistic electrons and within some 6 minutes of the relativistic electrons, but in some 30% of the cases, there was a delayed proton release. Near-relativistic electron releases and type III burst onsets occurred within 2–42 minutes of each other, with corresponding CME heights at electron release ranging from about 2 to 9 $R_{\odot}$.

The authors remarked that there probably is a close relation between the acceleration mechanisms of near-relativistic electrons and protons. Prakash et al. (2017) looked into associations between flares, CMEs, and type II radio bursts in 1997–2012, with or without concomitant $>$ 10 MeV proton events. They found that 65% of metric-to-decametric and hectometric (i.e. propagating from the corona to the interplanetary medium) type II bursts related to CMEs led to a proton event. A positive correlation exists between CME speeds (both projected and projection-corrected) and the logarithm of proton peak intensity in SEP events, albeit with a great deal of scatter in the data points; this was noted to be consistent with Papaioannou et al. (2016) and other similar studies. The SEP-associated and non-SEP-associated flares were not distinctive as to their rise times, and the same was true for the delays between the flare and type II burst onset in these categories. In contrast, the starting frequencies of metric type II bursts did show a significant difference, which was greater for SEP-associated events. More importantly, the propagation speed and frequency drifting rate of metric type II bursts were greater for SEP cases than non-SEP cases, as was the duration of decametric–hectometric type II bursts in SEP events. The radio bursts were surmised to form slightly lower in the solar corona in SEP events than otherwise. In 65% of the SEP events, some level of CME interaction seemed to be present based on position angles and propagation of the CMEs, as well as a visual check of LASCO movies.

Focussing on radio observations, Ameri et al. (2019) investigated the relationship between SEP events, the particle release times, and radio bursts (types II, III, and IV). Over 96% of the considered 58 events were associated with type IIs, all were associated with type IIIs, and 55% with metric type IVs. In about half of all cases, VDA results indicated that protons and electrons were released (and perhaps accelerated) more or less simultaneously, but in a large majority of the others, protons were released later. However, the cause of the delay in the proton release times compared to the release times of electrons and type III radio burst onsets remained uncertain. Two categories appeared to be present in the data, judging by radio burst activity: events where only metric type II burst is present, or if a decametric–hectometric type II also appears, protons are released before the onset of the latter; and events where only decametric–hectometric type II burst appears, or if metric type II appears as well, protons are released during or after the onset of the former. A possible interpretation is that the SEPs in cases belonging to the first group are accelerated at low altitudes, while CME-driven shocks high in the corona dominate for particle events of the second group.

Firoz et al. (2019) considered 34 large proton events (of which 13 were GLEs) from 1997–2012, all associated with at least M4.6-class GOES X-ray flares, with respect to their radio burst (type II), flare, and CME associations. $>$ 10 MeV integral proton intensity profiles were shifted back to the Sun using VDA, and the delays between the X-ray flares and radio bursts and estimated particle injections were cal-

culated. It was concluded that MeV particles are injected before GeV particles at the Sun in GLEs, in the initial phases of the associated X-ray flare (which occurs prior to CME liftoff), and later accelerated to GeV energies; conversely, in non-GLE events the MeV particles are typically injected during the impulsive phase of the flare. Firoz et al. (2022) revisited these events, considering proton fluences at three integral energy channels (> 10, > 30, and > 60 MeV), with a correction for the solar longitude of SEP source (based on the treatment in Lario et al., 2013) additionally applied. The event fluence was discovered to be almost directly proportional to duration in the two lower energy ranges, a few unusual cases aside, and the mean duration at > 10 MeV was found to be similar for GLEs and non-GLEs. Even so, proton fluences are on average some three times greater in GLEs than non-GLE events and the energy spectra of the former are harder.

Lario et al. (2020) examined the CDAW SOHO LASCO CME Catalog for fast and wide (more than 1000 km/s and 120°) CMEs between 2009 and 2014 and found 11 cases out of a total of 123 where no > 20 MeV proton event followed the CME at either of the two STEREO spacecraft or SOHO. They found that such CMEs tend to be narrower and contain less kinetic energy and mass than those that are associated with proton events. The shock volumes with high Mach numbers were also typically narrow (as estimated from white-light and EUV images) in non-SEP event cases, meaning that the observing spacecraft are connected to low-Mach regions, and they often involve weak or absent type III radio bursts in the decametre–hectometre range. The latter was considered to signify that there is in fact no substantial SEP release during the CME liftoff and propagation, which is probably the main reason for the lack of an SEP event at 1 AU.

Recently, Ameri et al. (2022) carried out an analysis of energetic storm particle (ESP) events—SEP intensity rises during passing interplanetary shocks—associated with CMEs faster than 400 km/s and wider than 120 degrees that originate from the front side of the Sun, as well as the corresponding solar proton events. 57% of well-defined interplanetary shocks detected at the Earth led to an ESP event, and 88% and 77% of the 66 identified ESP–CME events were associated with type II radio bursts and SEP events, respectively; only 28% of CMEs associated with SEP events lacked an ESP event. Average shock transit speeds were found to be much greater in ESP than in non-ESP cases, and ESP-associated CMEs were similarly faster and also wider on average than non-ESP CMEs, although these distributions overlap. The shock transit speed from the Sun to the Earth had the strongest correlation with the ESP peak intensity, while only a moderate level of correlation was discovered between the ESP peak intensity and CME speed, and a weak correlation between ESP peak intensity and the connection angle, consistent with the results of Kouloumvakos et al. (2019), who studied connections between coronal shock waves and SEPs observed in situ. SEP and ESP peak intensities were moderately to strongly correlated, the level of correlation increasing with particle energy.

A number of studies feature an explicit comparison between two or more solar cycles (e.g. Chandra et al., 2013; Gopalswamy et al., 2015a; Gopalswamy et al., 2015b; Bazilevskaya et al., 2021; Samwel and Miteva, 2021; Vlasova et al., 2022), often cycles 23 and 24, with regard to SEP events. These works report that a given part of cycle 23, or cycle 23 as a whole, was considerably more active in terms of sunspot numbers, flares, CMEs, and particle events than the corresponding part of cycle 24. Gopalswamy et al. (2014) gave a listing of all large frontside solar eruptions (59) from the rising phase of solar cycle 24 (from December 2008 up to until the end of January 2014), i.e. cases with at least an M5-class flare and a CME. Only 37% of the ones with a solar origin west of E15, and 27% in total, led to >10 MeV proton events at the Earth (according to GOES data); a similar percentage of cases featuring a flare smaller than M5 also caused an SEP event.

Gopalswamy et al. (2015a) proposed that the likely reasons for the paucity of high-energy SEP events at 1 AU during the early part of solar cycle 24 were weak heliospheric magnetic field, poor magnetic connectivity, and local ambient conditions in interplanetary space (possibly high Alfvén speed, making the environment less conducive for strong shocks). Raukunen et al. (2016), whose list of iron-rich events was adopted for Article III, additionally raised the possibility that SEP seed populations may have differed in composition between the two cycles. They found that cycle 23 had more iron-enriched days than cycle 24, and its rising phase in particular featured a considerable number of days with Fe enhanced in relation to C and O. Studying the near-Earth >25 MeV proton events detected during solar cycles 20 through 24 (1967–2015), Richardson et al. (2017) noted that the solar minimum after the conclusion of cycle 23 and before the commencement of cycle 24 was without significant proton events, whereas events occurred during other minima; extremely intense SEP events such as were observed in cycles 22 and 23 were absent in cycles 21 and 24. In a tangentially related work, Richardson et al. (2016) presented evidence that there was a six-month periodicity during the rising phase and possibly the early declining phase of solar cycle 24 in several phenomena in the Sun, such as the sunspot number and total area, 10.7 cm radio flux, CME occurrence rates, and >25 MeV proton events from a given solar hemisphere (northern or southern). The solar hemispheres seem to be independent from each other with regard to their SEP event rate and other activity, leading the authors to argue against a model proposed by McIntosh et al. (2015) that attempts to explain the six-month periodicity as a product of approximately annual and regular magnetic surging stemming from global processes in the deep solar interior.

3.3 Studies based on data from multiple viewpoints

Observing the same SEP event simultaneously from multiple locations in space appears very desirable, as the differences in the detected intensity profiles may provide

important clues about the processes involved in particle release and transport. Indeed, studies of this nature have been made for several decades (e.g. McKibben, 1972), but these efforts have often had to contend with sparse data coverage resulting from the technical challenges and costs involved in operating long-duration interplanetary missions. An important milestone in multi-spacecraft SEP studies occurred in 2006 when the twin STEREO spacecraft were launched into solar orbits. As they gradually receded from the Earth in opposite directions while remaining at approximately 1 AU from the Sun, it became possible in effect to study the entire surface of the Sun at once by combining the data collected by the STEREOs with those from near-Earth missions. Taking advantage of this opportunity, a proliferation of works on the statistical properties of SEP events published in the 2010s and early 2020s rely in part or entirely on STEREO data.

Lario et al. (2013) provided a listing of 35 events detected by two or more spacecraft—at 1 AU by SOHO, ACE, GOES, and the STEREOs, and closer to the Sun by the Mercury Surface Space Environment Geochemistry and Ranging spacecraft (MESSENGER; Leary et al., 2007)—during the rising phase of solar cycle 24. Energies and particle species studied were near-relativistic and relativistic electrons and 15–40 and 25–53 MeV protons. The dependence of the peak intensities of the events as observed at 1 AU on the connection angle was modelled with Gaussian curves, revealing a bias where the peak of the distribution lies to the east of the nominally best-connected region on the Sun. This confirmed an earlier result (Lario et al., 2006), and was in turn corroborated by e.g. Cohen et al. (2017), Richardson et al. (2017), He and Wan (2017), and Article II. The peak longitudes and longitudinal widths of the Gaussians as a function of the connection angle were obtained, respectively, as -16° ± 3° and 49° ± 2° (71–112 keV electrons), -13° ± 3° and 46° ± 2° (0.7–3.0 MeV electrons), -12° ± 3° and 43° ± 2° (15–40 MeV protons), and -12° ± 3° and 45° ± 1° (25–53 MeV protons). This was viewed as suggesting that the prompt SEP component does not form until the CME-driven shock has already moved a considerable distance away from the Sun, which might cause the relative central solar meridian of each observer to be favoured as the direction of the apparent source of the SEPs. The peak intensities of five near-relativistic electron events featuring a good magnetic connection between MESSENGER and one of the spacecraft at 1 AU were modelled with a power function of the form $R^{-\alpha}$ (where R is the radial distance from the Sun); the authors interpreted the results so that under a relatively undisturbed interplanetary magnetic field configuration, α falls below 3, while values greater than 3 follow from complicated magnetic field conditions that tend to hinder particle transport away from the Sun.

Focussing on ^{3}He-rich events, Wiedenbeck et al. (2013) found 17 multi-spacecraft cases in STEREO and ACE data during the period between January 2007 and January 2011, including one three-spacecraft event that extended to more than 136° in longitude. ^{3}He enhancements have traditionally been considered as a feature of impulsive

events, implying a flare-related, narrow injection and acceleration region that should be unlikely to give SEPs access to a large longitude range; earlier single-spacecraft observations tended to support this notion (e.g. Reames, 1999), and the dropout phenomenon would seem to do so as well. The authors considered a range of possible explanations, including magnetic field line random walk, extensive spreading of field lines between solar photosphere and the source surface (i.e. the distance where the interplanetary magnetic field assumes its radial-spiral shape), CME-induced shocks, and widely separated but virtually simultaneous flares, but did not reach definite conclusions, emphasising that all of these processes may be involved.

Dresing et al. (2014) extended the scope of multi-viewpoint studies to 55–105 keV electron events with a width of over 80°, as seen by both STEREO spacecraft and ACE between November 2009 and August 2013, identifying 21 such events. The peak intensities in the event sample as the function of the connection angle were modelled with Gaussian curves, and onset delays (time between the event-related type III radio burst onset and event onset at the observing spacecraft) and event intensity anisotropies were determined. All events in question were over 180 degrees wide, some almost 300 degrees. Peak intensities were found to depend on connection angle much as expected, but onset delays less unambiguously so, and intensity anisotropy still less clearly. Correlations between anisotropy and onset delay and event rise time were additionally studied, revealing that some level of correlation appears to be present. This, in all, was considered to suggest that both perpendicular transport and extended particle sources may be effective in these events, but the relative importance of these factors was not clear. Klassen et al. (2016) highlighted another four wide-longitude electron events where the peak intensities observed by the STEREOs show a drastic difference (up to a factor of 12) despite a similar magnetic connection to the source region, and the better connected of the observers surprisingly detected the event onsets later than the more poorly connected one. The peak intensity distribution as a function of connection angle was not described well by a simple uniform Gaussian shape but there appeared a rippling or ”fingers-and-valleys” pattern superposed on the Gaussian. The authors suggested that this might be due to open magnetic field lines giving the SEPs a fast path to some observers, whereas closed lines near the active regions and in the coronal holes along with the strong turbulence in their associated fast solar wind streams might block and scatter particles headed towards a separate nearby observer; other possible explanations include an asymmetric or multi-point injection or acceleration region, and the interplanetary magnetic field being non-uniform and differing starkly from the ideal Parker configuration.

Papaioannou et al. (2014) presented a catalogue[4] of all STEREO proton events

4 This is available online at `http://server.sepserver.eu`.

in the 6–10 MeV energy range during 2007 to 2014, including associated near-relativistic electron events. Proton intensity enhancements detected by the instruments that arose due to shocks, co-rotating interaction regions, and stream interaction regions were eliminated, and solar origins of the events were identified from radio and X-ray data. The final listing includes 130 cases for STEREO-A and 108 for STEREO-B, with 30 of these jointly seen by both probes. 85% of all proton events featured an electron signature, and 30% a high-energy (40–100 MeV) proton signature; a majority of all events were associated with a type III radio burst. Another comprehensive catalogue of proton events observed by the STEREOs (at > 25 MeV) is that of Richardson et al. (2014), who additionally considered the accompanying relativistic electron events and used SOHO/ERNE data for near-Earth observations. They found that event onset delays were generally longer for protons than for electrons, and short for well-connected, western hemisphere events, but with a small bias favouring footpoints to the east of the particle source site (cf. Lario et al., 2013). The peak intensities of three-spacecraft proton events were again modelled with Gaussian curves; the widths were found to be $43° \pm 13°$ for 14–24 MeV protons and $47° \pm 14°$ for (0.7–4 MeV) electrons, and the eastward bias mentioned above was confirmed ($15° \pm 35°$ for protons, $18° \pm 29°$ for electrons), although this fell inside the limits of statistical uncertainty. The authors pointed out that the results imply a close relationship between the acceleration of protons and electrons. A more recent study by Xie et al. (2019), based on a selection of 28 three-spacecraft proton ($\approx$ 20–30 MeV; STEREOs and Wind) and near-relativistic electron (STEREOs and ACE) events from January 2010 to April 2014, found average Gaussian widths of some 40° for both protons and electrons and a slight preference for the centre of the distribution to be located east of the magnetic footpoint ($15° \pm 16°$ for protons, $18° \pm 17°$ for electrons) that, nevertheless, is once more almost or entirely within the range of uncertainty.

With a view to investigating the usability of the data from the Standard Radiation Environment Monitor (SREM; Bühler et al., 1996) and also validating standardized, lightweight, low-cost SEP detectors as a concept, Georgoulis et al. (2018) reported on 22 energetic proton events, 14 of which were detected simultaneously by the units aboard International Gamma-Ray Astrophysics Laboratory (INTEGRAL; Winkler et al., 2003) and Rosetta (Glassmeier et al., 2007). It was shown that the SREMs and their data are sufficiently reliable for the purpose of studying SEPs; as for the events themselves, all were found to be associated with major solar eruptions (at least M-class flares, fast CMEs), as well as interplanetary shocks, and their intensity rise times exhibit a statistical peak at 9 hours.

Multi-viewpoint study of three-dimensional, SEP event-associated phenomena such as CMEs and coronal shocks offers obvious benefits since any single observer is limited to seeing these occurrences as two-dimensional projections against the sky plane. As an example, Park et al. (2017) investigated the peak proton intensi-

ties and the three-dimensional properties of CMEs in 18 wide-longitude events from 2010–2015. The true CME speeds in three dimensions were compared with two-dimensional estimates from the CDAW SOHO LASCO Catalog and found to be reasonably consistent, with the mean 3D speed being some 200 km/s greater than the mean 2D speed but with a large correlation coefficient. The highest peak intensities were generally observed by the best-connected spacecraft, and there is a statistically weak tendency for the peak proton intensity to increase as the three-dimensional speed and angular width of the event-associated CME increase. A weak correlation additionally exists between the peak intensity and the three-dimensional CME width. The peak intensities as functions of the connection angle were modelled with a Gaussian curve, yielding an overall result that is comparable to that of Lario et al. (2013) but indicates slightly larger event widths. The connection angle was found to be considerably better (anti-)correlated with proton maximum intensity than the CME parameters.

Kouloumvakos et al. (2019) made a comparison between coronal shock wave parameters from both three-dimensional modelling and observations and SEP event observations; the event list presented in Article II was used as a basis of the latter, with 33 three- or two-spacecraft events included. Shock information was based on white light and EUV images, and the shock waves were reconstructed with a three-dimensional technique of fitting a chosen geometric shape (Thernisien et al., 2006, 2009). Correlations between SEP peak intensity and several shock parameters were studied, as was the relation between shock wave evolution and SEP release. The best correlations were found between shock Mach numbers and SEP peak intensities. When the connection angle is less than about 120 degrees, the shock wave becomes supercritical (i.e. exceeds the local speed of sound) before it reaches the magnetic footpoints of the SEP event observers, possibly as a sign that it is triggers or is otherwise associated with particle release and acceleration, but this does not seem to hold for cases with larger connection angles, as the shocks at their footpoints tend to remain subcritical. Zhuang et al. (2020) considered 41 large multi-spacecraft proton cases where two successive CMEs, a slow preceding and a fast ”primary” one, have been identified within nine hours and as associated with an SEP event, deducing 11 of the 41 events to feature spatial overlap of the two CMEs (when modelling the CMEs in three dimensions by combining observations from three vantage points and applying the graduated cylindrical shell model as described by Thernisien et al., 2006). While the particle release probably occurred before the CMEs came in contact with each other in six cases, the peak proton intensity appeared to be substantially enhanced as a result of the CME interaction in the remaining events.

Works on SEP transport in wide-longitude events include the simulation study of Rodríguez-Gasén et al. (2014). This involved a series of gradual multi-spacecraft events simulated using a three-dimensional, co-rotational MHD code (Jacobs, 2007.). Virtual observers were placed at two radial distances (0.4 and 1.0 AU) and different

longitudes and latitudes with respect to event site of origin. A fast shock was then modelled by injecting a high-density plasma cloud, representing a CME, into the background solar wind. The plasma and magnetic field quantities were found to behave qualitatively similarly at both radial distances, and the shock was the strongest for the observer with the least lateral distance to the nose of the shock. SEP intensities were the highest for these observers at both distances, with the rise phase of the event being more intense for the near-Sun observer; in addition to the effect of the longitudinal distance to the shock nose on the observed SEP intensity profile, a difference in latitude was found to be able to cause a variation of an order of magnitude in the detected peak intensity, suggesting that the latitudinal distance component should be routinely included in calculations of magnetic connectivity. Dröge et al. (2016), in turn, investigated a series of three wide SEP events detected by the STEREOs in August 2010. The temporal variation of the intensity and anisotropy of near-relativistic electrons were considered and used as input for a three-dimensional stochastic particle transport model (as previously used by Dröge et al., 2014) that yields estimates for electron mean free path with regard to both field-aligned and perpendicular scattering in the corona. The mean free paths were shown to vary a great deal depending on the radial distance and longitude. The authors noted that the model would benefit from the identification of some mechanism that decreases perpendicular scattering close to the Sun, and noted that studying the possible correlations between the parallel and perpendicular mean free paths could lead to a better understanding on the processes involved.

Lario et al. (2017) concentrated on three wide-longitude proton and electron SEP events (from 2011, 2013, and 2014) with a view to their CME acceleration in solar corona, inferring shock properties from white light and EUV observations and particle injection times by applying VDA. An MHD model of the corona (designed by Lionello et al., 2009) was used in conjunction with observations to gain an understanding of the plasma conditions and processes at the shocks. For one event, a correspondence in the timing between increased (the fast magnetosonic) Mach number of the shock and SEP release was found, but not in the other two events for observers not well connected to the SEP origin site. Shock speed, as estimated by fitting to white-light and EUV images and assuming the shock to have a spherical or ellipsoidal three-dimensional shape, appeared to correlate well with the peak intensity of 25 MeV protons at 1 AU. While acknowledging the inherent uncertainties in the model, the authors suggested that unless there are low-intensity magnetic regions extending to a wide range of longitudes in the corona during particle injection, perpendicular transport must play an important role in wide SEP events.

The so-called reservoir effect, i.e. a situation where a magnetic trap that collects SEPs and releases them later forms between the Sun and a propagating ICME (see e.g. Anastasiadis et al., 2019, and references therein), is considered to be an important factor in the prolonged decay phases of certain large (gradual-type) SEP

events. The reservoir effect was specifically noted in three large three-spacecraft (SOHO and the STEREOs) $>$ 25 MeV proton events of 2012 by Struminsky (2015). Wang et al. (2021) identified a total of 62 reservoir events in deka-MeV proton data from 1976–1980 and 2010–2014, commenting that such cases are observed at virtually all longitudes at 1 AU; the authors viewed the longitudinal uniformity of proton intensities as pointing towards effective perpendicular diffusion.

Based on simultaneous multi-point observations of 32 events, Bruno and Richardson (2021) recently presented an empirical model for predicting proton event fluence and peak intensity between 10 and 130 MeV at 1 AU. The spatial distribution of the event peak intensity was modelled so that the intensity decrease when moving away from the global maximum behaves like a periodic Gaussian that depends on both the longitudinal and latitudinal distance. The magnetic connection was traced as a Parker spiral back to 2.5 $R_{\odot}$, and CME speed was additionally included in the prediction formula. When tested against a control sample of some 20 events, the model was found to be in a reasonably good agreement with the actual situation in most cases (usually predicting a somewhat softer energy spectrum than what is measured), although it might be significantly in error when, e.g., the particle source is unusually wide.

Aiming to derive a useful analytical function form to describe event time-intensity profiles, Wang et al. (2022) examined 59 large, three-spacecraft, gradual proton events. The radial diffusion equation was solved for the best-connected observer in each case, leading to a function that consists of a power law multiplied by an exponential and has four parameters. The parameters can be interpreted in terms of intensity rise and decay times. When the function was fitted to the observed data, it was seen that the rise time appeared to be strongly correlated with magnetic connection, being on the order of a few hours for a typical well-connected event. For this reason, it was regarded as a prime indicator for this type of particle transport processes on the premise that large rise time implies substantial perpendicular diffusion.

4 Data sources

4.1 Charged particles

4.1.1 Protons

The analysis carried out in Articles I and II relies in large part on differential proton intensity data provided by the Energetic and Relativistic Nuclei and Electron experiment (Torsti et al., 1995), included in the scientific instrumentation of the Solar and Heliospheric Observatory (SOHO) spacecraft. So as to be able to cover a large range of particle energies, ERNE was designed as two particle telescopes operating together, the Low Energy Detector (LED) and the High Energy Detector (HED). The former is made up of two silicon detector layers, and the latter is a stack of five layers of silicon detectors and two scintillators, the upper one consisting of a single block of CsI(Tl) and the lower one of five BGO crystals. Both telescopes include an anticoincidence shield. LED is sensitive to SEPs in the energy range of $\approx$ 2–13 MeV/nucleon, while HED covers the range of $\approx$ 13 MeV/nucleon to a few hundred MeV/nucleon, depending on the particle species. The highest kinetic energy of protons that can be detected and analysed by HED is approximately 130 MeV. ERNE/HED can identify elements from hydrogen to zinc and is able to distinguish between the most abundant isotopes of each element. Due to its directional sensitivity, it is capable of providing detailed data on SEP intensity anisotropies.

An additional source of near-Earth SEP proton intensity data, used for the study described in detail in Article III, was version 2.0 of the Reference Data Set (RDS) of the Solar Energetic Particle Environment Modeling (SEPEM) project (Crosby et al., 2015). RDS has been created through cross-calibrating (see Sandberg et al., 2014), energy re-binning and combining data recorded by the Geosynchronous Operational Environmental Satellite (GOES) spacecraft 5 through 13 (GOES/Space Environment Monitor; Onsager et al., 1996; Sellers and Hanser, 1996), Interplanetary Monitoring Platform 8/Goddard Medium Energy (GME; McGuire et al., 1986), as well as earlier Synchronous Meteorological Satellites. The resulting data set provides a nearly complete coverage of the years 1973–2015 for proton fluxes at 11 differential energy channels that span the energy range from 5 to 200 MeV, with a time resolution of 5 minutes. (Note that while newer versions of the RDS are available, they were not utilised for reasons explained in Article III.)

The corresponding proton data for observation locations other than the vicinity

of the Earth (in Article II) were collected by the In situ Measurements of Particles and CME Transients (IMPACT) investigation of the two-spacecraft Solar Terrestrial Relations Observatory (STEREO) mission. Both STEREO-A and STEREO-B are equipped with an IMPACT unit which includes, in addition to other instruments, two SEP detectors; these are called the High Energy Telescope (HET; von Rosenvinge et al., 2008) and the Low Energy Telescope (LET; Mewaldt et al., 2008). HET consists of a stack of planar ion-implanted silicon detectors covered by two entrance foils, designed to study the abundances and energy spectra of electrons and ions up to and including iron; LET, meanwhile, is a double-ended, ion-implanted silicon detector system, with one end facing the Sun and the other the anti-sunward direction. The design goal of LET is to measure the composition and energy spectra of ions from hydrogen to nickel in the energy range of a few MeV/nucleon to a few tens of MeV/nucleon. In the case of protons, LET is capable of detection and measurement in the kinetic energy range between some 1.8 MeV and 15 MeV, whereas the lower and upper bound are 13 MeV and 100 MeV, respectively, for HET.

4.1.2 Electrons

As the objective of the studies detailed in Articles I and II was to gain the most complete understanding possible of each SEP event considered, electron intensity observations were of interest alongside proton observations. For reasons of statistics and to facilitate performing the time shifting analysis (TSA) on electrons, the main focus of these studies was on near-relativistic electrons with kinetic energy between about 0.18 and 0.31 MeV (exact values depending on the available instrument). For observations in the vicinity of the Earth, we utilised data from the Electron, Proton, and Alpha Monitor (EPAM; Gold et al., 1998) aboard the Advanced Composition Explorer (ACE). EPAM consists of five particle telescope apertures in an orientation chosen to provide a near-complete angular coverage of the space around itself, and it sweeps the sky as its parent spacecraft spins. The instrument, which was adapted from the flight spare of a functionally identical unit included in the Ulysses mission, is designed to detect electrons with kinetic energies of 40 keV to about 350 keV and ions with kinetic energies from 50 keV to 4.8 MeV.

The STEREO spacecraft are equipped with a broadly comparable instrument called the Solar Electron and Proton Telescope (SEPT; Müller-Mellin et al., 2008). This is part of the IMPACT package mentioned above and consists of two pairs of double-ended particle telescopes sensitive to electrons (kinetic energies of 30 keV to 400 keV) and protons (60 keV to 7 MeV), oriented so that they are able to provide anisotropy information without the need to spin the spacecraft itself. STEREO/SEPT data were used in the electron-related studies in Article II.

To complement the overall picture of the SEP events obtained through near-relativistic electron data, relativistic electrons within the energy range of 0.7–3.0

MeV at the Earth were also analysed for event onset times in Article I. The data concerning these were obtained from SOHO/Electron Proton Helium Instrument (EPHIN; Müller-Mellin et al., 1995). EPHIN, which forms one component of the Comprehensive Suprathermal and Energetic Particle Analyzer (COSTEP) experiment, is a stack of six solid-state detectors designed to detect high-energy electrons (kinetic energies of 150 keV to more than 5 MeV), as well as mid-energy protons and alpha particles (4 MeV/nucleon to more than 53 MeV/nucleon).

4.2 Soft X-rays

The early generations of GOES satellites (up to and including GOES 7) operated by the National Oceanic and Atmospheric Administration (NOAA) of the United States carried two ion chamber-based X-ray sensor units (XRS; Garcia, 1994) as part of their scientific payload. These observed the Sun on one wavelength band each, namely 0.1–0.8 nm and 0.05–0.4 nm, with the former dubbed the ”long” or ”soft” channel and the latter the ”short” or ”hard” channel. While the design of the instrument was updated on GOES 8–15, its spectral bandpass is considered to have remained essentially identical to the previous type (Hanser and Sellers, 1996). Of note is the fact that the commonly used classification of solar X-ray flares is based on the peak flux (measured in W/m^2) detected by XRS on the soft channel, with a letter (A, B, C, M, or X) signifying the order of magnitude of the peak flux of the flare and a number representing the significand.

All articles included in this dissertation involved the use of GOES/XRS soft X-ray data. The solar locations of the event-related X-ray flares, which were considered to mark the approximate site of the SEP event origin, were taken from publicly available lists maintained by NOAA and others (see the articles for details).

4.3 Visible and ultraviolet light

For information on event-related CMEs, the studies detailed in Articles I and II relied on data from the SOHO/Large Angle and Spectrometric Coronagraph (LASCO; Brueckner et al., 1995) as processed and presented in The SOHO LASCO CME Catalog.[1] LASCO consists of three coronagraphs, one internally and two externally occulted, that image the solar corona at wavelengths between about 530 nm and 660 nm, with their combined field of view spanning radial solar distances from 1.1 $R_\odot$ to more than 30 $R_\odot$.

The analogous CME data for vantage points other than the Earth, required for the wide-longitude SEP event analysis in Article II, were derived from observa-

1 Accessible online at `http://cdaw.gsfc.nasa.gov/CME_list/`.

tions performed by the Coronagraph 1 and 2 (COR1 and COR2) instruments included in the Sun Earth Connection Coronal and Heliospheric Investigation (SECCHI; Howard et al., 2000) experiment carried by both STEREO spacecraft. COR1 and COR2 are Lyot-type coronagraphs (the former is internally occulted, the latter externally) operating on the 650–750 nm bandpass, and together they are designed to cover a field of view between 1.25 and 15 $R_\odot$. In cases where it was necessary to identify and locate potential event-related farside flares not included in any of the GOES/XRS-based X-ray flare listings, this information was complemented with STEREO/SECCHI/Extreme Ultraviolet Imager (EUVI) time-lapse movies provided by the STEREO COR1 CME Catalog.[2] EUVI is a Ritchey-Chrétien-type ultraviolet telescope operating on four nominal wavelengths between 17.1 nm (Fe IX) and 30.4 nm (He II); the radius of its field of view at 1 AU corresponds to about 1.7 $R_\odot$.

4.4 Radio waves

Even though radio frequency observations are not specifically covered in quantitative terms in any of the studies included in this dissertation, type III radio bursts were considered in the context of the solar departure times of the SEPs in Articles I and II. The pertinent data were collected by Wind/WAVES (Bougeret et al., 1995) and STEREO/WAVES (also referred to as S/WAVES; Bougeret et al., 2008). Wind/WAVES consists of three electric dipolar antenna systems (two coplanar and orthogonal wire antennae, one rigid spin-axis antenna) and three magnetic search coils, together with their associated amplifier and analyser electronics. Combined, these systems cover the electromagnetic frequency range of 0.3 Hz to about 14 MHz. The similarly-named but more recent STEREO/WAVES comprises three orthogonal monopole antennae, and it is sensitive to a continuous range of frequencies from a few decihertz to some 16 MHz. The radio receivers of these instruments operate on frequencies that span from 2.5 kHz (STEREO/WAVES) or 20 kHz (Wind/WAVES) to the upper bound of the respective instrument.

4.5 Thermal protons (solar wind speed)

The speed of the solar wind is relevant to the TSA analysis (see Articles I and II), and to estimate it, we made use of data from the Solar Wind Electron, Proton and Alpha Monitor (SWEPAM) aboard ACE (McComas et al., 1998).[3] Wind/Solar Wind Experiment (SWE; Ogilvie et al., 1995) data[4] were substituted for time periods for

2 These are available at `https://cor1.gsfc.nasa.gov/catalog/`.

3 These data are available at `http://www.srl.caltech.edu/ACE/ASC/level2/lvl2DATA_SWEPAM.html`.

4 `http://omniweb.gsfc.nasa.gov/ftpbrowser/wind_swe_2m.html`

which ACE/SWEPAM data were not available. Of these instruments, SWEPAM is electrostatic analyser designed to detect electrons, protons, and alpha particles; the energy range for the latter two is 260 eV/q–36 keV/q, where q is the electric charge of the incident particle. SWE, in turn, is made up of two Faraday cup sensors and a vector electron and ion spectrometer (and also a strahl sensor dedicated to investigating electrons near to the magnetic field direction), with a combined energy range spanning from 150 ev/q to 24.8 keV/q.

In Article II, the data mentioned above were additionally supplemented with comparable data from Plasma and Suprathermal Ion Composition (PLASTIC; Galvin et al., 2008) experiment of the STEREO mission. PLASTIC is a top hat-type electrostatic analyser featuring solid state detectors for energy measurement. As a whole, it monitors a kinetic energy range that spans from 0.3 keV/q to 80 keV/q, and it is capable of detecting and measuring ions of elements from hydrogen to iron.

5 Methods

5.1 Event onset determination

The primary method of determining SEP event onset used in our work is based on the Poisson-Cumulative sum (CUSUM) statistic. In this framework, the count of SEPs of interest per a unit of time is essentially regarded as a Poissonian process that is either under control (particle intensity remains at the background level) or out of control (an SEP event has commenced). An applied Poisson-CUSUM scheme is able to decide between these two alternatives and, if the latter situation prevails, when the loss of control (event onset) occurred. This is achieved by cumulating the difference between an observed variable Y_i (the particle count rate) and a reference value k; as soon as this sum exceeds a pre-determined threshold value h, control is considered to have been lost.

Since it is sufficient to limit the scheme to detecting only sudden increases in particle counts, the expression for the cumulative sum can be written as

$$S_i = \max\left(0, Y_i - k - S_{i-1}\right); S_0 = 0. \tag{3}$$

In the above equation, k is to be selected so that it falls between the acceptable process mean μ_a and the mean level of counts that is desired to trigger an alarm, μ_d. For the application in question, the following definitions are used:

$$k = \frac{\mu_d - \mu_a}{\ln\left(\mu_d\right) - \ln\left(\mu_a\right)}; \mu_d = \mu_a + 2.0\sigma_a. \tag{4}$$

Here, σ_a is the standard deviation of μ_a, the mean pre-event background particle count rate. The threshold value h is set to 1 when $k < 1$ and 2 otherwise. Due to the sensitivity of this criterion, 30 consecutive "out-of-control" signals are required for a positive determination of an event onset. If this condition is met, the first of the signals is considered to indicate the onset. For a more detailed description and discussion of the method outlined here, see Huttunen-Heikinmaa et al. (2005).

Figure 8 demonstrates the Poisson-CUSUM method in practice. The proton energy range studied is the 55–80 MeV channel of ERNE/HED at 1-minute time resolution. When the proton counting rates exhibit a rapid increase, the Poisson cumulative sum increases likewise and exceeds the threshold value h. Several small sporadic fluctuations preceding the event proper briefly trigger the primary condition, but they are disregarded because they do not satisfy the requirement for 30

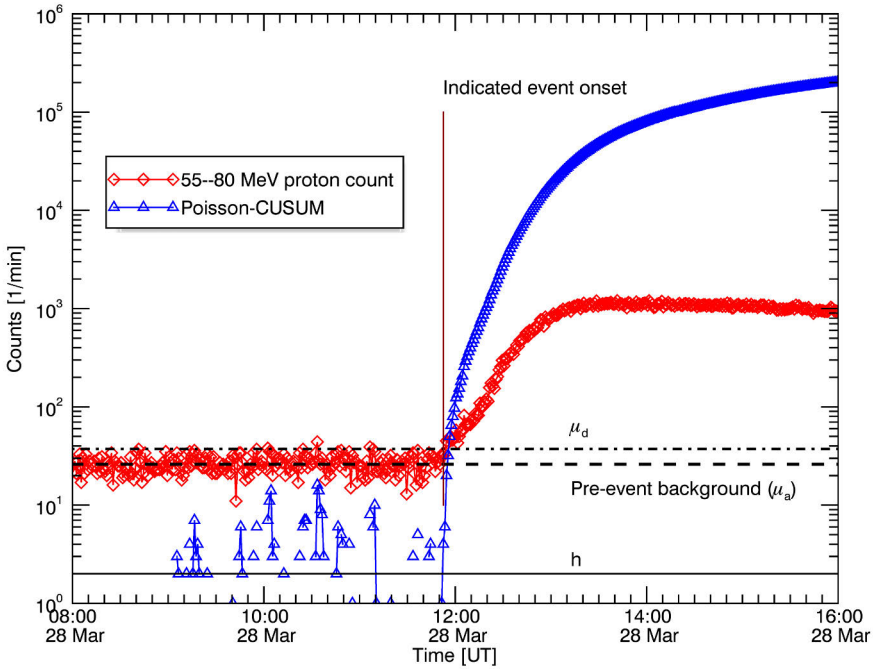

Figure 8. The count rate of 55–80 MeV proton channel (red diamonds) as recorded by ERNE/HED on 28 March 2022 and the corresponding Poisson-CUSUM value (blue triangles). The dashed black line denotes the mean pre-event background, the dashed-dotted black line denotes μ_d, and the solid thin black line the threshold value h (here, h = 2.0). The indicated event onset is marked with a vertical dark red line.

successive instances of $S_i > h$. As a result, the algorithm determines the time of event onset as 11:52 UT.

5.2 Time-shifting analysis

Time-shifting analysis (TSA) is a simple method of estimating the solar release time for SEPs of a given species and kinetic energy E when their time of arrival at a distant observer is known. If we assume the interplanetary magnetic field to be an Archimedean spiral in shape (see Chapter 1.1.2), the length of a field line that connects the solar centre and the observer, passing through the site of origin of the particle, can be calculated as

$$z(r) = \frac{a}{2}\left[\ln\left(\frac{r}{a} + \sqrt{1+\frac{r^2}{a^2}}\right) + \frac{r}{a}\sqrt{1+\frac{r^2}{a^2}}\right], \tag{5}$$

where $a = u_{\mathrm{SW}}/\omega_{\odot}$; u_{SW} is the solar wind speed and $2\pi/\omega_{\odot}$ is the rotation period of the Sun, usually taken as its equatorial value (about 24.47 d). If all scattering effects are neglected, the distance L travelled by the particle along the field line is then

$$L(u_{\mathrm{SW}}) = z(r_{\mathrm{SC}}) - z(\mathrm{R}_{\odot}). \tag{6}$$

In the above equation, r_{SC} and $\mathrm{R}_{\odot}$ are respectively the observer's radial distance from the Sun and the solar radius. These expressions yield an estimate for the release time of the particle, $t_{\mathrm{rel}}(E)$, as follows:

$$t_{\mathrm{rel}}(E) = t_{\mathrm{onset}}(E) - 8.33\,[\mathrm{min/AU}]\,L\,\beta^{-1}(E), \tag{7}$$

where $t_{\mathrm{onset}}(E)$ is the recorded onset and $\beta^{-1}(E)$ the reciprocal speed of the particle species of interest at kinetic energy E.

TSA was utilised in Articles I and II as an alternate or control method for estimating proton release times, as well as the sole method when working with electron data. The latter choice was due to the fact that electron intensities were generally only considered on two or three widely spaced energy channels, making velocity dispersion analysis (VDA; see below) difficult and unreliable. While electron intensity data are available for STEREO/SEPT on 15 channels, attempts at performing VDA with these failed almost without exception, probably because of instrument-related issues (see Article II).

5.3 Velocity dispersion analysis

In cases where SEPs are observed at multiple energy ranges at once and an estimate of the time of event onset can be obtained for each, velocity dispersion analysis (VDA) can be performed. If the release time and the apparent path length traversed by the first-arriving SEPs are assumed to be independent of their kinetic energy, the detected onset time t_{onset} of particles at the kinetic energy E can be expressed as

$$t_{\mathrm{onset}}(E) = t_0 + 8.33\,[\mathrm{min/AU}]\,s\,\beta^{-1}(E), \tag{8}$$

where t_0 is the time of release of the particles (in minutes), s is the apparent SEP path length (in AU) between the source and the observer, and $\beta^{-1}(E)$ is the reciprocal speed of the SEPs. A linear fit to t_{onset} as a function of $\beta^{-1}(E)$ yields estimates for t_0 and s. We used VDA as the primary method for estimating solar release times of protons in Articles I and II.

VDA tends to produce unreliable results in events where the onset determination is made difficult by small or gradual intensity enhancements or an elevated pre-event background, and such a situation often requires that at least some energy channels be dismissed from analysis. Additionally, it is not very uncommon for the linear fit to be statistically plausible yet indicate an obviously unphysical value for s, such as

less or a great deal more than 1 AU. As noted by several authors (e.g. Lintunen and Vainio, 2004; Sáiz et al., 2005; Vainio et al., 2013; see also Articles I and II), the method is susceptible to issues such as varying SEP injection and pre-event intensity conditions and its basic assumptions should not be regarded as strictly correct, even if it usually yields a workable estimate for the particle injection time in most cases.

5.4 SEP event time-intensity profile characterisation

Our study of SEP event time-intensity profiles, detailed in Article III, is in part inspired by Kahler and Ling (2017) who investigated different functional forms to be used for this purpose. They required that the function feature as few parameters as possible but simultaneously render observed profiles reasonably accurately. Using the earlier work of Wilks (1995) as a starting point in turn, they considered the Weibull function as a promising candidate when altered so that the customary independent variable x is replaced with time t and the shape parameter α is allowed to have negative values. This resulted in the following form, dubbed the modified Weibull function:

$$F(t) = \left(-\frac{\alpha}{\beta}\right)\left(\frac{t}{\beta}\right)^{\alpha-1} \exp\left(-\left(\frac{t}{\beta}\right)^{\alpha}\right). \tag{9}$$

The parameter α governs the general shape of the profile, and β scales it along the time axis. The values of the independent variable and parameters are constrained so that $t, \beta > 0$ and $\alpha < 0$.

We adopted this definition but added three new parameters to account for the intensity scaling, time shifting, and background intensity of the event; furthermore, we changed the parameter names (in order to avoid conflict with the magnetic connectivity parameters given in Barcewicz, 2019) and refer to α as a and β as b. Thus, the form the fit function featured in Article III is defined as follows:

$$F(t) = \begin{cases} A_0 \left(\frac{t-t_0}{b}\right)^{a-1} \exp\left(-\left(\frac{t-t_0}{b}\right)^{a}\right) + F_{\mathrm{bg}}; t > t_0 \\ F_{\mathrm{bg}}; t \leq t_0 \end{cases}. \tag{10}$$

Of the additional terms, A_0 scales the curve along the ordinate, t_0 is a time shift parameter, and F_{bg} the pre-event background intensity, here assumed to be constant. For the fit to be physically meaningful, we require that $A_0 > 0$. The time axis origin ($t = 0$) can be defined almost arbitrarily, but we chose it as the onset of the soft X-ray flare associated with the event, to ensure that the definition for the origin is consistent, related to an observable quantity, and precedes the event onset in the vast majority of cases. It should be noted, however, that because the parameters are not completely internally independent, t_0 is not directly equal to the actual physical delay between the onset times of the flare and the SEP event.

Given that the function defined in Equation 10 has a single maximum under the conditions specified above, we can take its derivative with respect to t, set the derivative to zero and solve for A_0:

$$A_0 = I_0 \left(\frac{a-1}{a} \right)^{\frac{1-a}{a}} \exp\left(\frac{a-1}{a} \right). \tag{11}$$

Here, I_0 is the modelled peak intensity in physical units. Plotted examples of modified Weibull curves are presented in Fig. 1 of Article III (q.v.).

We may further define the rise time (that is, the time required to reach the peak intensity after starting from the pre-event background), τ_{rise}, and the total delay between the flare onset ($t = 0$) and the intensity maximum, t_{max}, as

$$\tau_{\mathrm{rise}} = b \left(1 - \frac{1}{a} \right)^{\frac{1}{a}} \tag{12}$$

and

$$t_{\mathrm{max}} = t_0 + \tau_{\mathrm{rise}}. \tag{13}$$

These measures do not entail an explicitly laid out onset criterion for the modelled time-intensity profile, but imply that the event commences immediately when $F(t)$ exceeds F_{bg}.

In practice, we considered the normalised logarithms of observed proton intensity data to avoid possible problems stemming from comparing events that show widely varying maximum intensities. The modified Weibull function as given above was fitted to these applying the Levenberg–Marquardt algorithm. Since the software implementations of the algorithm usually require initial guesses for the fit parameters, and additionally to minimise the risk of the solution converging to a local instead of the global minimum of χ^2, we first constructed a large 5-dimensional matrix for these, with the values chosen so that each covered a range that was deemed reasonable. The routine was then executed with every combination of initial guess values, and of the mathematically successful attempts that found a converging solution, we selected the one that yielded the smallest value of χ^2 divided by the degrees of freedom for the fit. As the final step, the result was inspected visually to confirm that it was indeed sensible. (For additional details of the process, please refer to Appendix A of Article III.)

6 Summary of the original publications

Article I: Catalogue of 55–80 MeV solar proton events extending through solar cycles 23 and 24

In this article, we present a catalogue of near-Earth SEP events spanning the years from 1996 to 2016, i.e. solar cycle 23 and most of solar cycle 24. The 55–80 MeV proton intensity data recorded by SOHO/ERNE served as the basis for the identification of the events; data from other instruments and spacecraft were used to complement these observations in a bid to form a comprehensive picture of each event. In addition to SOHO/ERNE proton and heavy ion data, we made use of near-relativistic electron data from ACE/EPAM, relativistic electron data from SOHO/EPHIN, CME observations by SOHO/LASCO, and soft X-ray intensity data from the GOES spacecraft. Radio frequency observations of the Sun by Wind/WAVES and solar wind proton observations by ACE/SWEPAM and Wind/SWE were utilized in ancillary roles.

We identified and studied a total of 176 SEP events that had occurred during the time period of interest. Where possible, the proton event onset time and date, duration, maximum intensity, integral proton fluence, oxygen fluence (for the energy channel of 5–15 MeV/nucleon), and iron-to-oxygen ratio (for 5–15 MeV/nucleon) were determined, together with the onset time and date and maximum intensity for near-relativistic (0.18–0.31 MeV) and relativistic (0.7–3.0 MeV) electrons. Further, we deduced the likely X-ray flare and CME associations of the event and reported these, calculating additionally the time of maximum slope of the soft X-ray intensity in the cases where the flare/event association was considered at least reasonably securely established and sufficient X-ray data were available. Based on this information, we calculated the approximate solar release times of SEPs using both VDA and TSA for protons and TSA for near-relativistic electrons, which allowed us to perform a simple statistical comparison between three different methods of SEP solar release time estimation (TSA, VDA, and soft X-ray intensity time derivative maximum). Another comparison was made between the two solar cycles with regard to various quantities (TSA and VDA path lengths, solar longitude of the event-related flares, CME width).

Our results indicate that:

1. As also suggested by previous studies (e.g. Vainio et al., 2013), proton VDA

results that indicate a path length between 1 AU and some 3 AU appear to be generally useful, but any cases falling outside of these limits are unreliable in view of the release time estimates based on the event-related X-ray activity.

2. The maximum of time derivative of soft X-ray intensity appears to indicate the (global) solar release times of energetic electrons fairly reliably, and it usually concurs with the TSA-based estimate of the same. This is particularly true for well-connected events, with the difference between the two estimates generally increasing as the magnetic connection of the particle release site to the observer becomes poorer. (For a later, qualitatively similar result derived with a comparison of TSA results and type II radio burst onsets, see Xie et al., 2019.)

3. High-energy SEP events that feature large longitudinal distance between the event-associated X-ray flare and the observer (the Earth) were more frequent in solar cycle 24 than in solar cycle 23. We identified three well-documented events during the former that involved a flare site more than 60 degrees east of the solar central meridian, while none seem to have occurred during the latter; this may point to a characteristic increase of longitudinal width of SEP events in solar cycle 24.

4. While CMEs related to high-energy SEP events were mostly of the halo type (according to the CDAW SOHO LASCO CME Catalog) in both cycles, they were proportionally more frequent in solar cycle 24 than in solar cycle 23 (for a concurring result, see e.g. Gopalswamy et al., 2015b). If we assume the mass densities in the heliosphere to be similar during both cycles, one viable interpretation is that the total heliospheric pressure has been lower in cycle 24, thereby facilitating the formation of an interplanetary shock, which in turn could imply that CMEs have been able to accelerate SEPs towards the Earth from poorly connected sites more effectively during cycle 24 than during cycle 23.

We note that improved statistics might shed additional light on some of the remaining issues, especially with regard to the possible differences of the two solar cycles. Considering simultaneous observations from multiple vantage points (see Article II) is raised as a possibly interesting avenue of further research.

An extended electronic version of the event catalogue presented in this article was created for the Space Radiation Expert Service Centre (R-ESC), established as part of and funded through the Space Weather Service Network/Space Situational Awareness programme of the European Space Agency. This version, which includes graphic representations of the measured particle intensities, proton and oxygen fluences, and Fe/O ratios of the events, as well as concurrent solar X-ray observations, is accessible online at `http://swe.ssa.esa.int/web/guest/`

`utu-srl-federated`. It has been regularly updated by the author of this dissertation after initial release in 2017, and it currently covers 193 55–80 MeV proton events that occurred between September 1997 and March 2022.

Author's contribution

The author contributed to the research topic and approach of the article, performed the data analysis, prepared all of the figures and wrote most of the manuscript.

Article II: Catalogue of >55 MeV Wide-longitude Solar Proton Events Observed by SOHO, ACE, and the STEREOs at ≈1 AU During 2009–2016

In part as a continued investigation into the questions raised in Article I, this article presents and details a catalogue of 46 SEP events that exceed 45 degrees in longitudinal width at 1 AU, as observed from at least two separate locations. SEP species and energies considered are protons at >55 MeV and near-relativistic electrons at 0.18–0.31 MeV. In addition to near-Earth data from SOHO/ERNE (protons), SOHO/LASCO (CMEs), ACE/EPAM (electrons), and GOES (soft X-rays), we included observations by the STEREO-A and STEREO-B spacecraft concerning protons (STEREO/HET), electrons (STEREO/SEPT), CMEs (STEREO/SECCHI/COR1 and COR2), and extreme ultraviolet (STEREO/SECCHI/EUVI) to 1) establish the identity of the SEP events detected at different points in space and their associations with related solar phenomena, namely CMEs, X-ray/ultraviolet flares, and radio bursts, and 2) to study the effects of the longitudinal separation of observers on the characteristics of each event. To this end, we determined the onset times, peak intensities, rise times, durations, and proton fluences for these events. Additionally, in keeping with Article I, we estimated the solar release times of the SEPs by performing VDA and TSA for protons and TSA for electrons.

We found that the highest peak intensities in SEP events typically occur if the observer is magnetically connected to a solar region that lies at or somewhat to the west of the event-related flare. Estimating the mean event longitudinal width through modelling the dependence of the peak intensities on the connection angle with a Gaussian curve and taking the standard deviation of the curve to represent the mean width yields some 44 degrees for protons and some 50 degrees for electrons. These results are essentially in agreement with preceding studies (e.g. Lario et al., 2013; Dresing et al., 2014; Richardson et al., 2014) involving somewhat lower-energy SEPs and suggest that there probably is no strong dependence between event width and SEP energy.

Somewhat unexpectedly, the difference between the SEP release times as estimated with VDA and TSA on one hand and from the time derivative maximum of

the X-ray intensity of the associated flare on the other (called ”release delay” for short in the following) exhibits no straightforward dependence on the absolute value of the connection angle of the observer, with a considerable amount of scatter and conceivably more than one population of events present in the results. The same appears to be true for event rise times, i.e. the time between the onset and the peak intensity of the event. While a lack of clear correlation between the rise times and connection angles in electron events originating from eastern solar hemisphere had been reported earlier by Miteva et al. (2014), it is seen here that even in a larger event sample that contains relatively well-connected cases, a meaningful rise time–connection angle correlation appears to be all but absent. The clear implication is that the extent of the SEP source region together with the details and relative importance of the particle acceleration and transport mechanisms play a vital part in defining the salient characteristics of the event (see also e.g. Dresing et al., 2014). For instance, in cases where the release delay depends strongly on the connection angle, we might interpret this to reflect a diffusive transport from a compact source, while a weak dependence could rather point to a situation where emission from a laterally expanding coronal shock is the dominant mechanism.

There are some indications that although the CMEs related to wide SEP events probably do not differ significantly with respect to mean speed distribution when compared to all SEP events detected at the Earth, halo-type CMEs are more common for wide-longitude SEP events. Our study found that halo CMEs (again, according to the CDAW SOHO LASCO CME Catalog) were associated with 96% of wide-longitude events but with only 81% of all near-Earth events during the same time period.

Author’s contribution

The author contributed to the research topic and approach of the article, performed the data analysis, prepared all of the figures and wrote most of the manuscript.

Article III: Magnetic connectivity and solar energetic proton event intensity profiles at deka-MeV energy

This article features an analysis of the time-intensity profiles of 25 proton events observed near the Earth between the years 1996 and 2015. The profiles were derived by fitting a modified Weibull function to differential proton intensities at 18.2 MeV, obtained from the SEPEM RDS dataset version 2.0. Utilizing the results of a previous work (Barcewicz, 2019) that had studied the magnetic connectivity in a selection of iron-rich SEP events by applying a potential field source surface (PFSS) -based modelling of magnetic field lines in the solar corona (Altschuler and Newkirk, 1969), we were able to investigate the parameters of the fit function, the parameters char-

acterising the connectivity, and the iron-to-carbon ratio of the events in question for statistically significant correlations.

Our results show that the fit function parameter primarily controlling the rise phase and the overall shape of the time-intensity profile is either not dependent, or only weakly dependent at the most, on the magnetic connectivity or the iron-to-carbon ratio of the SEP event. This would seem to indicate that contrary to an intuitive expectation, there are no systematic and definite differences between the time-intensity profiles of well-connected and poorly connected SEP events or between those of iron-rich and nominal-abundance events, if all other conditions are equal. However, the time scaling of the profile is likely at least moderately correlated with magnetic connectivity and the Fe/C abundance ratio: well-connected and iron-rich events tend to be shorter in relative duration than weakly connected and nominal-abundance events. A very similar situation exists with respect to the event rise times and the delay between the event-related flare onset and modelled event intensity maximum, in that these are generally longer for poorly connected and nominal-abundance events than for well-connected and iron-rich events. Broadly speaking, the latter two results conform to the classic categorisation of impulsive and gradual events and their typical features (e.g. Reames, 1988 and others; see also Chapter 1.1).

The first result highlighted above presumably arises because of the combined effect of different transport processes that act on the particles on their way from the source site to the observer in interplanetary space, whereas the second largely accords with established knowledge concerning the intensity profile shapes of SEP events *vis-à-vis* their magnetic connectivity and heavy ion abundances. We note that in order to advance the current understanding substantially, it appears to be necessary to widen the scope of the study in the future by attempting to model the particle transport effects and by including other (especially higher) particle energies so as to improve the statistical underpinnings of the analysis and the conclusions.

The overall data analysis approach of this article was, in part, drawn upon in the design and implementation of the software for the SAWS-ASPECS SEP event forecasting tool (see Chapter 2.1.1). In particular, the ASPECS component responsible for estimating the shape of the time-intensity profile of a predicted or on-going SEP event based on observed data relies on the function fitting method and some of the results featured in Article III, in addition to synthetic profiles generated through numerical simulations.

Author's contribution

The author contributed to the research topic and approach of the article, performed the data analysis, prepared all of the figures and wrote most of the manuscript.

7 Conclusions and outlook

The main focus of the studies presented in this dissertation lies on the quantitative properties of SEP events. Combining the energetic particle measurements with other pertinent data of concurrent solar phenomena, most importantly X-ray and ultraviolet radiation, CMEs and type III radio bursts, allows one to gain an understanding of the associations between these (even if the details of the physical processes involved and their exact relationships may not always be straightforward to uncover) and thereby estimate the location and time of the SEP release at the Sun. This knowledge, in turn, is vital in determining the magnetic connectivity between the SEP site of origin and the observer, which plays an essential role in the transport of electrically charged particles through interplanetary space (e.g. Cane et al., 1988), and its overall impact on the event as observed at a given radial and longitudinal distance from the SEP source. Models that reliably connect solar observables such as the X-ray emissions from a flare with the size and shape of the potentially resulting SEP event would be extremely valuable in predicting space weather and protecting human activity from its adverse effects (e.g. Vainio et al., 2009; Cucinotta et al., 2010; Mishev, 2014; Eastwood et al., 2017), a consideration that has been an important motivation in our research.

In each of the included articles, we have approached the central topic outlined above by studying a large number (several tens) of SEP events. Our chief strategy has been to gain the fullest possible information coverage of every event and, after deriving a numerical measure for the magnetic connectivity, compare this with other important characteristics of the event so as to find statistically significant dependencies. Any such dependencies may then be used as a valuable guide to future research. This sort of an approach can, of course, only produce meaningful results when it is applied to a large set of cases, and it stands in something of a contrast to highly involved studies of single events: the latter might be regarded as most important in shedding light on the details of the physical processes relevant to SEP acceleration and bringing intriguing individual events to the fore, while the former is more oriented towards reaching a general understanding first and then proceeding to study single cases.

The results of the work presented herein show that the early phases of SEP events as recorded at 1 AU do not show any simple type of dependence on the longitudinal distance or the magnetic connectivity (characterised as an angular measurement)

between the particle source and the observer. This conclusion is primarily based on investigating the difference between the VDA/TSA-derived and the X-ray flare-derived particle release times, the event profile rise times (Articles I and II), and the analytical function fits to the SEP event time-intensity profiles (Article III). This observation has important implications on event profile modelling as it shows quite conclusively that correlations useful for describing well-connected and large SEP events (e.g. Ji et al., 2014 and Wang et al., 2022) are not straightforward to generalise to all events. Even though there exist some indications of correlations that seem intuitively plausible and expected—i.e. a poorly connected event exhibits a slow rise, a relatively low peak, and a generally gradual intensity profile shape (see e.g. Reames, 1999; Lario et al., 2006, 2013)—every selection of events featured in this dissertation would appear to contain cases that are highly variable in this respect, or perhaps different populations or classes of cases. Our interpretation of this result is that the transport processes and mechanisms to which the SEPs are exposed on the way from the Sun to the observer have such a strong and complicated effect on the profiles of SEP events that they probably have to be modelled in at least some detail before significant progress towards a better understanding of the wide variety of SEP event shapes can be attained.

The rise times, delays between the onset of the event-related X-ray flare and the modelled onset of the event, and the relative durations of SEP events appear to be somewhat dependent on the magnetic connectivity and the iron abundance of the event, namely so that a poorly connected and nominal-abundance event usually rises more slowly and lasts longer than an otherwise comparable well-connected and iron-rich event (Article III). This, in contrast to the preceding result, essentially conforms to expectations and agrees with the general picture presented in previous studies (e.g. Reames, 1988; Cane et al., 2006).

In addition, we found that the longitudinal width of large SEP events is not strongly dependent or possibly not dependent at all on particle energy (Article II), but may depend to some extent on the conditions prevailing in interplanetary space during the solar cycle of interest (Article I; see also Gopalswamy et al., 2015b and Dagnew et al., 2020). Suggestive of this interpretation is the result that halo CMEs related to SEP events were generally more frequent in solar cycle 24 than in cycle 23 although the former was in general terms quieter than the latter. Nonetheless, this observation and interpretation must be regarded with due caution owing to the fact that our statistics concerning wide events in solar cycle 23 are poorer than what would be desirable. Furthermore, directly comparable multi-spacecraft observations from widely separated locations, which might help settle the issue and such as were utilized in Article II, are not available for solar cycle 23.

Our work has mainly relied on common, well-established methods (such as VDA) widely used in space physics. However, the large number and variety of the studied events has allowed them to be tested thoroughly here, and the results clearly show

the merits of these methods: in many or even most cases, they tend to yield plausible results that can be considered at least roughly correct. At the same time, their shortcomings, principally stemming from various assumptions and simplifications, are also apparent since the methods plainly fail in certain other cases. Indeed, this study as a whole may be regarded as having found a limit of sorts beyond which decidedly more advanced tools and approaches are needed to improve our understanding of SEP events. From a more immediately practical viewpoint, it has produced a comprehensive catalogue of almost 200 SEP events that can serve as a basis for further statistical studies, as well as contributing to an essential part of an online event forecasting system.

Several paths of further research, some already touched upon in the foregoing, seem attractive on the grounds of the results. For the purposes of this discussion, they can be broadly divided into two main categories, observation-based and simulation-based.

Observation-based approaches rely on accumulating more data on SEPs and related solar phenomena in order to improve statistics, which, together with new and refined analysis techniques, should allow one to reach firmer conclusions on the correlations and dependencies already discovered, as well as possibly leading to other discoveries. A logical and straightforward extension of the current work would be to apply the PFSS modelling as featured in Article III to a larger event list (for instance, those in Articles I and II) and other particle energies. Another potentially interesting source of additional information and insight is the SEP data from recent space missions such as Parker Solar Probe and Solar Orbiter. These monitor the Sun at distances significantly less than ≈ 1 AU, meaning that they can be expected to encounter SEPs that have undergone less scattering than those at 1 AU. The role of the transport processes in shaping SEP event profiles might thus become clearer by studying the differences in SEP events as observed by these spacecraft and the ones further away from the Sun.

In Article II, we carried out a brief investigation into the possible relationship between the height of the event-related CME at the VDA-estimated particle release time and the apparent path length indicated by VDA. Such a correlation, if present, could point to a dependence of proton pitch angle scattering on the SEP release height; none was found to exist in our data. However, in view of the limitations of this simple approach, the PFSS modelling and event intensity profile characterisation (Article III) in connection with studying the event-related CMEs might conceivably offer further possibilities to explore the conditions pertaining to the particle release at the Sun, as might a detailed modelling of the three-dimensional geometry of the CME itself. Recent work involving these topics include studies by Isavnin (2016), Zhang (2021), and Dai (2022) on CME geometry, and numerical simulations by Kong et al. (2019) and Kozarev et al. (2022) concerning the initial SEP acceleration by CME-induced shocks in the solar corona.

At any rate, advanced simulations of SEP transport appear to be a necessary complement to the observation-based approaches, especially in view of disentangling the en route effects from the characteristics of the initial particle injection. Among desired qualities for such a simulation would be the self-consistent modelling of the SEP source, inclusion of transport phenomena perpendicular to the nominal interplanetary magnetic field lines, and the ability to run on reasonable computing resources. It is well to note, however, that a number of open questions exist as to the details of the configuration of the interplanetary magnetic field and other related issues, so a great deal of both theoretical and empirical work remains to be done in this field.

List of References

Altschuler, M. D., Newkirk, G. Magnetic Fields and the Structure of the Solar Corona. I: Methods of Calculating Coronal Fields. *Solar Physics*, 9(1):131–149, 1969. doi:10.1007/BF00145734

Ameri, D., Valtonen, E., Al-Sawad, A., Vainio, R. Relationships between energetic storm particle events and interplanetary shocks driven by full and partial halo coronal mass ejections. *Advances in Space Research*, 2022. ISSN 0273-1177. doi:10.1016/j.asr.2022.12.014

Ameri, D., Valtonen, E., Pohjolainen, S. Properties of High-Energy Solar Particle Events Associated with Solar Radio Emissions. *Solar Physics*, 294(9):122, 2019. doi:10.1007/s11207-019-1512-9

Aminalragia-Giamini, S., Sandberg, I., Papadimitriou, C., Daglis, I., Jiggens, P. The virtual enhancements - solar proton event radiation (VESPER) model. *Journal of Space Weather and Space Climate*, 8:A06, 2018. doi:10.1051/swsc/2017040

Anastasiadis, A., Lario, D., Papaioannou, A., Kouloumvakos, A., Vourlidas, A. Solar energetic particles in the inner heliosphere: status and open questions. *Philosophical Transactions of the Royal Society of London Series A*, 377(2148):20180100, 2019. doi:10.1098/rsta.2018.0100

Anderson, H. R. Mariner II: High-Energy-Radiation Experiment. *Science*, 139(3549):42–45, 1963. doi:10.1126/science.139.3549.42

Anglin, J. D., Dietrich, W. F., Simpson, J. A. Super Enrichments of Fe-Group Nuclei in Solar Flares and their Association with Large ^{3}He Enrichments. In *International Cosmic Ray Conference*, volume 5 of *International Cosmic Ray Conference*, page 43. 1977

Aran, A., Agueda, N., Afanasiev, A., Sanahuja, B. *Charged Particle Transport in the Interplanetary Medium*, chapter 4, pages 63–78. Springer International Publishing, Cham, 2018. ISBN 978-3-319-60051-2. doi:10.1007/978-3-319-60051-2_4

Aran, A., Sanahuja, B., Lario, D. SOLPENCO: A solar particle engineering code. *Advances in Space Research*, 37(6):1240–1246, 2006. doi:10.1016/j.asr.2005.09.019

Arge, C. N., Luhmann, J. G., Odstrcil, D., Schrijver, C. J., Li, Y. Stream structure and coronal sources of the solar wind during the May 12th, 1997 CME. *Journal of Atmospheric and Solar-Terrestrial Physics*, 66(15–16):1295–1309, 2004. doi:10.1016/j.jastp.2004.03.018

Asvestari, E., Willamo, T., Gil, A., Usoskin, I. G., Kovaltsov, G. A., Mikhailov, V. V., Mayorov, A. Analysis of Ground Level Enhancements (GLE): Extreme solar energetic particle events have hard spectra. *Advances in Space Research*, 60(4):781–787, 2017. doi:10.1016/j.asr.2016.08.043

Babcock, H. W. The Topology of the Sun's Magnetic Field and the 22-Year Cycle. *The Astrophysical Journal*, 133:572, 1961. doi:10.1086/147060

Balch, C. C. SEC proton prediction model: verification and analysis. *Radiation Measurements*, 30(3):231–250, 1999. ISSN 1350-4487. doi:10.1016/S1350-4487(99)00052-9

Barcewicz, S. *Magnetic connectivity in SEP events*. Master's thesis, Department of Physics and Astronomy, University of Turku, 2019

Battarbee, M., Dalla, S., Marsh, M. S. Solar Energetic Particle Transport Near a Heliospheric Current Sheet. *The Astrophysical Journal*, 836(1):138, 2017. doi:10.3847/1538-4357/836/1/138

Battarbee, M., Dalla, S., Marsh, M. S. Modeling Solar Energetic Particle Transport near a Wavy Heliospheric Current Sheet. *The Astrophysical Journal*, 854(1):23, 2018. doi:10.3847/1538-4357/aaa3fa

Bazilevskaya, G. A., Daibog, E. I., Logachev, Y. I., Vlasova, N. A., Ginzburg, E. A., Ishkov, V. N., Lazutin, L. L., Nguyen, M. D., Surova, G. M., Yakovchouk, O. S. Characteris-

tic Features of Solar Cosmic Rays in the 21st-24th Solar-Activity Cycles According to Data from Catalogs of Solar Proton Events. *Geomagnetism and Aeronomy*, 61(1):6–13, 2021. doi:10.1134/S0016793221010023

Beer, J., Vonmoos, M., Muscheler, R. Solar Variability Over the Past Several Millennia. *Space Science Reviews*, 125(1–4):67–79, 2006. doi:10.1007/s11214-006-9047-4

Bell, A. R. The acceleration of cosmic rays in shock fronts - I. *Monthly Notices of the Royal Astronomical Society*, 182:147–156, 1978. doi:10.1093/mnras/182.2.147

Belov, A., Abunin, A., Abunina, M., Eroshenko, E., Oleneva, V., Yanke, V., Papaioannou, A., Mavromichalaki, H., Gopalswamy, N., Yashiro, S. Coronal Mass Ejections and Non-recurrent Forbush Decreases. *Solar Physics*, 289(10):3949–3960, 2014. doi:10.1007/s11207-014-0534-6

Bieber, J. W., Dröge, W., Evenson, P. A., Pyle, R., Ruffolo, D., Pinsook, U., Tooprakai, P., Rujiwarodom, M., Khumlumlert, T., Krucker, S. Energetic Particle Observations during the 2000 July 14 Solar Event. *The Astrophysical Journal*, 567(1):622, 2002. doi:10.1086/338246

Biji, M. S., Prince, P. R. A study of the characteristic properties of SEP events observed by SOHO ERNE during solar cycle 24. *Advances in Space Research*, 69(7):2902–2920, 2022. doi:10.1016/j.asr.2022.01.024

Boteler, D. H. Geomagnetic effects on the pipe-to-soil potentials of a continental pipeline. *Advances in Space Research*, 26(1):15–20, 2000. ISSN 0273-1177. doi:10.1016/S0273-1177(99)01020-0. Space Weather: Physics and Applications.

Boteler, D. H. A 21st Century View of the March 1989 Magnetic Storm. *Space Weather*, 17(10):1427–1441, 2019. doi:10.1029/2019SW002278

Bougeret, J. L., Goetz, K., Kaiser, M. L., Bale, S. D., Kellogg, P. J., Maksimovic, M., Monge, N., Monson, S. J., Astier, P. L., Davy, S., Dekkali, M., Hinze, J. J., Manning, R. E., Aguilar-Rodriguez, E., Bonnin, X., Briand, C., Cairns, I. H., Cattell, C. A., Cecconi, B., Eastwood, J., Ergun, R. E., Fainberg, J., Hoang, S., Huttunen, K. E. J., Krucker, S., Lecacheux, A., MacDowall, R. J., Macher, W., Mangeney, A., Meetre, C. A., Moussas, X., Nguyen, Q. N., Oswald, T. H., Pulupa, M., Reiner, M. J., Robinson, P. A., Rucker, H., Salem, C., Santolik, O., Silvis, J. M., Ullrich, R., Zarka, P., Zouganelis, I. S/WAVES: The Radio and Plasma Wave Investigation on the STEREO Mission. *Space Science Reviews*, 136(1–4):487–528, 2008. doi:10.1007/s11214-007-9298-8

Bougeret, J. L., Kaiser, M. L., Kellogg, P. J., Manning, R., Goetz, K., Monson, S. J., Monge, N., Friel, L., Meetre, C. A., Perche, C., Sitruk, L., Hoang, S. Waves: The Radio and Plasma Wave Investigation on the Wind Spacecraft. *Space Science Reviews*, 71(1–4):231–263, 1995. doi:10.1007/BF00751331

Bronarska, K., Michalek, G. Characteristics of active regions associated to large solar energetic proton events. *Advances in Space Research*, 59(1):384–392, 2017. doi:10.1016/j.asr.2016.09.011

Brueckner, G. E., Howard, R. A., Koomen, M. J., Korendyke, C. M., Michels, D. J., Moses, J. D., Socker, D. G., Dere, K. P., Lamy, P. L., Llebaria, A., Bout, M. V., Schwenn, R., Simnett, G. M., Bedford, D. K., Eyles, C. J. The Large Angle Spectroscopic Coronagraph (LASCO). *Solar Physics*, 162(1–2):357–402, 1995. doi:10.1007/BF00733434

Bruno, A., Bazilevskaya, G. A., Boezio, M., Christian, E. R., de Nolfo, G. A., Martucci, M., Merge', M., Mikhailov, V. V., Munini, R., Richardson, I. G., Ryan, J. M., Stochaj, S., Adriani, O., Barbarino, G. C., Bellotti, R., Bogomolov, E. A., Bongi, M., Bonvicini, V., Bottai, S., Cafagna, F., Campana, D., Carlson, P., Casolino, M., Castellini, G., De Santis, C., Di Felice, V., Galper, A. M., Karelin, A. V., Koldashov, S. V., Koldobskiy, S., Krutkov, S. Y., Kvashnin, A. N., Leonov, A., Malakhov, V., Marcelli, L., Mayorov, A. G., Menn, W., Mocchiutti, E., Monaco, A., Mori, N., Osteria, G., Panico, B., Papini, P., Pearce, M., Picozza, P., Ricci, M., Ricciarini, S. B., Simon, M., Sparvoli, R., Spillantini, P., Stozhkov, Y. I., Vacchi, A., Vannuccini, E., Vasilyev, G. I., Voronov, S. A., Yurkin, Y. T., Zampa, G., Zampa, N. Solar Energetic Particle Events Observed by the PAMELA Mission. *The Astrophysical Journal*, 862(2):97, 2018. doi:10.3847/1538-4357/aacc26

Bruno, A., Richardson, I. G. Empirical Model of 10 - 130 MeV Solar Energetic Particle Spectra at 1 AU Based on Coronal Mass Ejection Speed and Direction. *Solar Physics*, 296(2):36, 2021. doi:10.1007/s11207-021-01779-4

Bruno, R., Carbone, V. The Solar Wind as a Turbulence Laboratory. *Living Reviews in Solar Physics*, 10(1):2, 2013. doi:10.12942/lrsp-2013-2

Bühler, P., Desorgher, L., Zehnder, A. Simple Instruments for Continuous Measurement of Trapped Particles. In T. D. Guyenne, A. Hilgers (editors), *Environment Modeling for Space-Based Applications*, volume 392 of *ESA Special Publication*, page 87. 1996

Burrell, M. O. The risk of solar proton events to space missions. *Proceedings of the National Symposium on Natural and Manmade Radiation in Space*, pages 310–323, 1972

Cade III, W. B., Chan-Park, C. The Origin of "Space Weather". *Space Weather*, 13(2):99–103, 2015. doi:10.1002/2014SW001141

Cairns, I. H., Knock, S. A., Robinson, P. A., Kuncic, Z. Type II Solar Radio Bursts: Theory and Space Weather Implications. *Space Science Reviews*, 107:27–34, 2003. doi:10.1023/A:1025503201687

Cane, H. V., Erickson, W. C., Prestage, N. P. Solar flares, type III radio bursts, coronal mass ejections, and energetic particles. *Journal of Geophysical Research (Space Physics)*, 107(A10):1315, 2002. doi:10.1029/2001JA000320

Cane, H. V., McGuire, R. E., von Rosenvinge, T. T. Two Classes of Solar Energetic Particle Events Associated with Impulsive and Long-Duration Soft X-Ray Flares. *The Astrophysical Journal*, 301:448, 1986. doi:10.1086/163913

Cane, H. V., Mewaldt, R. A., Cohen, C. M. S., von Rosenvinge, T. T. Role of flares and shocks in determining solar energetic particle abundances. *Journal of Geophysical Research (Space Physics)*, 111(A6):A06S90, 2006. doi:10.1029/2005JA011071

Cane, H. V., Reames, D. V., von Rosenvinge, T. T. The role of interplanetary shocks in the longitude distribution of solar energetic particles. *Journal of Geophysical Research*, 93(A9):9555–9567, 1988. doi:10.1029/JA093iA09p09555

Cane, H. V., Richardson, I. G., St. Cyr, O. C. Coronal mass ejections, interplanetary ejecta and geomagnetic storms. *Geophysical Research Letters*, 27(21):3591–3594, 2000. doi:10.1029/2000GL000111

Cane, H. V., Richardson, I. G., von Rosenvinge, T. T. A study of solar energetic particle events of 1997–2006: Their composition and associations. *Journal of Geophysical Research (Space Physics)*, 115(A8):A08101, 2010. doi:10.1029/2009JA014848

Carrington, R. C. Description of a Singular Appearance seen in the Sun on September 1, 1859. *Monthly Notices of the Royal Astronomical Society*, 20:13–15, 1859. doi:10.1093/mnras/20.1.13

Chandra, R., Gopalswamy, N., Mäkelä, P., Xie, H., Yashiro, S., Akiyama, S., Uddin, W., Srivastava, A. K., Joshi, N. C., Jain, R., Awasthi, A. K., Manoharan, P. K., Mahalakshmi, K., Dwivedi, V. C., Choudhary, D. P., Nitta, N. V. Solar energetic particle events during the rise phases of solar cycles 23 and 24. *Advances in Space Research*, 52(12):2102–2111, 2013. doi:10.1016/j.asr.2013.09.006

Charbonneau, P. Dynamo Models of the Solar Cycle. *Living Reviews in Solar Physics*, 7(1):3, 2010. doi:10.12942/lrsp-2010-3

Clark, D. H., Stephenson, F. R. An Interpretation of the Pre-Telescopic Sunspot Records from the Orient. *Quarterly Journal of the Royal Astronomical Society*, 19:387, 1978

Clauset, A., Rohilla Shalizi, C., Newman, M. E. J. Power-law distributions in empirical data. *arXiv e-prints*, arXiv:0706.1062, 2007

Cliver, E. W., D'Huys, E. Size Distributions of Solar Proton Events and Their Associated Soft X-Ray Flares: Application of the Maximum Likelihood Estimator. *The Astrophysical Journal*, 864(1):48, 2018. doi:10.3847/1538-4357/aad043

Cliver, E. W., Kahler, S. W., Shea, M. A., Smart, D. F. Injection onsets of 2 GeV protons, 1 MeV electrons, and 100 keV electrons in solar cosmic ray flares. *The Astrophysical Journal*, 260:362–370, 1982. doi:10.1086/160261

Cohen, C. M. S., Mason, G. M., Mewaldt, R. A. Characteristics of Solar Energetic Ions as a Function of Longitude. *The Astrophysical Journal*, 843(2):132, 2017. doi:10.3847/1538-4357/aa7513

Crosby, N., Heynderickx, D., Jiggens, P., Aran, A., Sanahuja, B., Truscott, P., Lei, F., Jacobs, C., Poedts, S., Gabriel, S., Sandberg, I., Glover, A., Hilgers, A. SEPEM: A tool for statisti-

cal modeling the solar energetic particle environment. *Space Weather*, 13(7):406–426, 2015. doi:10.1002/2013SW001008

Crosby, N. B., Aschwanden, M. J., Dennis, B. R. Frequency distributions and correlations of solar X-ray flare parameters. *Solar Physics*, 143(2):275–299, 1993. doi:10.1007/BF00646488

Cucinotta, F. A., Hu, S., Schwadron, N. A., Kozarev, K., Townsend, L. W., Kim, M.-H. Y. Space radiation risk limits and Earth-Moon-Mars environmental models. *Space Weather*, 8:S00E09, 2010. doi:10.1029/2010SW000572

Dagnew, F. K., Gopalswamy, N., Tessema, S. B., Akiyama, S., Yashiro, S., Tesfu, T. Y. Intercycle and Intracycle Variation of Halo CME Rate Obtained from SOHO/LASCO Observations. *The Astrophysical Journal*, 903(2):118, 2020. doi:10.3847/1538-4357/abb887

Dai, X. A Time-dependent Self-similar Reconstruction of Solar Coronal Mass Ejections Based on the Gibson-Low Model. *The Astrophysical Journal*, 925(1):24, 2022. doi:10.3847/1538-4357/ac3eda

Dalla, S., Marsh, M. S., Battarbee, M. Solar Energetic Particle Drifts and the Energy Dependence of 1 AU Charge States. *The Astrophysical Journal*, 834(2):167, 2017. doi:10.3847/1538-4357/834/2/167

Dalla, S., Marsh, M. S., Laitinen, T. Drift-induced Deceleration of Solar Energetic Particles. *The Astrophysical Journal*, 808(1):62, 2015. doi:10.1088/0004-637X/808/1/62

Decker, R. B. Computer Modeling of Test Particle Acceleration at Oblique Shocks. *Space Science Reviews*, 48(3–4):195–262, 1988. doi:10.1007/BF00226009

Decker, R. B. Particle acceleration at shocks with surface ripples. *Journal of Geophysical Research*, 95:11993–12003, 1990. doi:10.1029/JA095iA08p11993

Dennis, B. R., Zarro, D. M. The Neupert Effect - what can it Tell up about the Impulsive and Gradual Phases of Solar Flares. *Solar Physics*, 146(1):177–190, 1993. doi:10.1007/BF00662178

Desai, M., Giacalone, J. Large gradual solar energetic particle events. *Living Reviews in Solar Physics*, 13(1):3, 2016. doi:10.1007/s41116-016-0002-5

Dierckxsens, M., Tziotziou, K., Dalla, S., Patsou, I., Marsh, M. S., Crosby, N. B., Malandraki, O., Tsiropoula, G. Relationship between Solar Energetic Particles and Properties of Flares and CMEs: Statistical Analysis of Solar Cycle 23 Events. *Solar Physics*, 290(3):841–874, 2015. doi:10.1007/s11207-014-0641-4

Dodd, P. E., Massengill, L. W. Basic mechanisms and modeling of single-event upset in digital microelectronics. *IEEE Transactions on Nuclear Science*, 50(3):583–602, 2003. doi:10.1109/TNS.2003.813129

Domingo, V., Fleck, B., Poland, A. I. The SOHO Mission: an Overview. *Solar Physics*, 162(1–2):1–37, 1995. doi:10.1007/BF00733425

Donnelly, E. H., Nemhauser, J. B., Smith, J. M., Kazzi, Z. N., Farfán, E. B., Chang, A. S., Naeem, S. F. Acute radiation syndrome: assessment and management. *Southern Medical Journal*, 103(6):541–546, 2010. doi:10.1097/SMJ.0b013e3181ddd571

Drake, J. F., Cassak, P. A., Shay, M. A., Swisdak, M., Quataert, E. A Magnetic Reconnection Mechanism for Ion Acceleration and Abundance Enhancements in Impulsive Flares. *The Astrophysical Journal Letters*, 700(1):L16–L20, 2009. doi:10.1088/0004-637X/700/1/L16

Drake, J. F., Swisdak, M. Ion Heating and Acceleration During Magnetic Reconnection Relevant to the Corona. *Space Science Reviews*, 172(1–4):227–240, 2012. doi:10.1007/s11214-012-9903-3

Dresing, N., Effenberger, F., Gómez-Herrero, R., Heber, B., Klassen, A., Kollhoff, A., Richardson, I., Theesen, S. Statistical Results for Solar Energetic Electron Spectra Observed over 12 yr with STEREO/SEPT. *The Astrophysical Journal*, 889(2):143, 2020. doi:10.3847/1538-4357/ab64e5

Dresing, N., Gómez-Herrero, R., Heber, B., Klassen, A., Malandraki, O., Dröge, W., Kartavykh, Y. Statistical survey of widely spread out solar electron events observed with STEREO and ACE with special attention to anisotropies. *Astronomy & Astrophysics*, 567:A27, 2014. doi:10.1051/0004-6361/201423789

Dresing, N., Gómez-Herrero, R., Klassen, A., Heber, B., Kartavykh, Y., Dröge, W. The Large Longitudinal Spread of Solar Energetic Particles During the 17 January 2010 Solar Event. *Solar Physics*, 281(1):281–300, 2012. doi:10.1007/s11207-012-0049-y

Dröge, W. Particle Scattering by Magnetic Fields. *Cosmic Rays and Earth*, pages 121–151, 2000. doi:10.1023/A:1026588210726

Dröge, W., Kartavykh, Y. Y., Dresing, N., Heber, B., Klassen, A. Wide longitudinal distribution of interplanetary electrons following the 7 February 2010 solar event: Observations and transport modeling. *Journal of Geophysical Research (Space Physics)*, 119(8):6074–6094, 2014. doi:10.1002/2014JA019933

Dröge, W., Kartavykh, Y. Y., Dresing, N., Klassen, A. Multi-spacecraft Observations and Transport Modeling of Energetic Electrons for a Series of Solar Particle Events in August 2010. *The Astrophysical Journal*, 826(2):134, 2016. doi:10.3847/0004-637X/826/2/134

Dulk, G. A. Radio emission from the Sun and stars. *Annual Review of Astronomy and Astrophysics*, 23:169–224, 1985. doi:10.1146/annurev.aa.23.090185.001125

Eastwood, J. P., Biffis, E., Hapgood, M. A., Green, L., Bisi, M. M., Bentley, R. D., Wicks, R., McKinnell, L. A., Gibbs, M., Burnett, C. The Economic Impact of Space Weather: Where Do We Stand? *Risk Analysis*, 37(2):206–218, 2017. doi:10.1111/risa.12765

Eddy, J. A. The Maunder Minimum. *Science*, 192(4245):1189–1202, 1976. doi:10.1126/science.192.4245.1189

Eichler, D. Ultraheavy Element Enrichment in Impulsive Solar Flares. *The Astrophysical Journal*, 794(1):6, 2014. doi:10.1088/0004-637X/794/1/6

Elgarøy, E. Ø. *Solar noise storms*. Pergamon Press, Oxford, 1977

Emslie, A. G., Dennis, B. R., Shih, A. Y., Chamberlin, P. C., Mewaldt, R. A., Moore, C. S., Share, G. H., Vourlidas, A., Welsch, B. T. Global Energetics of Thirty-eight Large Solar Eruptive Events. *The Astrophysical Journal*, 759(1):71, 2012. doi:10.1088/0004-637X/759/1/71

Engelbrecht, N. E., Strauss, R. D., le Roux, J. A., Burger, R. A. Toward a Greater Understanding of the Reduction of Drift Coefficients in the Presence of Turbulence. *The Astrophysical Journal*, 841(2):107, 2017. doi:10.3847/1538-4357/aa7058

Engell, A. J., Falconer, D. A., Schuh, M., Loomis, J., Bissett, D. SPRINTS: A Framework for Solar-Driven Event Forecasting and Research. *Space Weather*, 15(10):1321–1346, 2017. doi:10.1002/2017SW001660

Feynman, J., Armstrong, T. P., Dao-Gibner, L., Silverman, S. New interplanetary proton fluence model. *Journal of Spacecraft and Rockets*, 27:403–410, 1990. doi:10.2514/3.26157

Feynman, J., Gabriel, S. B. Period and phase of the 88-year solar cycle and the Maunder minimum: Evidence for a chaotic sun. *Solar Physics*, 127(2):393–403, 1990. doi:10.1007/BF00152176

Feynman, J., Spitale, G., Wang, J., Gabriel, S. Interplanetary proton fluence model: JPL 1991. *Journal of Geophysical Research*, 98(A8):13281–13294, 1993. doi:10.1029/92JA02670

Firoz, K. A., Gan, W. Q., Li, Y. P., Rodríguez-Pacheco, J., Dorman, L. I. Duration and Fluence of Major Solar Energetic Particle (SEP) Events. *Solar Physics*, 297(6):71, 2022. doi:10.1007/s11207-022-01994-7

Firoz, K. A., Gan, W. Q., Li, Y. P., Rodríguez-Pacheco, J., Kudela, K. On the Possible Mechanism of GLE Initiation. *The Astrophysical Journal*, 872(2):178, 2019. doi:10.3847/1538-4357/ab0381

Fisk, L. A. ^{3}He-rich flares: A possible explanation. *The Astrophysical Journal*, 224:1048–1055, 1978. doi:10.1086/156456

Forbush, S. E. On the Effects in Cosmic-Ray Intensity Observed During the Recent Magnetic Storm. *Physical Review*, 51(12):1108–1109, 1937. doi:10.1103/PhysRev.51.1108.3

Forbush, S. E. Three Unusual Cosmic-Ray Increases Possibly Due to Charged Particles from the Sun. *Physical Review*, 70(9–10):771–772, 1946. doi:10.1103/PhysRev.70.771

Fox, N. J., Velli, M. C., Bale, S. D., Decker, R., Driesman, A., Howard, R. A., Kasper, J. C., Kinnison, J., Kusterer, M., Lario, D., Lockwood, M. K., McComas, D. J., Raouafi, N. E., Szabo, A. The Solar Probe Plus Mission: Humanity's First Visit to Our Star. *Space Science Reviews*, 204(1–4):7–48, 2016. doi:10.1007/s11214-015-0211-6

Frederickson, A. Upsets related to spacecraft charging. *IEEE Transactions on Nuclear Science*, 43(2):426–441, 1996. doi:10.1109/23.490891

Fröhlich, C. Total Solar Irradiance Observations. *Surveys in Geophysics*, 33(3–4):453–473, 2012. doi:10.1007/s10712-011-9168-5

Galvin, A. B., Kistler, L. M., Popecki, M. A., Farrugia, C. J., Simunac, K. D. C., Ellis, L., Möbius, E., Lee, M. A., Boehm, M., Carroll, J., Crawshaw, A., Conti, M., Demaine, P., Ellis, S., Gaidos, J. A., Googins, J., Granoff, M., Gustafson, A., Heirtzler, D., King, B., Knauss, U., Levasseur, J., Longworth, S., Singer, K., Turco, S., Vachon, P., Vosbury, M., Widholm, M., Blush, L. M., Karrer, R., Bochsler, P., Daoudi, H., Etter, A., Fischer, J., Jost, J., Opitz, A., Sigrist, M., Wurz, P., Klecker, B., Ertl, M., Seidenschwang, E., Wimmer-Schweingruber, R. F., Koeten, M., Thompson, B., Steinfeld, D. The Plasma and Suprathermal Ion Composition (PLASTIC) Investigation on the STEREO Observatories. *Space Science Reviews*, 136(1–4):437–486, 2008. doi:10.1007/s11214-007-9296-x

Garcia, H. A. Temperature and Emission Measure from GOES Soft X-Ray Measurements. *Solar Physics*, 154(2):275–308, 1994. doi:10.1007/BF00681100

Georgoulis, M. K., Papaioannou, A., Sandberg, I., Anastasiadis, A., Daglis, I. A., Rodríguez-Gasén, R., Aran, A., Sanahuja, B., Nieminen, P. Analysis and interpretation of inner-heliospheric SEP events with the ESA Standard Radiation Environment Monitor (SREM) onboard the INTEGRAL and Rosetta Missions. *Journal of Space Weather and Space Climate*, 8:A40, 2018. doi:10.1051/swsc/2018027

Gergely, T. E., Erickson, W. C. Decameter Storm Radiation, I. *Solar Physics*, 42(2):467–486, 1975. doi:10.1007/BF00149927

Giacalone, J., Jokipii, J. R., Mazur, J. E. Small-scale Gradients and Large-scale Diffusion of Charged Particles in the Heliospheric Magnetic Field. *The Astrophysical Journal*, 532(1):L75–L78, 2000. doi:10.1086/312564

Glassmeier, K.-H., Boehnhardt, H., Koschny, D., Kührt, E., Richter, I. The Rosetta Mission: Flying Towards the Origin of the Solar System. *Space Science Reviews*, 128(1–4):1–21, 2007. doi:10.1007/s11214-006-9140-8

Gleissberg, W. A long-periodic fluctuation of the sun-spot numbers. *The Observatory*, 62:158–159, 1939

Gold, R. E., Krimigis, S. M., Hawkins III, S. E., Haggerty, D. K., Lohr, D. A., Fiore, E., Armstrong, T. P., Holland, G., Lanzerotti, L. J. Electron, Proton, and Alpha Monitor on the Advanced Composition Explorer spacecraft. *Space Science Reviews*, 86:541–562, 1998. doi:10.1023/A:1005088115759

Gopalswamy, N. Corona Mass Ejections: a Summary of Recent Results. In I. Dorotovic (editor), *20th National Solar Physics Meeting*, volume 20, pages 108–130. 2010

Gopalswamy, N., Akiyama, S., Yashiro, S., Mäkelä, P. Coronal Mass Ejections from Sunspot and Non-Sunspot Regions. In *Magnetic Coupling between the Interior and Atmosphere of the Sun*, volume 19 of *Astrophysics and Space Science Proceedings*, pages 289–307. 2010. doi:10.1007/978-3-642-02859-5_24

Gopalswamy, N., Mäkelä, P., Yashiro, S., Xie, H., Akiyama, S., Thakur, N. High-energy solar particle events in cycle 24. In *Journal of Physics Conference Series*, volume 642 of *Journal of Physics Conference Series*, page 012012. 2015a. doi:10.1088/1742-6596/642/1/012012

Gopalswamy, N., Xie, H., Akiyama, S., Mäkelä, P., Yashiro, S., Michalek, G. The Peculiar Behavior of Halo Coronal Mass Ejections in Solar Cycle 24. *The Astrophysical Journal Letters*, 804(1):L23, 2015b. doi:10.1088/2041-8205/804/1/L23

Gopalswamy, N., Xie, H., Akiyama, S., Mäkelä, P. A., Yashiro, S. Major solar eruptions and high-energy particle events during solar cycle 24. *Earth, Planets and Space*, 66:104, 2014. doi:10.1186/1880-5981-66-104

Gopalswamy, N., Xie, H., Yashiro, S., Akiyama, S., Mäkelä, P., Usoskin, I. G. Properties of Ground Level Enhancement Events and the Associated Solar Eruptions During Solar Cycle 23. *Space Science Reviews*, 171(1–4):23–60, 2012. doi:10.1007/s11214-012-9890-4

Gopalswamy, N., Yashiro, S., Michalek, G., Stenborg, G., Vourlidas, A., Freeland, S., Howard, R. The SOHO/LASCO CME Catalog. *Earth, Moon, and Planets*, 104(1–4):295–313, 2009. doi:10.1007/s11038-008-9282-7

Gordon, B. E., Lee, M. A., Möbius, E., Trattner, K. J. Coupled hydromagnetic wave excitation and ion acceleration at interplanetary traveling shocks and Earth's bow shock revisited. *Journal of Geophysical Research*, 104(A12):28263–28278, 1999. doi:10.1029/1999JA900356

Gosling, J. T., McComas, D. J., Phillips, J. L., Bame, S. J. Geomagnetic activity associated with earth passage of interplanetary shock disturbances and coronal mass ejections. *Journal of Geophysical Research*, 96(A5):7831–7839, 1991. doi:10.1029/91JA00316

Green, L. M., Matthews, S. A., van Driel-Gesztelyi, L., Harra, L. K., Culhanan, J. L. Multi-wavelength observations of an X-class flare without a coronal mass ejection. *Solar Physics*, 205:325–339, 2002. doi:10.1023/A:1014211528863

Greenkorn, R. A. Analysis of Sunspot Activity Cycles. *Solar Physics*, 255(2):301–323, 2009. doi:10.1007/s11207-009-9331-z

Guo, F., Jokipii, J. R., Kota, J. Particle Acceleration by Collisionless Shocks Containing Large-scale Magnetic-field Variations. *The Astrophysical Journal*, 725(1):128–133, 2010. doi:10.1088/0004-637X/725/1/128

Hale, G. E. On the Probable Existence of a Magnetic Field in Sun-Spots. *The Astrophysical Journal*, 28:315, 1908. doi:10.1086/141602

Hale, G. E., Ellerman, F., Nicholson, S. B., Joy, A. H. The Magnetic Polarity of Sun-Spots. *The Astrophysical Journal*, 49:153, 1919. doi:10.1086/142452

Hanser, F. A., Sellers, F. B. Design and calibration of the GOES-8 solar X-ray sensor: the XRS. In E. R. Washwell (editor), *GOES-8 and Beyond*, volume 2812, pages 344–352. International Society for Optics and Photonics, SPIE, 1996. doi:10.1117/12.254082

Hart, S. T., Dayeh, M. A., Bučík, R., Desai, M. I., Ebert, R. W., Ho, G. C., Li, G., Mason, G. M. Statistical Study and Live Catalog of Multispacecraft ^{3}He-rich Time Periods over Solar Cycles 23, 24, and 25. *The Astrophysical Journal Supplement Series*, 263(2):22, 2022. doi:10.3847/1538-4365/ac91c1

Hathaway, D. H. The Solar Cycle. *Living Reviews in Solar Physics*, 12(1):4, 2015. doi:10.1007/lrsp-2015-4

He, H. Q., Wan, W. On the east-west longitudinally asymmetric distribution of solar proton events. *Monthly Notices of the Royal Astronomical Society*, 464(1):85–93, 2017. doi:10.1093/mnras/stw2255

Hess, V. On the Observations of the Penetrating Radiation during Seven Balloon Flights. *arXiv e-prints*, arXiv:1808.02927, 1912

Hey, J. S. Solar Radiations in the 4–6 Metre Radio Wave-Length Band. *Nature*, 157(3976):47–48, 1946. doi:10.1038/157047b0

Hillaris, A., Bouratzis, C., Nindos, A. Interplanetary Type IV Bursts. *Solar Physics*, 291(7):2049–2069, 2016. doi:10.1007/s11207-016-0946-6

Hodgson, R. On a curious Appearance seen in the Sun. *Monthly Notices of the Royal Astronomical Society*, 20:15–16, 1859. doi:10.1093/mnras/20.1.15

Howard, R. A., Moses, J. D., Socker, D. G. Sun-Earth connection coronal and heliospheric investigation (SECCHI). In S. Fineschi, C. M. Korendyke, O. H. Siegmund, B. E. Woodgate (editors), *Instrumentation for UV/EUV Astronomy and Solar Missions*, volume 4139 of *Society of Photo-Optical Instrumentation Engineers (SPIE) Conference Series*, pages 259–283. 2000. doi:10.1117/12.410527

Hoyt, D. V., Schatten, K. H. Group Sunspot Numbers: A New Solar Activity Reconstruction. *Solar Physics*, 179:189–219, 1998a. doi:10.1023/A:1005007527816

Hoyt, D. V., Schatten, K. H. Group Sunspot Numbers: A New Solar Activity Reconstruction. *Solar Physics*, 181:491–512, 1998b. doi:10.1023/A:1005056326158

Hsieh, K. C., Simpson, J. A. The Relative Abundances and Energy Spectra of ^{3}He and ^{4}He from Solar Flares. *The Astrophysical Journal*, 162:L191, 1970. doi:10.1086/180652

Hua, X.-M., Kozlovsky, B., Lingenfelter, R. E., Ramaty, R., Stupp, A. Angular and Energy-dependent Neutron Emission from Solar Flare Magnetic Loops. *The Astrophysical Journal Supplement Series*, 140(2):563–579, 2002. doi:10.1086/339372

Hudson, H. S. Global Properties of Solar Flares. *Space Science Reviews*, 158(1):5–41, 2011. doi:10.1007/s11214-010-9721-4

Huttunen-Heikinmaa, K., Valtonen, E., Laitinen, T. Proton and helium release times in SEP events observed with SOHO/ERNE. *Astronomy & Astrophysics*, 442(2):673–685, 2005. doi:10.1051/0004-6361:20042620

Isavnin, A. FRiED: A Novel Three-dimensional Model of Coronal Mass Ejections. *The Astrophysical Journal*, 833(2):267, 2016. doi:10.3847/1538-4357/833/2/267

Iwai, K., Yashiro, S., Nitta, N. V., Kubo, Y. Spectral Structures of Type II Solar Radio Bursts and Solar Energetic Particles. *The Astrophysical Journal*, 888(1):50, 2020. doi:10.3847/1538-4357/ab57ff

Jacobs, C. *Magnetohydrodynamic modelling of the solar wind and coronal mass ejections*. Master's thesis, Katholieke Universiteit Leuven, 2007.

Jaynes, E. T. Information Theory and Statistical Mechanics. *Physical Review*, 106(4):620–630, 1957. doi:10.1103/PhysRev.106.620

Ji, E.-Y., Moon, Y.-J., Park, J. Forecast of solar proton flux profiles for well-connected events. *Journal of Geophysical Research (Space Physics)*, 119(12):9383–9394, 2014. doi:10.1002/2014JA020333

Jiggens, P., Varotsou, A., Truscott, P., Heynderickx, D., Lei, F., Evans, H., Daly, E. The Solar Accumulated and Peak Proton and Heavy Ion Radiation Environment (SAPPHIRE) Model. *IEEE Transactions on Nuclear Science*, 65(2):698–711, 2018. doi:10.1109/TNS.2017.2786581

Jiggens, P. T. A., Gabriel, S. B., Heynderickx, D., Crosby, N., Glover, A., Hilgers, A. ESA SEPEM Project: Peak Flux and Fluence Model. *IEEE Transactions on Nuclear Science*, 59(4):1066–1077, 2012. doi:10.1109/TNS.2012.2198242

Jokipii, J. R. Particle drift, diffusion, and acceleration at shocks. *The Astrophysical Journal*, 255:716–720, 1982. doi:10.1086/159870

Jones, F. C., Jokipii, J. R., Baring, M. G. Charged-Particle Motion in Electromagnetic Fields Having at Least One Ignorable Spatial Coordinate. *The Astrophysical Journal*, 509(1):238–243, 1998. doi:10.1086/306480

Jones, J. A., Casey, R. C., Karouia, F. 14.10 - Ionizing Radiation as a Carcinogen. In McQueen, Charlene A. (editor), *Comprehensive Toxicology*, pages 181–228. Elsevier, Oxford, second edition, 2010. ISBN 978-0-08-046884-6. doi:10.1016/B978-0-08-046884-6.01411-1

Kahler, S. W. Solar Energetic Particle Event Onsets: Far Backside Solar Sources and the East-West Hemispheric Asymmetry. *The Astrophysical Journal*, 819(2):105, 2016. doi:10.3847/0004-637X/819/2/105

Kahler, S. W., Hildner, E., Van Hollebeke, M. A. I. Prompt solar proton events and coronal mass ejections. *Solar Physics*, 57(2):429–443, 1978. doi:10.1007/BF00160116

Kahler, S. W., Ling, A. G. Characterizing Solar Energetic Particle Event Profiles with Two-Parameter Fits. *Solar Physics*, 292(4):59, 2017. doi:10.1007/s11207-017-1085-4

Kahler, S. W., Ling, A. G. Suprathermal Ion Backgrounds of Solar Energetic Particle Events. *The Astrophysical Journal*, 872(1):89, 2019. doi:10.3847/1538-4357/aafb03

Kahler, S. W., Reames, D. V., Sheeley, J., N. R. Coronal Mass Ejections Associated with Impulsive Solar Energetic Particle Events. *The Astrophysical Journal*, 562(1):558–565, 2001. doi:10.1086/323847

Kahler, S. W., Vourlidas, A. Solar Energetic Particle Events in Different Types of Solar Wind. *The Astrophysical Journal*, 791(1):4, 2014. doi:10.1088/0004-637X/791/1/4

Kallenrode, M. B., Cliver, E. W., Wibberenz, G. Composition and Azimuthal Spread of Solar Energetic Particles from Impulsive and Gradual Flares. *The Astrophysical Journal*, 391:370, 1992. doi:10.1086/171352

King, J. H. Solar Proton Fluences for 1977-1983 Space Missions. *Journal of Spacecraft and Rockets*, 11:401, 1974. doi:10.2514/3.62088

Kivelson, M. G., Russell, C. T. *Introduction to Space Physics*. Cambridge atmospheric and space science series. Cambridge University Press, 1995. ISBN 9780521457149

Klassen, A., Dresing, N., Gómez-Herrero, R., Heber, B., Müller-Mellin, R. Unexpected spatial intensity distributions and onset timing of solar electron events observed by closely spaced STEREO spacecraft. *Astronomy & Astrophysics*, 593:A31, 2016. doi:10.1051/0004-6361/201628734

Kocharov, L., Torsti, J. Hybrid Solar Energetic Particle Events Observed on Board SOHO. *Solar Physics*, 207:149–157, 2002. doi:10.1023/A:1015540311183

Kong, X., Guo, F., Chen, Y., Giacalone, J. The Acceleration of Energetic Particles at Coronal Shocks and Emergence of a Double Power-law Feature in Particle Energy Spectra. *The Astrophysical Journal*, 883(1):49, 2019. doi:10.3847/1538-4357/ab3848

Kouloumvakos, A., Nindos, A., Valtonen, E., Alissandrakis, C. E., Malandraki, O., Tsitsipis, P., Kontogeorgos, A., Moussas, X., Hillaris, A. Properties of solar energetic particle events inferred from their associated radio emission. *Astronomy & Astrophysics*, 580:A80, 2015. doi:10.1051/0004-6361/201424397

Kouloumvakos, A., Rouillard, A. P., Wu, Y., Vainio, R., Vourlidas, A., Plotnikov, I., Afanasiev, A., Önel, H. Connecting the Properties of Coronal Shock Waves with Those of Solar Energetic Particles. *The Astrophysical Journal*, 876(1):80, 2019. doi:10.3847/1538-4357/ab15d7

Kozarev, K., Nedal, M., Miteva, R., Dechev, M., Zucca, P. A Multi-Event Study of Early-Stage SEP Acceleration by CME-Driven Shocks—Sun to 1 AU. *Frontiers in Astronomy and Space Sciences*, 9:801429, 2022. doi:10.3389/fspas.2022.801429

Kühl, P., Dresing, N., Heber, B., Klassen, A. Solar Energetic Particle Events with Protons Above 500 MeV Between 1995 and 2015 Measured with SOHO/EPHIN. *Solar Physics*, 292(1):10, 2017. doi:10.1007/s11207-016-1033-8

Kumar, R., Eichler, D., Gaspari, M., Spitkovsky, A. Preferential Heating and Acceleration of Heavy Ions in Impulsive Solar Flares. *The Astrophysical Journal*, 835(2):295, 2017. doi:10.3847/1538-4357/835/2/295

Laitinen, T., Dalla, S., Marriott, D. Early propagation of energetic particles across the mean field in turbulent plasmas. *Monthly Notices of the Royal Astronomical Society*, 470(3):3149–3158, 2017. doi:10.1093/mnras/stx1509

Laitinen, T., Kopp, A., Effenberger, F., Dalla, S., Marsh, M. S. Solar energetic particle access to distant longitudes through turbulent field-line meandering. *Astronomy & Astrophysics*, 591:A18, 2016. doi:10.1051/0004-6361/201527801

Lakhina, G. S., Tsurutani, B. T., Gonzalez, W. D., Alex, S. *Alexander Von Humboldt And Magnetic Storms*, pages 404–406. Springer Netherlands, Dordrecht, 2007. ISBN 978-1-4020-4423-6. doi:10.1007/978-1-4020-4423-6_141

Lampa, F., Kallenrode, M. B. Perpendicular Transport in the Inner Heliosphere: A Quick and Dirty Approach. *Solar Physics*, 260(2):423–440, 2009. doi:10.1007/s11207-009-9465-z

Lamy, P. L., Floyd, O., Boclet, B., Wojak, J., Gilardy, H., Barlyaeva, T. Coronal Mass Ejections over Solar Cycles 23 and 24. *Space Science Reviews*, 215(5):39, 2019. doi:10.1007/s11214-019-0605-y

Landi, R., Moreno, G., Storini, M., Antalová, A. Coronal mass ejections, flares, and geomagnetic storms. *Journal of Geophysical Research*, 103(A9):20553–20560, 1998. doi:10.1029/98JA01818

Lanzerotti, L. J. *Solar and Space Weather Radiophysics: Current Status and Future Developments*, chapter Solar and Solar Radio Effects on Technologies. Astrophysics and Space Science Library 314. Springer Netherlands, 1 edition, 2005. ISBN 978-1-4020-2813-7,978-1-4020-2814-4

Lario, D., Aran, A., Gómez-Herrero, R., Dresing, N., Heber, B., Ho, G. C., Decker, R. B., Roelof, E. C. Longitudinal and Radial Dependence of Solar Energetic Particle Peak Intensities: STEREO, ACE, SOHO, GOES, and MESSENGER Observations. *The Astrophysical Journal*, 767(1):41, 2013. doi:10.1088/0004-637X/767/1/41

Lario, D., Kallenrode, M. B., Decker, R. B., Roelof, E. C., Krimigis, S. M., Aran, A., Sanahuja, B. Radial and Longitudinal Dependence of Solar 4–13 MeV and 27–37 MeV Proton Peak Intensities

and Fluences: Helios and IMP 8 Observations. *The Astrophysical Journal*, 653(2):1531–1544, 2006. doi:10.1086/508982

Lario, D., Karelitz, A. Influence of interplanetary coronal mass ejections on the peak intensity of solar energetic particle events. *Journal of Geophysical Research (Space Physics)*, 119(6):4185–4209, 2014. doi:10.1002/2014JA019771

Lario, D., Kwon, R. Y., Balmaceda, L., Richardson, I. G., Krupar, V., Thompson, B. J., Cyr, O. C. S., Zhao, L., Zhang, M. Fast and Wide CMEs without Observed >20 MeV Protons. *The Astrophysical Journal*, 889(2):92, 2020. doi:10.3847/1538-4357/ab64e1

Lario, D., Kwon, R. Y., Riley, P., Raouafi, N. E. On the Link between the Release of Solar Energetic Particles Measured at Widespread Heliolongitudes and the Properties of the Associated Coronal Shocks. *The Astrophysical Journal*, 847(2):103, 2017. doi:10.3847/1538-4357/aa89e3

Lario, D., Kwon, R. Y., Vourlidas, A., Raouafi, N. E., Haggerty, D. K., Ho, G. C., Anderson, B. J., Papaioannou, A., Gómez-Herrero, R., Dresing, N., et al. Longitudinal Properties of a Widespread Solar Energetic Particle Event on 2014 February 25: Evolution of the Associated CME Shock. *The Astrophysical Journal*, 819(1):72, 2016. doi:10.3847/0004-637X/819/1/72

Le, G.-M., Li, C., Zhang, X.-F. Dependence of E $\geq$ 100 MeV protons on the associated flares and CMEs. *Research in Astronomy and Astrophysics*, 17(7):073, 2017. doi:10.1088/1674-4527/17/7/73

Le, G.-M., Zhang, X.-F. Dependence of large SEP events with different energies on the associated flares and CMEs. *Research in Astronomy and Astrophysics*, 17(12):123, 2017. doi:10.1088/1674-4527/17/12/123

Leary, J. C., Conde, R. F., Dakermanji, G., Engelbrecht, C. S., Ercol, C. J., Fielhauer, K. B., Grant, D. G., Hartka, T. J., Hill, T. A., Jaskulek, S. E., Mirantes, M. A., Mosher, L. E., Paul, M. V., Persons, D. F., Rodberg, E. H., Srinivasan, D. K., Vaughan, R. M., Wiley, S. R. The MESSENGER Spacecraft. *Space Science Reviews*, 131(1–4):187–217, 2007. doi:10.1007/s11214-007-9269-0

Li, G., Moore, R., Mewaldt, R. A., Zhao, L., Labrador, A. W. A Twin-CME Scenario for Ground Level Enhancement Events. *Space Science Reviews*, 171(1–4):141–160, 2012. doi:10.1007/s11214-011-9823-7

Lintunen, J., Vainio, R. Solar energetic particle event onset as analyzed from simulated data. *Astronomy & Astrophysics*, 420:343–350, 2004. doi:10.1051/0004-6361:20034247

Lionello, R., Linker, J. A., Mikić, Z. Multispectral Emission of the Sun During the First Whole Sun Month: Magnetohydrodynamic Simulations. *The Astrophysical Journal*, 690(1):902–912, 2009. doi:10.1088/0004-637X/690/1/902

Liu, S., Petrosian, V., Mason, G. M. Stochastic Acceleration of ^{3}He and ^{4}He by Parallel Propagating Plasma Waves. *The Astrophysical Journal*, 613(1):L81–L84, 2004. doi:10.1086/425070

Love, J. J., Lucas, G. M., Rigler, E. J., Murphy, B. S., Kelbert, A., Bedrosian, P. A. Mapping a Magnetic Superstorm: March 1989 Geoelectric Hazards and Impacts on United States Power Systems. *Space Weather*, 20(5):e2021SW003030, 2022. doi:10.1029/2021SW003030. E2021SW003030 2021SW003030

Luhmann, J. G., Mays, M. L., Odstrcil, D., Li, Y., Bain, H., Lee, C. O., Galvin, A. B., Mewaldt, R. A., Cohen, C. M. S., Leske, R. A., Larson, D., Futaana, Y. Modeling solar energetic particle events using ENLIL heliosphere simulations. *Space Weather*, 15(7):934–954, 2017. doi:10.1002/2017SW001617

MacQueen, R. M., Eddy, J. A., Gosling, J. T., Hildner, E., Munro, R. H., Newkirk, J., G. A., Poland, A. I., Ross, C. L. The Outer Solar Corona as Observed from Skylab: Preliminary Results. *The Astrophysical Journal*, 187:L85, 1974. doi:10.1086/181402

Marsh, M. S., Dalla, S., Kelly, J., Laitinen, T. Drift-induced Perpendicular Transport of Solar Energetic Particles. *The Astrophysical Journal*, 774(1):4, 2013. doi:10.1088/0004-637X/774/1/4

Marshall, P. W., Dale, C. J., Burke, E. A. Proton-induced displacement damage fluctuations in silicon microvolumes. *Nuclear Instruments and Methods in Physics Research Section B: Beam Interactions with Materials and Atoms*, 56:847–850, 1991

Mason, G. M., Gloeckler, G., Hovestadt, D. Temporal variations of nucleonic abundances in solar flare energetic particle events. II - Evidence for large-scale shock acceleration. *The Astrophysical Journal*, 280:902–916, 1984. doi:10.1086/162066

Mason, G. M., Mazur, J. E., Dwyer, J. R. ^{3}He Enhancements in Large Solar Energetic Particle Events. *The Astrophysical Journal*, 525(2):L133–L136, 1999. doi:10.1086/312349

Mason, G. M., Mazur, J. E., Dwyer, J. R., Jokipii, J. R., Gold, R. E., Krimigis, S. M. Abundances of Heavy and Ultraheavy Ions in ^{3}He-rich Solar Flares. *The Astrophysical Journal*, 606(1):555–564, 2004. doi:10.1086/382864

Mason, G. M., Reames, D. V., Klecker, B., Hovestadt, D., von Rosenvinge, T. T. The Heavy-Ion Compositional Signature in ^{3}He-rich Solar Particle Events. *The Astrophysical Journal*, 303:849, 1986. doi:10.1086/164133

Maunder, E. W. Greenwich, Royal Observatory, the "great" magnetic storms, 1875 to 1903, and their association with sun-spots. *Monthly Notices of the Royal Astronomical Society*, 64:205, 1904. doi:10.1093/mnras/64.3.205

Mazur, J. E., Mason, G. M., Dwyer, J. R., Giacalone, J., Jokipii, J. R., Stone, E. C. Interplanetary Magnetic Field Line Mixing Deduced from Impulsive Solar Flare Particles. *The Astrophysical Journal*, 532(1):L79–L82, 2000. doi:10.1086/312561

Mazur, J. E., Mason, G. M., Klecker, B., McGuire, R. E. The Energy Spectra of Solar Flare Hydrogen, Helium, Oxygen, and Iron: Evidence for Stochastic Acceleration. *The Astrophysical Journal*, 401:398, 1992. doi:10.1086/172071

Mazur, J. E., Mason, G. M., Klecker, B., McGuire, R. E. The Abundances of Hydrogen, Helium, Oxygen, and Iron Accelerated in Large Solar Particle Events. *The Astrophysical Journal*, 404:810, 1993. doi:10.1086/172336

McComas, D. J., Bame, S. J., Barker, P., Feldman, W. C., Phillips, J. L., Riley, P., Griffee, J. W. Solar Wind Electron Proton Alpha Monitor (SWEPAM) for the Advanced Composition Explorer. *Space Science Reviews*, 86:563–612, 1998. doi:10.1023/A:1005040232597

McComas, D. J., Schwadron, N. A. An explanation of the Voyager paradox: Particle acceleration at a blunt termination shock. *Geophysical Research Letters*, 33(4):L04102, 2006. doi:10.1029/2005GL025437

McGuire, R. E., von Rosenvinge, T. T., McDonald, F. B. The Composition of Solar Energetic Particles. *The Astrophysical Journal*, 301:938, 1986. doi:10.1086/163958

McIntosh, S. W., Leamon, R. J., Krista, L. D., Title, A. M., Hudson, H. S., Riley, P., Harder, J. W., Kopp, G., Snow, M., Woods, T. N., Kasper, J. C., Stevens, M. L., Ulrich, R. K. The solar magnetic activity band interaction and instabilities that shape quasi-periodic variability. *Nature Communications*, 6:6491, 2015. doi:10.1038/ncomms7491

McKibben, R. B. Observations of Solar Proton Events Made from Very Widely Separated Spacecraft. In *Bulletin of the American Astronomical Society*, volume 4, page 387. 1972

McNulty, P. J. Single-event effects experienced by astronauts and microelectronic circuits flown in space. *IEEE Transactions on Nuclear Science*, 43(2):475–482, 1996. doi:10.1109/23.490894

McTiernan, J. M., Fisher, G. H., Li, P. The Solar Flare Soft X-Ray Differential Emission Measure and the Neupert Effect at Different Temperatures. *The Astrophysical Journal*, 514(1):472–483, 1999. doi:10.1086/306924

Mewaldt, R. A., Cohen, C. M. S., Cook, W. R., Cummings, A. C., Davis, A. J., Geier, S., Kecman, B., Klemic, J., Labrador, A. W., Leske, R. A., Miyasaka, H., Nguyen, V., Ogliore, R. C., Stone, E. C., Radocinski, R. G., Wiedenbeck, M. E., Hawk, J., Shuman, S., von Rosenvinge, T. T., Wortman, K. The Low-Energy Telescope (LET) and SEP Central Electronics for the STEREO Mission. *Space Science Reviews*, 136(1–4):285–362, 2008. doi:10.1007/s11214-007-9288-x

Miller, J. A. Particle Acceleration in Impulsive Solar Flares. *Space Science Reviews*, 86:79–105, 1998. doi:10.1023/A:1005066209536

Mishev, A. L. Computation of radiation environment during ground level enhancements 65, 69 and 70 at equatorial region and flight altitudes. *Advances in Space Research*, 54:528–535, 2014. doi:10.1016/j.asr.2013.10.010

Miteva, R., Klein, K. L., Kienreich, I., Temmer, M., Veronig, A., Malandraki, O. E. Solar Energetic Particles and Associated EIT Disturbances in Solar Cycle 23. *Solar Physics*, 289(7):2601–2631, 2014. doi:10.1007/s11207-014-0499-5

Miteva, R., Klein, K. L., Malandraki, O., Dorrian, G. Solar Energetic Particle Events in the 23rd Solar Cycle: Interplanetary Magnetic Field Configuration and Statistical Relationship with Flares and CMEs. *Solar Physics*, 282(2):579–613, 2013. doi:10.1007/s11207-012-0195-2

Miteva, R., Samwel, S. W., Costa-Duarte, M. V. Solar energetic particle catalogs: Assumptions, uncertainties and validity of reports. *Journal of Atmospheric and Solar-Terrestrial Physics*, 180:26–34, 2018a. doi:10.1016/j.jastp.2017.05.003

Miteva, R., Samwel, S. W., Costa-Duarte, M. V. The Wind/EPACT Proton Event Catalog (1996 – 2016). *Solar Physics*, 293(2):27, 2018b. doi:10.1007/s11207-018-1241-5

Miteva, R., Samwel, S. W., Costa-Duarte, M. V., Malandraki, O. E. Solar cycle dependence of Wind/EPACT protons, solar flares and coronal mass ejections. *Sun and Geosphere*, 12:11–19, 2017a

Miteva, R., Samwel, S. W., Krupar, V. Solar energetic particles and radio burst emission. *Journal of Space Weather and Space Climate*, 7:A37, 2017b. doi:10.1051/swsc/2017035

Miteva, R., Samwel, S. W., Zabunov, S. Solar Radio Bursts Associated with In Situ Detected Energetic Electrons in Solar Cycles 23 and 24. *Universe*, 8(5):275, 2022. doi:10.3390/universe8050275

Müller, D., Marsden, R. G., St. Cyr, O. C., Gilbert, H. R., Solar Orbiter Team. Solar Orbiter . Exploring the Sun-Heliosphere Connection. *Solar Physics*, 285(1-2):25–70, 2013. doi:10.1007/s11207-012-0085-7

Müller-Mellin, R., Böttcher, S., Falenski, J., Rode, E., Duvet, L., Sanderson, T., Butler, B., Johlander, B., Smit, H. The Solar Electron and Proton Telescope for the STEREO Mission. *Space Science Reviews*, 136(1–4):363–389, 2008. doi:10.1007/s11214-007-9204-4

Müller-Mellin, R., Kunow, H., Fleißner, V., Pehlke, E., Rode, E., Röschmann, N., Scharmberg, C., Sierks, H., Rusznyak, P., Mckenna-Lawlor, S., Elendt, I., Sequeiros, J., Meziat, D., Sanchez, S., Medina, J., del Peral, L., Witte, M., Marsden, R., Henrion, J. COSTEP - Comprehensive Suprathermal and Energetic Particle Analyser. *Solar Physics*, 162(1–2):483–504, 1995. doi:10.1007/BF00733437

Mursula, K., Usoskin, I. G., Maris, G. Introduction to Space Climate. *Advances in Space Research*, 40(7):885–887, 2007. doi:10.1016/j.asr.2007.07.046

Nagata, T. Solar Flare Effect on the Geomagnetic Field. *Journal of Geomagnetism and Geoelectricity*, 18(2):197–219, 1966. doi:10.5636/jgg.18.197

Neupert, W. M. Comparison of Solar X-Ray Line Emission with Microwave Emission during Flares. *The Astrophysical Journal*, 153:L59, 1968. doi:10.1086/180220

Ning, Z., Cao, W. Investigation of Chromospheric Evaporation in a Neupert-type Solar Flare. *The Astrophysical Journal*, 717(2):1232–1242, 2010. doi:10.1088/0004-637X/717/2/1232

Nitta, N. V., Mason, G. M., Wiedenbeck, M. E., Cohen, C. M. S., Krucker, S., Hannah, I. G., Shimojo, M., Shibata, K. Coronal Jet Observed by Hinode as the Source of a ^{3}He-rich Solar Energetic Particle Event. *The Astrophysical Journal*, 675(2):L125, 2008. doi:10.1086/533438

Nymmik, R. A. Radiation environment induced by cosmic ray particle fluxes in the international space station orbit according to recent galactic and solar cosmic ray models. *Advances in Space Research*, 21(12):1689–1698, 1998. ISSN 0273-1177. doi:10.1016/S0273-1177(98)00015-5

Nymmik, R. A. Probabilistic model for fluences and peak fluxes of solar energetic particles. *Radiation Measurements*, 30(3):287–296, 1999. ISSN 1350–4487. doi:10.1016/S1350-4487(99)00065-7

Nymmik, R. A. Improved environment radiation models. *Advances in Space Research*, 40(3):313–320, 2007. doi:10.1016/j.asr.2006.12.028

Odstrcil, D., Riley, P., Zhao, X. P. Numerical simulation of the 12 May 1997 interplanetary CME event. *Journal of Geophysical Research (Space Physics)*, 109(A2):A02116, 2004. doi:10.1029/2003JA010135

Ogilvie, K. W., Chornay, D. J., Fritzenreiter, R. J., Hunsaker, F., Keller, J., Lobell, J., Miller, G., Scudder, J. D., Sittler, J., E. C., Torbert, R. B., Bodet, D., Needell, G., Lazarus, A. J., Steinberg,

J. T., Tappan, J. H., Mavretic, A., Gergin, E. SWE, A Comprehensive Plasma Instrument for the Wind Spacecraft. *Space Science Reviews*, 71(1–4):55–77, 1995. doi:10.1007/BF00751326

Onsager, T., Grubb, R., Kunches, J., Matheson, L., Speich, D., Zwickl, R., Sauer, H. Operational uses of the GOES energetic particle detectors. In E. R. Washwell (editor), *GOES-8 and Beyond*, volume 2812, pages 281–290. International Society for Optics and Photonics, SPIE, 1996. doi:10.1117/12.254075

Ossendrijver, M. The solar dynamo. *The Astronomy and Astrophysics Review*, 11(4):287–367, 2003. doi:10.1007/s00159-003-0019-3

Owens, M. J., Lockwood, M., Hawkins, E., Usoskin, I., Jones, G. S., Barnard, L., Schurer, A., Fasullo, J. The Maunder minimum and the Little Ice Age: an update from recent reconstructions and climate simulations. *Journal of Space Weather and Space Climate*, 7:A33, 2017. doi:10.1051/swsc/2017034

Pallavicini, R., Serio, S., Vaiana, G. S. A survey of soft X-ray limb flare images: the relation between their structure in the corona and other physical parameters. *The Astrophysical Journal*, 216:108–122, 1977. doi:10.1086/155452

Papaioannou, A., Anastasiadis, A., Kouloumvakos, A., Paassilta, M., Vainio, R., Valtonen, E., Belov, A., Eroshenko, E., Abunina, M., Abunin, A. Nowcasting Solar Energetic Particle Events Using Principal Component Analysis. *Solar Physics*, 293(7):100, 2018. doi:10.1007/s11207-018-1320-7

Papaioannou, A., Belov, A., Abunina, M., Eroshenko, E., Abunin, A., Anastasiadis, A., Patsourakos, S., Mavromichalaki, H. Interplanetary Coronal Mass Ejections as the Driver of Non-recurrent Forbush Decreases. *The Astrophysical Journal*, 890(2):101, 2020. doi:10.3847/1538-4357/ab6bd1

Papaioannou, A., Malandraki, O. E., Dresing, N., Heber, B., Klein, K. L., Vainio, R., Rodríguez-Gasén, R., Klassen, A., Nindos, A., Heynderickx, D., Mewaldt, R. A., Gómez-Herrero, R., Vilmer, N., Kouloumvakos, A., Tziotziou, K., Tsiropoula, G. SEPServer catalogues of solar energetic particle events at 1 AU based on STEREO recordings: 2007–2012. *Astronomy & Astrophysics*, 569:A96, 2014. doi:10.1051/0004-6361/201323336

Papaioannou, A., Sandberg, I., Anastasiadis, A., Kouloumvakos, A., Georgoulis, M. K., Tziotziou, K., Tsiropoula, G., Jiggens, P., Hilgers, A. Solar flares, coronal mass ejections and solar energetic particle event characteristics. *Journal of Space Weather and Space Climate*, 6:A42, 2016. doi:10.1051/swsc/2016035

Papaioannou, A., Vainio, R., Raukunen, O., Jiggens, P., Aran, A., Dierckxsens, M., Mallios, S. A., Paassilta, M., Anastasiadis, A. The probabilistic solar particle event forecasting (PROSPER) model. *Journal of Space Weather and Space Climate*, 12:24, 2022. doi:10.1051/swsc/2022019

Park, J., Moon, Y. J. What flare and CME parameters control the occurrence of solar proton events? *Journal of Geophysical Research (Space Physics)*, 119(12):9456–9463, 2014. doi:10.1002/2014JA020272

Park, J., Moon, Y. J., Lee, H. Dependence of the Peak Fluxes of Solar Energetic Particles on CME 3D Parameters from STEREO and SOHO. *The Astrophysical Journal*, 844(1):17, 2017. doi:10.3847/1538-4357/aa794a

Parker, E. N. Dynamics of the Interplanetary Gas and Magnetic Fields. *The Astrophysical Journal*, 128:664, 1958. doi:10.1086/146579

Parker, E. N. The passage of energetic charged particles through interplanetary space. *Planetary and Space Science*, 13(1):9–49, 1965. doi:10.1016/0032-0633(65)90131-5

Pick, M., Mason, G. M., Wang, Y. M., Tan, C., Wang, L. Solar Source Regions for ^{3}He-rich Solar Energetic Particle Events Identified Using Imaging Radio, Optical, and Energetic Particle Observations. *The Astrophysical Journal*, 648(2):1247–1255, 2006. doi:10.1086/505926

Pohjolainen, S., Al-Hamadani, F., Valtonen, E. Propagation of Solar Energetic Particles During Multiple Coronal Mass Ejection Events. *Solar Physics*, 291(2):487–511, 2016. doi:10.1007/s11207-015-0835-4

Poluianov, S. V., Usoskin, I. G., Mishev, A. L., Shea, M. A., Smart, D. F. GLE and Sub-GLE Redefinition in the Light of High-Altitude Polar Neutron Monitors. *Solar Physics*, 292(11):176, 2017. doi:10.1007/s11207-017-1202-4

Pomoell, J., Poedts, S. EUHFORIA: European heliospheric forecasting information asset. *Journal of Space Weather and Space Climate*, 8:A35, 2018. doi:10.1051/swsc/2018020

Posner, A. Up to 1-hour forecasting of radiation hazards from solar energetic ion events with relativistic electrons. *Space Weather*, 5(5):05001, 2007. doi:10.1029/2006SW000268

Prakash, O., Feng, L., Michalek, G., Gan, W., Lu, L., Shanmugaraju, A., Umapathy, S. Characteristics of events with metric-to-decahectometric type II radio bursts associated with CMEs and flares in relation to SEP events. *Astrophysics and Space Science*, 362(3):56, 2017. doi:10.1007/s10509-017-3034-y

Ramaty, R., Murphy, R. J. Nuclear Processes and Accelerated Particles in Solar Flares. *Space Science Reviews*, 45(3–4):213–268, 1987. doi:10.1007/BF00171995

Raukunen, O., Paassilta, M., Vainio, R., Rodriguez, J. V., Eronen, T., Crosby, N., Dierckxsens, M., Jiggens, P., Heynderickx, D., Sandberg, I. Very high energy proton peak flux model. *Journal of Space Weather and Space Climate*, 10:24, 2020. doi:10.1051/swsc/2020024

Raukunen, O., Vainio, R., Tylka, A. J., Dietrich, W. F., Jiggens, P., Heynderickx, D., Dierckxsens, M., Crosby, N., Ganse, U., Siipola, R. Two solar proton fluence models based on ground level enhancement observations. *Journal of Space Weather and Space Climate*, 8:A04, 2018. doi:10.1051/swsc/2017031

Raukunen, O., Valtonen, E., Vainio, R. Iron-rich solar particle events measured by SOHO/ERNE during two solar cycles. *Astronomy & Astrophysics*, 589:A138, 2016. doi:10.1051/0004-6361/201527462

Reames, D. V. Bimodal Abundances in the Energetic Particles of Solar and Interplanetary Origin. *The Astrophysical Journal*, 330:L71, 1988. doi:10.1086/185207

Reames, D. V. Energetic Particles from Impulsive Solar Flares. *The Astrophysical Journal Supplement Series*, 73:235, 1990. doi:10.1086/191456

Reames, D. V. Particle acceleration at the Sun and in the heliosphere. *Space Science Reviews*, 90:413–491, 1999. doi:10.1023/A:1005105831781

Reames, D. V. The Two Sources of Solar Energetic Particles. *Space Science Reviews*, 175:53–92, 2013. doi:10.1007/s11214-013-9958-9

Reames, D. V. Sixty Years of Element Abundance Measurements in Solar Energetic Particles. *Space Science Reviews*, 217(6):72, 2021. doi:10.1007/s11214-021-00845-4

Reber, G. Cosmic Static. *The Astrophysical Journal*, 100:279, 1944. doi:10.1086/144668

Reeves, G. D., Friedel, R. H. W., Belian, R. D., Meier, M. M., Henderson, M. G., Onsager, T., Singer, H. J., Baker, D. N., Li, X., Blake, J. B. The relativistic electron response at geosynchronous orbit during the January 1997 magnetic storm. *Journal of Geophysical Research*, 103(A8):17559–17570, 1998. doi:10.1029/97JA03236

Reid, H. A. S., Ratcliffe, H. A review of solar type III radio bursts. *Research in Astronomy and Astrophysics*, 14(7):773–804, 2014. doi:10.1088/1674-4527/14/7/003

Richardson, I. G., von Rosenvinge, T. T., Cane, H. V. The Properties of Solar Energetic Particle Event-Associated Coronal Mass Ejections Reported in Different CME Catalogs. *Solar Physics*, 290(6):1741–1759, 2015. doi:10.1007/s11207-015-0701-4

Richardson, I. G., von Rosenvinge, T. T., Cane, H. V. North/South Hemispheric Periodicities in the {¿} 25 MeV Solar Proton Event Rate During the Rising and Peak Phases of Solar Cycle 24. *Solar Physics*, 291(7):2117–2134, 2016. doi:10.1007/s11207-016-0948-4

Richardson, I. G., von Rosenvinge, T. T., Cane, H. V. 25 MeV solar proton events in Cycle 24 and previous cycles. *Advances in Space Research*, 60(4):755–767, 2017. doi:10.1016/j.asr.2016.07.035

Richardson, I. G., von Rosenvinge, T. T., Cane, H. V., Christian, E. R., Cohen, C. M. S., Labrador, A. W., Leske, R. A., Mewaldt, R. A., Wiedenbeck, M. E., Stone, E. C. $>$ 25 MeV Proton Events Observed by the High Energy Telescopes on the STEREO A and B Spacecraft and/or at Earth

During the First $\sim$ Seven Years of the STEREO Mission. *Solar Physics*, 289(8):3059–3107, 2014. doi:10.1007/s11207-014-0524-8

Rigozo, N. R., Echer, E., Vieira, L. E. A., Nordemann, D. J. R. Reconstruction of Wolf Sunspot Numbers on the Basis of Spectral Characteristics and Estimates of Associated Radio Flux and Solar Wind Parameters for the Last Millennium. *Space Science Reviews*, 203:179–191, 2001. doi:10.1023/A:1012745612022

Rodríguez-Gasén, R., Aran, A., Sanahuja, B., Jacobs, C., Poedts, S. Variation of Proton Flux Profiles with the Observer's Latitude in Simulated Gradual SEP Events. *Solar Physics*, 289(5):1745–1762, 2014. doi:10.1007/s11207-013-0442-1

Rosenqvist, L., Hilgers, A., Evans, H., Daly, E., Hapgood, M., Stamper, R., Zwickl, R., Bourdarie, S., Boscher, D. Toolkit for Updating Interplanetary Proton Cumulated Fluence Models. *Journal of Spacecraft and Rockets*, 42(6):1077–1090, 2005. doi:10.2514/1.8211

Rotti, S., Aydin, B., Georgoulis, M. K., Martens, P. C. Integrated Geostationary Solar Energetic Particle Events Catalog: GSEP. *The Astrophysical Journal Supplement Series*, 262(1):29, 2022. doi:10.3847/1538-4365/ac87ac

Rozelot, J. P. On the chaotic behaviour of the solar activity. *Astronomy & Astrophysics*, 297:L45, 1995

Sáiz, A., Evenson, P., Ruffolo, D., Bieber, J. W. On the Estimation of Solar Energetic Particle Injection Timing from Onset Times near Earth. *The Astrophysical Journal*, 626(2):1131–1137, 2005. doi:10.1086/430293

Samwel, S. W., Miteva, R. Catalogue of in situ observed solar energetic electrons from ACE/EPAM instrument. *Monthly Notices of the Royal Astronomical Society*, 505(4):5212–5227, 2021. doi:10.1093/mnras/stab1564

Sandberg, I., Jiggens, P., Heynderickx, D., Daglis, I. A. Cross calibration of NOAA GOES solar proton detectors using corrected NASA IMP-8/GME data. *Geophysical Research Letters*, 41(13):4435–4441, 2014. doi:10.1002/2014GL060469

Sandroos, A., Vainio, R. Simulation Results for Heavy Ion Spectral Variability in Large Gradual Solar Energetic Particle Events. *The Astrophysical Journal*, 662(2):L127–L130, 2007. doi:10.1086/519378

Sandroos, A., Vainio, R. Reacceleration of Flare Ions in Coronal and Interplanetary Shock Waves. *The Astrophysical Journal Supplement Series*, 181(1):183–196, 2009. doi:10.1088/0067-0049/181/1/183

Schmahl, E. J., Schmelz, J. T., Saba, J. L. R., Strong, K. T., Kundu, M. R. Microwave and X-Ray Observations of a Major Confined Solar Flare. *The Astrophysical Journal*, 358:654, 1990. doi:10.1086/169018

Schou, J., Antia, H. M., Basu, S., Bogart, R. S., Bush, R. I., Chitre, S. M., Christensen-Dalsgaard, J., Di Mauro, M. P., Dziembowski, W. A., Eff-Darwich, A., Gough, D. O., Haber, D. A., Hoeksema, J. T., Howe, R., Korzennik, S. G., Kosovichev, A. G., Larsen, R. M., Pijpers, F. P., Scherrer, P. H., Sekii, T., Tarbell, T. D., Title, A. M., Thompson, M. J., Toomre, J. Helioseismic Studies of Differential Rotation in the Solar Envelope by the Solar Oscillations Investigation Using the Michelson Doppler Imager. *The Astrophysical Journal*, 505(1):390–417, 1998. doi:10.1086/306146

Schwabe, H. Sonnenbeobachtungen im Jahre 1843. Von Herrn Hofrath Schwabe in Dessau. *Astronomische Nachrichten*, 21(15):233, 1844. doi:10.1002/asna.18440211505

Schwadron, N. A., Townsend, L., Kozarev, K., Dayeh, M. A., Cucinotta, F., Desai, M., Golightly, M., Hassler, D., Hatcher, R., Kim, M. Y., Posner, A., PourArsalan, M., Spence, H. E., Squier, R. K. Earth-Moon-Mars Radiation Environment Module framework. *Space Weather*, 8(10):S00E02, 2010. doi:10.1029/2009SW000523

Sellers, F. B., Hanser, F. A. Design and calibration of the GOES-8 particle sensors: the EPS and HEPAD. In E. R. Washwell (editor), *GOES-8 and Beyond*, volume 2812, pages 353–364. International Society for Optics and Photonics, SPIE, 1996. doi:10.1117/12.254083

Sexton, F. W. Destructive single-event effects in semiconductor devices and ics. *IEEE Transactions on Nuclear Science*, 50(3):603–621, 2003. doi:10.1109/TNS.2003.813137

Shalchi, A. *Nonlinear Cosmic Ray Diffusion Theories*. Astrophysics and Space Science Library. Springer Berlin, Heidelberg, 2009. ISBN 978-3-642-00308-0. doi:10.1007/978-3-642-00309-7

Shalchi, A. Perpendicular diffusion in magnetostatic slab turbulence: The theorem on reduced dimensionality and microscopic diffusion. *Journal of Atmospheric and Solar-Terrestrial Physics*, 97:37–42, 2013. doi:10.1016/j.jastp.2013.02.012

Shea, M. A., Smart, D. F. A Summary of Major Solar Proton Events. *Solar Physics*, 127(2):297–320, 1990. doi:10.1007/BF00152170

Sheeley, N. R., Walters, J. H., Wang, Y. M., Howard, R. A. Continuous tracking of coronal outflows: Two kinds of coronal mass ejections. *Journal of Geophysical Research*, 104(A11):24739–24768, 1999. doi:10.1029/1999JA900308

Shen, F., Shen, C., Xu, M., Liu, Y., Feng, X., Wang, Y. Propagation characteristics of coronal mass ejections (CMEs) in the corona and interplanetary space. *Reviews of Modern Plasma Physics*, 6(1):8, 2022. doi:10.1007/s41614-022-00069-1

Simpson, J. A. The Cosmic Ray Nucleonic Component: The Invention and Scientific Uses of the Neutron Monitor – (Keynote Lecture). *Space Science Reviews*, 93:11–32, 2000. doi:10.1023/A:1026567706183

Smart, D. F., Shea, M. A. PPS-87: A new event oriented solar proton prediction model. *Advances in Space Research*, 9(10):281–284, 1989. ISSN 0273-1177. doi:10.1016/0273-1177(89)90450-X

Smith, D. S., Scalo, J. Solar X-ray flare hazards on the surface of Mars. *Planetary and Space Science*, 55(4):517–527, 2007. doi:10.1016/j.pss.2006.10.001

Solanki, S. K., Usoskin, I. G., Kromer, B., Schüssler, M., Beer, J. Unusual activity of the Sun during recent decades compared to the previous 11,000 years. *Nature*, 431(7012):1084–1087, 2004. doi:10.1038/nature02995

Sonett, C. P. Very long solar periods and the radiocarbon record. *Reviews of Geophysics*, 22(3):239–254, 1984. doi:10.1029/RG022i003p00239

Spörer, F. W. G., Maunder, E. W. Prof. Spoerer's researches on Sun-spots. *Monthly Notices of the Royal Astronomical Society*, 50:251, 1890. doi:10.1093/mnras/50.4.251

Spörer, G. F. W. *Ueber die Periodicität er Sonnenflecken seit dem Jahre 1618*, volume 53. Blochmann, 1889

Steyn, R., Strauss, D. T., Effenberger, F., Pacheco, D. The soft X-ray Neupert effect as a proxy for solar energetic particle injection. A proof-of-concept physics-based forecasting model. *Journal of Space Weather and Space Climate*, 10:64, 2020. doi:10.1051/swsc/2020067

Strauss, R. D. T., Dresing, N., Engelbrecht, N. E. Perpendicular Diffusion of Solar Energetic Particles: Model Results and Implications for Electrons. *The Astrophysical Journal*, 837(1):43, 2017. doi:10.3847/1538-4357/aa5df5

Struminsky, A. B. Longitudinal distribution of solar cosmic rays observed in the events of 2012. *Bulletin of the Russian Academy of Sciences, Physics*, 79(5):566–569, 2015. doi:10.3103/S106287381505038X

Suess, H. E. The radiocarbon record in tree rings of the last 8000 years. *Radiocarbon*, 22(2):200–209, 1980

Tan, L. C. Electron-Ion Intensity Dropouts in Gradual Solar Energetic Particle Events during Solar Cycle 23. *The Astrophysical Journal*, 846(1):18, 2017. doi:10.3847/1538-4357/aa81d1

Tan, L. C. Electron Spectral Breaking Caused by Magnetic Reconnection in Impulsive Flare Events. *The Astrophysical Journal*, 858(1):25, 2018. doi:10.3847/1538-4357/aaba7e

Tan, L. C., Reames, D. V. Dropout of Directional Electron Intensities in Large Solar Energetic Particle Events. *The Astrophysical Journal*, 816(2):93, 2016. doi:10.3847/0004-637X/816/2/93

Tang, J. F., Wu, D. J., Tan, C. M. Electron Cyclotron Maser Emission in Coronal Arches and Solar Radio Type V Bursts. *The Astrophysical Journal*, 779(1):83, 2013. doi:10.1088/0004-637X/779/1/83

Tapping, K., Morgan, C. Changing Relationships Between Sunspot Number, Total Sunspot Area and $F_{10.7}$ in Cycles 23 and 24. *Solar Physics*, 292(6):73, 2017. doi:10.1007/s11207-017-1111-6

Tapping, K. F. The 10.7 cm solar radio flux ($F_{10.7}$). *Space Weather*, 11(7):394–406, 2013. doi:10.1002/swe.20064

Temerin, M., Roth, I. The Production of 3He and Heavy Ion Enrichments in 3He-rich Flares by Electromagnetic Hydrogen Cyclotron Waves. *The Astrophysical Journal*, 391:L105, 1992. doi:10.1086/186408

Temmer, M. Space weather: the solar perspective. *Living Reviews in Solar Physics*, 18(1):4, 2021. doi:10.1007/s41116-021-00030-3

Temmer, M., Veronig, A. M., Vršnak, B., Rybák, J., Gömöry, P., Stoiser, S., Maričić, D. Acceleration in Fast Halo CMEs and Synchronized Flare HXR Bursts. *The Astrophysical Journal Letters*, 673(1):L95, 2008. doi:10.1086/527414

Thernisien, A., Vourlidas, A., Howard, R. A. Forward Modeling of Coronal Mass Ejections Using STEREO/SECCHI Data. *Solar Physics*, 256(1–2):111–130, 2009. doi:10.1007/s11207-009-9346-5

Thernisien, A. F. R., Howard, R. A., Vourlidas, A. Modeling of Flux Rope Coronal Mass Ejections. *The Astrophysical Journal*, 652(1):763–773, 2006. doi:10.1086/508254

Thompson, B. J., Plunkett, S. P., Gurman, J. B., Newmark, J. S., St. Cyr, O. C., Michels, D. J. SOHO/EIT observations of an Earth-directed coronal mass ejection on May 12, 1997. *Geophysical Research Letters*, 25(14):2465–2468, 1998. doi:10.1029/98GL50429

Tobiska, W. K., Atwell, W., Beck, P., Benton, E., Copeland, K., Dyer, C., Gersey, B., Getley, I., Hands, A., Holland, M., Hong, S., Hwang, J., Jones, B., Malone, K., Meier, M. M., Mertens, C., Phillips, T., Ryden, K., Schwadron, N., Wender, S. A., Wilkins, R., Xapsos, M. A. Advances in Atmospheric Radiation Measurements and Modeling Needed to Improve Air Safety. *Space Weather*, 13(4):202–210, 2015. doi:10.1002/2015SW001169

Toriumi, S., Wang, H. Flare-productive active regions. *Living Reviews in Solar Physics*, 16(1):3, 2019. doi:10.1007/s41116-019-0019-7

Torsti, J., Valtonen, E., Lumme, M., Peltonen, P., Eronen, T., Louhola, M., Riihonen, E., Schultz, G., Teittinen, M., Ahola, K., Holmlund, C., Kelhä, V., Leppälä, K., Ruuska, P., Strömmer, E. Energetic Particle Experiment ERNE. *Solar Physics*, 162(1–2):505–531, 1995. doi:10.1007/BF00733438

Tousey, R. The solar corona. In *Space Research Conference*, volume 2, pages 713–730. 1973

Trottet, G., Samwel, S., Klein, K. L., Dudok de Wit, T., Miteva, R. Statistical Evidence for Contributions of Flares and Coronal Mass Ejections to Major Solar Energetic Particle Events. *Solar Physics*, 290(3):819–839, 2015. doi:10.1007/s11207-014-0628-1

Tsurutani, B. T., Gonzalez, W. D., Lakhina, G. S., Alex, S. The extreme magnetic storm of 1-2 September 1859. *Journal of Geophysical Research (Space Physics)*, 108(A7):1268, 2003. doi:10.1029/2002JA009504

Tylka, A. J., Cohen, C. M. S., Dietrich, W. F., Lee, M. A., Maclennan, C. G., Mewaldt, R. A., Ng, C. K., Reames, D. V. Shock Geometry, Seed Populations, and the Origin of Variable Elemental Composition at High Energies in Large Gradual Solar Particle Events. *The Astrophysical Journal*, 625(1):474, 2005. doi:10.1086/429384

Usoskin, I. G. A history of solar activity over millennia. *Living Reviews in Solar Physics*, 14(1):3, 2017. doi:10.1007/s41116-017-0006-9

Usoskin, I. G., Gallet, Y., Lopes, F., Kovaltsov, G. A., Hulot, G. Solar activity during the Holocene: the Hallstatt cycle and its consequence for grand minima and maxima. *Astronomy & Astrophysics*, 587:A150, 2016. doi:10.1051/0004-6361/201527295

Usoskin, I. G., Solanki, S. K., Schüssler, M., Mursula, K., Alanko, K. Millennium-Scale Sunspot Number Reconstruction: Evidence for an Unusually Active Sun since the 1940s. *Physical Review Letters*, 91(21):211101, 2003. doi:10.1103/PhysRevLett.91.211101

Vainio, R., Desorgher, L., Heynderickx, D., Storini, M., Flückiger, E., Horne, R. B., Kovaltsov, G. A., Kudela, K., Laurenza, M., McKenna-Lawlor, S., Rothkaehl, H., Usoskin, I. G. Dynamics of the Earth's Particle Radiation Environment. *Space Science Reviews*, 147:187–231, 2009. doi:10.1007/s11214-009-9496-7

Vainio, R., Valtonen, E., Heber, B., Malandraki, O. E., Papaioannou, A., Klein, K.-L., Afanasiev, A., Agueda, N., Aurass, H., Battarbee, M., Braune, S., Dröge, W., Ganse, U., Hamadache, C., Heynderickx, D., Huttunen-Heikinmaa, K., Kiener, J., Kilian, P., Kopp, A., Kouloumvakos, A., Maisala, S., Mishev, A., Miteva, R., Nindos, A., Oittinen, T., Raukunen, O., Riihonen, E., Rodríguez-Gasén, R., Saloniemi, O., Sanahuja, B., Scherer, R., Spanier, F., Tatischeff, V., Tziotziou, K., Usoskin, I. G., Vilmer, N. The first SEPServer event catalogue ~68-MeV solar proton events observed at 1 AU in 1996–2010. *Journal of Space Weather and Space Climate*, 3:A12, 2013. doi:10.1051/swsc/2013030

van den Berg, J., Strauss, D. T., Effenberger, F. A Primer on Focused Solar Energetic Particle Transport. *Space Science Reviews*, 216(8):1–57, 2020. doi:10.1007/s11214-020-00771-x

Vasiliev, S. S., Dergachev, V. A. The ~2400-year cycle in atmospheric radiocarbon concentration: bispectrum of ^{14}C data over the last 8000 years. *Annales Geophysicae*, 20(1):115–120, 2002. doi:10.5194/angeo-20-115-2002

Veronig, A., Vršnak, B., Dennis, B. R., Temmer, M., Hanslmeier, A., Magdalenić, J. Investigation of the Neupert effect in solar flares - I. Statistical properties and the evaporation model. *Astronomy & Astrophysics*, 392(2):699–712, 2002. doi:10.1051/0004-6361:20020947

Vlahos, L., Anastasiadis, A., Papaioannou, A., Kouloumvakos, A., Isliker, H. Sources of solar energetic particles. *Philosophical Transactions of the Royal Society of London Series A*, 377(2148):20180095, 2019. doi:10.1098/rsta.2018.0095

Vlasova, N. A., Logachev, Y. I., Bazilevskaya, G. A., Ginzburg, E. A., Daibog, E. I., Ishkov, V. N., Kalegaev, V. V., Lazutin, L. L., Nguyen, M. D., Surova, G. M., Yakovchuk, O. S. Catalogs of Solar Proton Events as a Tool for Studying Space Weather. *Cosmic Research*, 60(3):151–164, 2022. doi:10.1134/S001095252203008X

von Rosenvinge, T. T., Reames, D. V., Baker, R., Hawk, J., Nolan, J. T., Ryan, L., Shuman, S., Wortman, K. A., Mewaldt, R. A., Cummings, A. C., Cook, W. R., Labrador, A. W., Leske, R. A., Wiedenbeck, M. E. The High Energy Telescope for STEREO. *Space Science Reviews*, 136(1–4):391–435, 2008. doi:10.1007/s11214-007-9300-5

Vourlidas, A., Howard, R. A., Esfandiari, E., Patsourakos, S., Yashiro, S., Michalek, G. Comprehensive Analysis of Coronal Mass Ejection Mass and Energy Properties Over a Full Solar Cycle. *The Astrophysical Journal*, 722(2):1522–1538, 2010. doi:10.1088/0004-637X/722/2/1522

Vršnak, B., Maričić, D., Stanger, A. L., Veronig, A. Coronal Mass Ejection of 15 May 2001: II. Coupling of the Cme Acceleration and the Flare Energy Release. *Solar Physics*, 225(2):355–378, 2004. doi:10.1007/s11207-004-4995-x

Wang, Y., Lyu, D., Wu, X., Qin, G. The Quantitative Relation of the Time Profiles of Intensities in the Well-connected Solar Energetic Particle Events. *The Astrophysical Journal*, 940(1):67, 2022. doi:10.3847/1538-4357/ac99da

Wang, Y., Lyu, D., Xiao, B., Qin, G., Zhong, Y., Lian, L. Statistical Survey of Reservoir Phenomenon in Energetic Proton Events Observed by Multiple Spacecraft. *The Astrophysical Journal*, 909(2):110, 2021. doi:10.3847/1538-4357/abda39

Webb, D. F., Cliver, E. W., Crooker, N. U., Cry, O. C. S., Thompson, B. J. Relationship of halo coronal mass ejections, magnetic clouds, and magnetic storms. *Journal of Geophysical Research*, 105(A4):7491–7508, 2000. doi:10.1029/1999JA000275

Weiss, A. A. The Type IV Solar Radio Burst at Metre Wavelengths. *Australian Journal of Physics*, 16:526, 1963. doi:10.1071/PH630526

Whitman, K., Egeland, R., Richardson, I. G., Allison, C., Quinn, P., Barzilla, J., Kitiashvili, I., Viacheslav, S., Bain, H. M., Dierckxsens, M., Mays, M. L., Tadesse, T., Lee, K. T., Semones, E., Luhmann, J. G., Núñez, M., White, S. M., Kahler, S. W., Ling, A. G., Smart, D. F., Shea, M. A., Tenishev, V., Boubrahimi, S. F., Aydin, B., Martens, P., Angryk, R., Marsh, M. S., Dalla, S., Crosby, N., Schwadron, N. A., Kozarev, K., Gorby, M., Young, M. A., Laurenza, M., Cliver, E. W., Alberti, T., Stumpo, M., Benella, S., Papaioannou, A., Anastasiadis, A., Sandberg, I., Georgoulis, M. K., Ji, A., Kempton, D., Pandey, C., Li, G., Hu, J., Zank, G. P., Lavasa, E., Giannopoulos, G., Falconer, D., Kadadi, Y., Fernandes, I., Dayeh, M. A., Muñoz-Jaramillo, A.,

Chatterjee, S., Moreland, K. D., Sokolov, I. V., Roussev, I. I., Taktakishvili, A., Effenberger, F., Gombosi, T., Huang, Z., Zhao, L., Wijsen, N., Aran, A., Poedts, S., Kouloumvakos, A., Paassilta, M., Vainio, R., Belov, A., Eroshenko, E. A., Abunina, M. A., Abunin, A. A., Balch, C. C., Malandraki, O., Karavolos, M., Heber, B., Labrenz, J., Kühl, P., Kosovichev, A. G., Oria, V., Nita, G. M., Illarionov, E., O'Keefe, P. M., Jiang, Y., Fereira, S. H., Ali, A., Paouris, E., Aminalragia-Giamini, S., Jiggens, P., Jin, M., Lee, C. O., Palmerio, E., Bruno, A., Kasapis, S., Wang, X., Chen, Y., Sanahuja, B., Lario, D., Jacobs, C., Strauss, D. T., Steyn, R., van den Berg, J., Swalwell, B., Waterfall, C., Nedal, M., Miteva, R., Dechev, M., Zucca, P., Engell, A., Maze, B., Farmer, H., Kerber, T., Barnett, B., Loomis, J., Grey, N., Thompson, B. J., Linker, J. A., Caplan, R. M., Downs, C., Török, T., Lionello, R., Titov, V., Zhang, M., Hosseinzadeh, P. Review of solar energetic particle models. *Advances in Space Research*, 2022. ISSN 0273-1177. doi:10.1016/j.asr.2022.08.006

Wiedenbeck, M. E., Mason, G. M., Cohen, C. M. S., Nitta, N. V., Gómez-Herrero, R., Haggerty, D. K. Observations of Solar Energetic Particles from ^{3}He-rich Events over a Wide Range of Heliographic Longitude. *The Astrophysical Journal*, 762(1):54, 2013. doi:10.1088/0004-637X/762/1/54

Wijsen, N., Aran, A., Pomoell, J., Poedts, S. Modelling three-dimensional transport of solar energetic protons in a corotating interaction region generated with EUHFORIA. *Astronomy & Astrophysics*, 622:A28, 2019. doi:10.1051/0004-6361/201833958

Wild, J. P., Smerd, S. F., Weiss, A. A. Solar Bursts. *Annual Review of Astronomy and Astrophysics*, 1:291, 1963. doi:10.1146/annurev.aa.01.090163.001451

Wilks, D. S. *Statistical Methods in the Atmospheric Sciences*. Academic Press, San Diego, first edition, 1995. ISBN 978-0-12-815823-4. doi:10.1016/C2017-0-03921-6

Winkler, C., Courvoisier, T. J. L., Di Cocco, G., Gehrels, N., Giménez, A., Grebenev, S., Hermsen, W., Mas-Hesse, J. M., Lebrun, F., Lund, N., Palumbo, G. G. C., Paul, J., Roques, J. P., Schnopper, H., Schönfelder, V., Sunyaev, R., Teegarden, B., Ubertini, P., Vedrenne, G., Dean, A. J. The INTEGRAL mission. *Astronomy & Astrophysics*, 411:L1–L6, 2003. doi:10.1051/0004-6361:20031288

Wolf, R. Bericht über neue Untersuchungen über die Periode der Sonnenflecken und ihrer Bedeutung von Herrn Prof. Wolf. *Astronomische Nachrichten*, 35(25):369, 1852. doi:10.1002/asna.18530352504

Xapsos, M. A., Stauffer, C., Barth, J. L., Burke, E. A. Solar Particle Events and Self-Organized Criticality: Are Deterministic Predictions of Events Possible? *IEEE Transactions on Nuclear Science*, 53(4):1839–1843, 2006. doi:10.1109/TNS.2006.880576

Xapsos, M. A., Summers, G. P., Barth, J. L., Stassinopoulos, E. G., Burke, E. A. Probability model for worst case solar proton event fluences. *IEEE Transactions on Nuclear Science*, 46(6):1481–1485, 1999. doi:10.1109/23.819111

Xapsos, M. A., Summers, G. P., Barth, J. L., Stassinopoulos, E. G., Burke, E. A. Probability model for cumulative solar proton event fluences. *IEEE Transactions on Nuclear Science*, 47(3):486–490, 2000. doi:10.1109/23.856469

Xapsos, M. A., Summers, G. P., Burke, E. A. Probability model for peak fluxes of solar proton events. *IEEE Transactions on Nuclear Science*, 45(6):2948–2953, 1998. doi:10.1109/23.736551

Xie, H., Mäkelä, P., Gopalswamy, N., St. Cyr, O. C. Energy dependence of SEP electron and proton onset times. *Journal of Geophysical Research (Space Physics)*, 121(7):6168–6183, 2016. doi:10.1002/2015JA021422

Xie, H., St. Cyr, O. C., Mäkelä, P., Gopalswamy, N. Statistical Study on Multispacecraft Widespread Solar Energetic Particle Events During Solar Cycle 24. *Journal of Geophysical Research (Space Physics)*, 124(8):6384–6402, 2019. doi:10.1029/2019JA026832

Zhang, J., Dere, K. P., Howard, R. A., Kundu, M. R., White, S. M. On the Temporal Relationship between Coronal Mass Ejections and Flares. *The Astrophysical Journal*, 559(1):452–462, 2001. doi:10.1086/322405

Zhang, M., Low, B. C. The Hydromagnetic Nature of Solar Coronal Mass Ejections. *Annual Review of Astronomy & Astrophysics*, 43(1):103–137, 2005. doi:10.1146/annurev.astro.43.072103.150602

Zhang, M., Qin, G., Rassoul, H. Propagation of Solar Energetic Particles in Three-Dimensional Interplanetary Magnetic Fields. *The Astrophysical Journal*, 692(1):109–132, 2009. doi:10.1088/0004-637X/692/1/109

Zhang, Q. M. A revised cone model and its application to non-radial prominence eruptions. *Astronomy & Astrophysics*, 653:L2, 2021. doi:10.1051/0004-6361/202141982

Zhang, T. X. An Explanation for Huge Enhancements of Ultraheavy Ions in Solar ^{3}He-rich Events. *The Astrophysical Journal*, 617(1):L77–L80, 2004. doi:10.1086/427169

Zhuang, B., Lugaz, N., Gou, T., Ding, L., Wang, Y. The Role of Successive and Interacting CMEs in the Acceleration and Release of Solar Energetic Particles: Multi-viewpoint Observations. *The Astrophysical Journal*, 901(1):45, 2020. doi:10.3847/1538-4357/abaef9

TURUN
YLIOPISTO
UNIVERSITY
OF TURKU

ISBN 978-951-29-9256-0 (PRINT)
ISBN 978-951-29-9257-7 (PDF)
ISSN 0082-7002 (Print)
ISSN 2343-3175 (Online)

Painosalama Oy, Turku, Finland 2023